The Role of RNAi in Mammalian Cells in Response to Sindbis virus infection

Andras Donaszi-Ivanov

PhD 2013

Contents

Abstract

Viruses are obligate intracellular parasites that need to interact with their host in order to replicate successfully. The understanding of this complex interaction between host and virus is essential for developing new therapeutic strategies as viral infections pose a serious challenge in healthcare, and also because viruses impose enormous costs on the economy. This study focused on the role of RNA interference in the interaction between an RNA virus (Sindbis virus) and its mammalian host cell.

A sensitive image–based viral replication assay was developed to follow Sindbis virus replication in HEK293C cells and the main anti-viral innate responses to virus infection described. Virus replication increased in Dicer and RNA helicase A (RHA) knockout cells, but not when the central regulator of interferon synthesis IRF3 was knocked out. High-throughput Solexa Illumina sequencing was used to detect small viral RNA (svRNA) in Sindbis virus (SINV) infected human cells, and to detect changes in the cellular microRNA (miRNA) expression profile. Very few vsRNA sequences were detected by sequencing during virus infection, and I argue that they are random degradation products, not Dicer-generated svRNAs. Due to the very low level of svRNAs, these were undetectable using northern blotting. We have also found that the expression profile for cellular miRNAs did not change in the early stages of virus infection according to the sequencing data, a finding which was verified by northern blotting. A functional RNAi assay was developed to assess the activity and function of the RNAi system in cells subjected to cellular stress, type I interferon, infection and dsRNA, and northern blotting was used to verify the sequencing data. I have found that certain stress signals -double stranded RNA and SINV infection- decrease the efficiency of siRNA knockdowns in a siRNA-based knockdown assay system.

I have identified two host factors important in Sindbis replication (Dicer, RHA). The lack of vsRNA fragments led to the conclusion that during virus infection the siRNA pathway is suppressed by either the cell or the virus itself, although SINV has been shown not to have any RNAi suppressors in previous studies conducted on its insect vector. This can be explained by the fact that both RNAi and the innate immunity detect the same molecule, dsRNA, placing these two systems into direct competition for the same substrate. My hypothesis is that the siRNA pathway of RNAi is suppressed so that Dicer does not process the long dsRNA into small, 21nt fragments, which are invisible to the innate immune system.

Keywords: Sindbis virus, RNA interference, Dicer, RHA, Interferon, innate immunity, mammalian, high-throughput sequencing, virus titration

List of figures

List of abbreviations

AGO - Argonaut protein
ATP – adenosine triphosphate
bp – base pairs
CARD – Caspase recruitment domains
cDNA - complementary DNA
DAPI - 4',6-diamidino-2-phenylindole
DENG - Dengue Virus
DNA – Deoxyribonucleic Acid
dntps - deoxyribonucleotidetriphosphates
dsRNA – double stranded RNA
eIF2α - eukaryotic initiation factor 2 alpha
ER - Endoplasmic Reticulum
FHV - Flock House Virus
GAPDH - Glyceraldehyde 3-phosphate dehydrogenase
IFNα/β/γ – interferon alpha/beta/gamma
IFNAR - Type I Interferon α/β Receptor
IRES - Internal Ribosome Entry Site
IRF – IFN-regulatory factor
ISRE – Interferon-Sensitive Response Element
hpi – hours post infection
LPG2 - laboratory of genetics and physiology 2
MAVS - mitochondrial antiviral signalling
MDA5 - melanoma differentiation–associated gene 5
miRNA - microRNA
MOI – multiplicity of infection
mRNP - messenger ribonucleoprotein particles
OAS - 2'-5'-oligoadenylate synthetase 1
PAMP – pathogen associated molecular pattern
PB - Processing Body
PCR – Polymerase Chain Reaction
piRNAs - Piwi-interacting RNAs
PKR - dsRNA-dependent *protein kinase*
polyI:C - Polyinosinic:polycytidylic acid
PRR – pattern recognition receptor
RHA – RNA helicase A
RIG-I – Retinoic acid inducible gene -I
RLR – RIG-I like receptors
RNA - Ribonucleic Acid
RNAi - RNA interference
RT – Reverse transcription
SBS - Sequencing by Synthesis
SG - Stress Granule
SINV – Sindbis virus
siRNA - small interfering RNA
snRNA - small nuclear RNA
sRNA - short RNA
ssRNA – single stranded RNA
TCID50 - Median tissue culture infective dose
TLR – Toll like receptor
TNF-α – Tumour necrosis factor alpha
TRBP - TAR RNA binding protein
VSR – Viral Suppressor of RNAi
vsRNA -small RNA molecules with perfect complimentarily to the infecting viral genome

Acknowledgements

1. Introduction

1.1 .RNA interference

RNA interference (RNAi or posttranscriptional gene silencing) is the process by which long double stranded RNA is processed into small 21-24mer RNAs homologous to endogenous mRNA to inhibit expression. RNAi occurs in a wide range of eukaryotic organisms. It has been shown to be involved in gene expression regulation, control of cellular metabolism, growth and differentiation, and the maintenance of genome integrity, including protection of the cell against viruses and mobile genetic elements (Moazed 2009). Around 30% of the human genome is estimated to be controlled by a class of small regulatory RNA species called microRNA (miRNA), underscoring the significance of RNA interference (Lewis et al. 2005). Since in different organisms both the mechanism and the role of RNAi can be markedly different, in this short review I will only focus on the aspects of this process that are relevant to mammalian cells.

Posttranscriptional gene silencing is based on small, non-coding RNA sequences that are partially or completely complementary to the transcript they regulate. There are three main classes of small regulatory RNAs: microRNAs (miRNA), small interfering RNAs (siRNA), and PIWI-interacting RNAs (piRNA) (Moazed 2009, Tijsterman & Plasterk 2004, Jinek & Doudna 2009, Obbard et al. 2009, H. Siomi & M. C. Siomi 2009, Kutter & Svoboda 2008). The boundaries between the different types of small regulatory RNAs are blurred and their origin and function can be overlapping (H. Siomi & M. C. Siomi 2009). These molecules differ in their effector function and biogenesis, but are similar in chemical composition and structure, and share the same cellular machinery downstream of their initial processing. miRNAs and siRNAs are generated from long, double stranded RNA precursors, or single stranded RNA molecules with

extensive secondary structure, by Dicer, an RNase III family protein (Jinek & Doudna 2009). The products of Dicer cleavage, small, 20-25bp long double stranded sequences, then associate with the members of the Argonaut (AGO) family of proteins. AGO proteins form the core of the protein-RNA effector complex, called RNA-induced silencing complex (RISC). Here the double stranded RNA is unwound, one strand (the passenger strand) is discarded, and the guide strand is used for sequence specific silencing of messenger RNAs (mRNAs) either by degradation, or by translational repression (K. Kim et al. 2007, Jaronczyk et al. 2005). Biogenesis of the piRNA class of small RNAs also involves the members of the Argonaute family, but it differs from that of the miRNA and siRNA and will not be covered in this review (Moazed 2009, Jinek & Doudna 2009).

1.1.1. Biogenesis of small RNAs

Three main categories of small regulatory RNAs have been described on the basis of their precursors: microRNA, small inhibitory RNA and piwiRNA. Here I am focusing on only the miRNA and siRNA classes of small RNAs (**Figure 1.1**).

1.1.1.1. siRNA biogenesis

Small interfering RNA (siRNA) is formed when double stranded RNA is present in the cytoplasm (**Figure 1.1A**). Dicer, an RNaseIII enzyme, generates the signature 20-25 nucleotide siRNA fragments from their longer, dsRNA precursors (MacRae et al. 2007). In this respect Dicer acts as a dsRNA sensor, homologous of the RIG-I like receptors (RLRs), which, along with Dicer, are members of the DExD/H box RNA helicase family. The Dicer-generated siRNA duplexes have a phosphate group on their 5' end, and a two nucleotide overhang on the 3' end. This is a hallmark of RNaseIII mediated cleavage (MacRae & Doudna 2007). Dicer itself contains an N-terminal DExD/H box

domain, a PAZ domain, which binds to the 3' end of the RNA molecule, adjoined by a connector helix to two tandem RNaseIII domains (K. S. Yan et al. 2003, Macrae et al. 2006) (**Figure 1.2**). The connector helix keeps the PAZ domain at a distance of 65Å from the intramolecular dimer formed by the RNase domains. This molecular structure acts a molecular ruler, responsible for the size of the cleavage products (Macrae et al. 2006).

The exact substrate requirements for Dicer are not yet clear. Dicer processes the dsRNA into small, 21-25 nucleotide long double stranded siRNA fragments, and with the help of other proteins (such as RHA or TRBP, etc) loads them into a protein complex, called RISC (RNA induced silencing complex). In humans the siRNA is attached to AGO2, a member of the Argonaut (AGO) protein family (Joshua-Tor 2006, Meister et al. 2004). The RNA-AGO complex forms the core of RISC (Rivas et al. 2005): the RNA molecule is responsible for target recognition, and the Argonaut protein forms the catalytic component (responsible for slicing or translational repression). There are several members of this family (the number is dependent on the species in question), with different small RNA specificity and enzymatic function (Farazi et al. 2008). Once AGO binds the guide strand of the small dsRNA, it discards the passenger strand and the RISC complex is ready. siRNA sequences in mammals are fully complementary to their mRNA targets, and induce their degradation in a catalytic manner (slicing) (**Figure 1.1A**) (Doench et al. 2003, Chiu & Rana 2002, Jinek & Doudna 2009).

1.1.1.2. miRNA biogenesis

Similarly to siRNAs, miRNAs are short (20-25 nucleotides) double stranded RNA molecules, where both strand carry a phosphate group on the 5', and a 2 nucleotide overhang on the 3' end. Their biogenesis and function, however, are different from that

of the siRNAs (Jinek & Doudna 2009, R. J. Jackson & Standart 2007, Schickel et al.).

The primary precursors of miRNAs (pri-miRNAs) are transcribed from the genome by

RNA polymerase II (in some cases by RNA polymerase III). This pri-miRNA contains

stem-loop structures that are cleaved by the microprocessor complex in the nucleus. The

microprocessor complex contains Drosha, another RNaseIII enzyme, and its cofactor,

DGCR8 (called Pasha in Drosophila) (J. Han et al. 2004, Gregory et al. 2004, J. Han et

al. 2006). DGCR8 binds to the base of the hairpin of the pri-miRNA, and it positions

Drosha to cut the stem at the distance of 11 nucleotides from the junction between the

duplex stem and the flanking ssRNA regions (**Figure 1.1B**). DGCR8 is thought to be a

trans acting specificity determinant, analogous to the PAZ domain of Dicer, which acts

in *cis*. The resulting pre-miRNA is an approximately 70 nucleotide long molecule

containing a hairpin structure. This is exported to the cytoplasm via Exportin-5, where

Dicer completes the maturation process. After Dicer cleaved the pre-miRNA into a 21-

25 nucleotide long miRNA, it is loaded onto a RISC complex, similarly to the siRNA

pathway, where the passenger strand is ejected, and RISC becomes operational. miRNA

molecules in mammals are usually only partially complementary to the 3' untranslated

region (UTR) of their mRNA targets, and upon binding they cause translational

repression, not slicing. The exact mechanism is not yet fully understood, but it involves

translational inhibition of mRNA molecules, induction of de-amylation and RNA decay

(R. J. Jackson & Standart 2007). The partial complementarily also means that one

miRNA can suppress multiple target mRNAs (Lewis et al. 2005). There are a few

notable differences between the miRNA and siRNA pathways in mammals. The AGO

proteins involved in the miRNA pathway are AGO1, 2, 3 and 4. miRNA containing

RISC does not work in a catalytic manner. While AGO2-containing RISC can process

many target RNA molecules in the siRNA pathway (slicing), in the miRNA pathway

the posttranscriptional gene silencing is achieved in a slicer-independent manner. The

RISC complex must remain bound to the repressed mRNA to maintain repression

(**Figure 1.1B**) (Jinek & Doudna 2009).
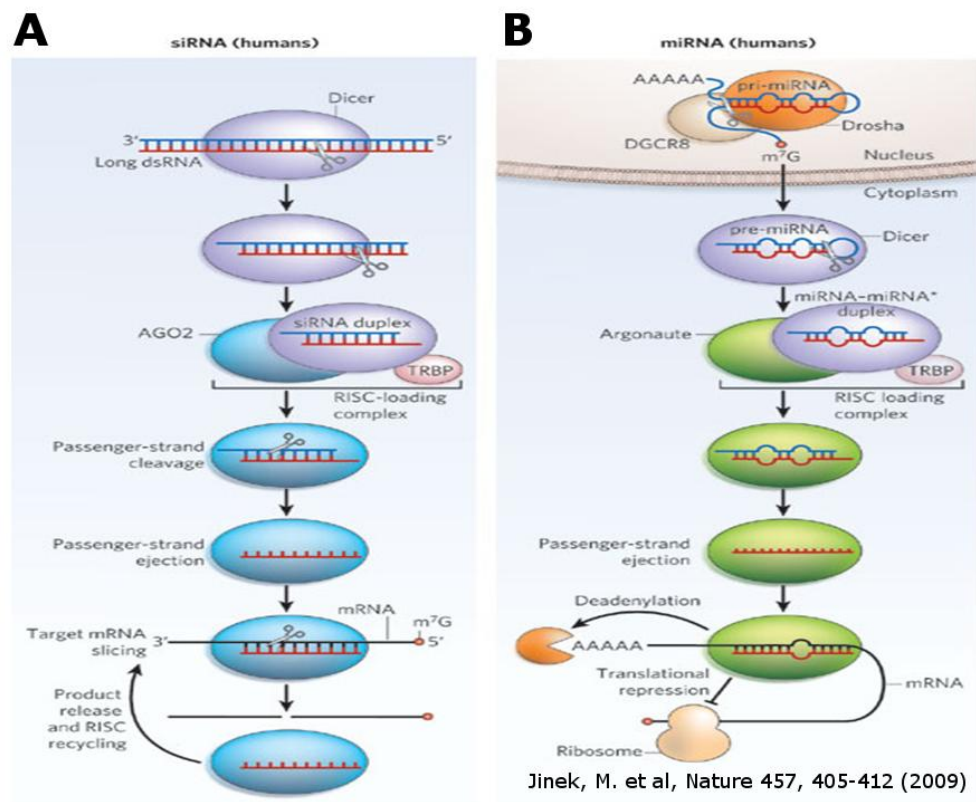
Figure 1.1 A) An overview of the siRNA pathway: dsRNA of exogenous or endogenous origin is processed by Dicer into 20-23nt siRNA, and loaded onto RISC. The siRNA duplex is separated, and one strand is used to target complementary mRNA for degradation by AGO2. **B).** An overview of the miRNA pathway: the precursor of miRNA (pri-miRNA) is coded in the genome and processed by the Microprocessor complex in the nucleus into pre-miRNA, which is transported into the cytosol, and further processed by Dicer into 20-23nt miRNA duplexes. It is loaded onto a RISC complex, and used in the translational repression of target genes.

1.1.2. RNAi as an antiviral mechanism

This study focuses on the role of RNAi as an antiviral defence in mammalian cells. The role of mammalian RNAi as an innate cellular defence mechanism against virus infection is not yet clear (B. R. Cullen 2006, Bagasra & Prilliman 2004a, Yeung et al. 2007). RNAi is used against viral pathogens in plants and invertebrates (Q. Xie & Guo 2006; Saleh et al. 2009), but mammals have a highly effective and sophisticated system to detect and eliminate viruses –the innate and the adaptive immune systems. Longer than 30mer dsRNA sequences in mammalian cells trigger innate immune responses, and short (20-25nt) sequences are directed towards the RNAi pathway (Tijsterman & Plasterk 2004; Svoboda P 2007).

1.1.2.1. RNAi as an antiviral mechanism in insects

It has been demonstrated that invertebrates, such as the vectors of arboviruses, utilize the RNAi pathway against viral infections. vsRNA sequences have been detected and characterized using high-throughput sequencing technologies, and were verified by northern blotting (Sanchez-Vargas et al. 2004; Fragkoudis et al. 2009; Myles et al. 2009; Sánchez-Vargas et al. 2009). The origin of vsRNS can either be double stranded replication intermediates or single stranded RNA molecules with secondary structures, and depends on both the host cell and the virus. In plants, viral genomes and replication intermediates were described as sources of vsRNA (T. Ho et al. 2006; Molnar et al. 2005; Itaya et al. 2007; Q. Xie & Guo 2006). In Drosophila, Flock House Virus infection produced an approximately equal ratio of (+) and (-) polarity vsRNA suggesting that the Dicer-2 substrate was the double stranded replication intermediate (van Rij & Berezikov 2009; Aliyari et al. 2008; Flynt et al. 2009). As cells usually contain much higher proportion of RNA with the same polarity as the viral genome than the RNA with the template polarity, sequences with the same polarity as the viral

genome are expected to be in the majority if the vsRNA is either produced from highly structured ssRNA molecules, or are the results of random degradation. vsRNA profiles produced by alphaviruses Sindbis (SINV) and O'nyong'nyong virus (ONNV) in insects showed that the vsRNA produced is overwhelmingly (+) polarity (Myles et al. 2009; Campbell et al. 2008). This suggests that the vsRNA is derived mostly from the genomic RNA or mRNA, and not from the double-stranded replication intermediates. In both cases hot-spots -areas of the viral genome where vsRNA was produced with a much higher abundance- were prominent.

The same study investigated the abundance of Dengue (DEN) vsRNA, and surprisingly it found that only 0.01-0.05% per 12 million reads mapped to the DEN genome. In case of alphaviruses, SINV infected mosquitoes had a significantly higher proportion of vsRNA (5-10%). The differences in virus evasion strategies or the accessibility of the viral genome may explain these differences.

1.1.2.2. RNAi and Mammalian Innate Immunity

In theory, RNAi (nucleic acid based immunity), which is immediately active, could work in conjunction with the protein based immunity, which only becomes active hours after the viral infection. Cytosolic short double stranded RNA sequences readily enter the RNAi pathway (Tijsterman & Plasterk 2004; Svoboda P 2007). The presence of long (more than 30bp) dsRNA, however, triggers a number of pattern recognition receptors (dsRNA-dependent protein kinase (PKR), RIG-I-like receptors (RLRs), Toll-like receptors (TLRs)), and they, in turn, induce type I interferons, activate non-specific RNases (mainly through PKR and RNase L), and trigger a global translational shutoff (Ishii et al. 2008; Kawai & Shizuo Akira 2006; Koyama et al. 2008).

There are several arguments put against RNAi as part of the innate immune response. While mammals have only one Dicer gene, Arabidopsis has four, encoding four distinct Dicer proteins that have the potential to recognize different types of dsRNA (Z. Xie et al. 2004). In mammals the mechanisms helping to amplify and spread the RNAi signals between cells are also thought to be lacking, making the process of RNAi cell-autonomous (Stein 2003).

There is mounting evidence however, that cells and viruses both utilize the RNAi pathway for their own purposes in mammalian systems. The host-pathogen interaction between is very complex and encompasses all levels of cell regulation, the RNA interference pathway included (Aliyari & S.-W. Ding 2009; Ben Berkhout & Joost Haasnoot 2006; Collins & X. Cheng 2006).

One possible clue to the importance of the RNAi machinery during viral infections is that suppressing the RNAi response increases the replication rate of certain viruses. Plant and invertebrate viruses encode RNAi suppressors (VSRs- viral suppressor of RNAi), and can replicate better in cells with defective RNAi system (Vance & Vaucheret 2001; Aliyari & S.-W. Ding 2009). De Vries et al. reported that blocking the RNAi system caused the replication of several types of viruses (adenovirus, alphavirus and lentivirus) to increase dramatically (W de Vries et al. 2008). My own studies have shown similar results.

External siRNA can be effectively used to suppress virus replication, which suggests that even if RNAi is not the part of innate immunity; the cellular machinery can be used against viral infection (J. Zhou & J. J. Rossi 2011; Joost Haasnoot et al. 2007).

Viruses have evolved countermeasures against the non-specific innate immune responses (Randall & Goodbourn 2008) For example: Adenovirus VA sequeresters PKR (O'Malley & Mathews 1986), the Porcine Rotavirus NSP3 protein and the Influenza A virus NS1 protein sequester dsRNA, and prevents stimulation of the type I interferon response (Langland et al. 1994; Bergmann et al. 2000a). HCV protease NS3/4A cleaves RIG-I signalling partner IPS-1 (Y. M. Loo 2006). There are several viral proteins (and RNA molecules) isolated from mammalian viruses identified as VSRs (Saumet & C.-H. Lecellier 2006; Bagasra & Prilliman 2004b; Walter de Vries & Ben Berkhout 2008). These proteins have diverse functions. They either interfere with Dicer (HIV-1 Tat), sequester and hide viral RNA (influenza NS1, Vaccinia E3L; W.-X. Li et al. 2004; Sullivan & Ganem 2005), or provide decoys at different stages of the RNAi process (i.e. adenovirus virus-associated RNAI-II is used as a decoy for Exportin-5, Dicer and RISC). TRBP, which is important in RISC loading, also binds to HIV-I TAR RNA, and inhibits RNA-activated Protein Kinase (PKR), an important interferon-activator (Gatignol et al. 2005). Several of these viral proteins can suppress RNAi in plant cells (Bucher et al. 2004; Lichner et al. 2003). This suppressive activity suggests that these viruses are targets of the RNAi machinery, and that they evolved means to evade it.

Are these viral proteins real VSRs, though? An alternative explanation for the VSR activity of these proteins is that they could be artefacts of the experimental systems they were used in (Lichner et al. 2003; Umbach & B. R. Cullen 2009). The VSR role of mammalian viral proteins was generally studied by overexpressing them, and not in the context of infection. NS1, for example, is crucial for the influenza virus reproduction; the absence of the protein hinders virus replication. The absence of virus replication,

however, does not manifest in IFN-deficient cells, suggesting that the main function of NS1 is the evasion of the immune response (Bergmann et al. 2000b).

Viruses have been shown to directly interact with the RNA interference machinery of their host cells by affecting the miRNa expression of their host cells, or encoding microRNAs themselves (Skalsky & Bryan R Cullen 2010; Ghosh et al. 2009). DNA viruses (Epstein-Bar virus (EBV; Pfeffer et al. 2004), Kaposi's sarcoma-associated herpesvirus (KSHV) or cytomegalovirus (CMV) were found to be encoding miRNAs that regulate cellular proliferation, apoptosis and transcription.

Cell-encoded miRNAs that block virus production have also been found, as in the case of miR-32 and primate foamy virus (PFV-1) (C. H. Lecellier et al. 2005). A potential target site for miR-32 was identified in the PFV-1 genome using computer analysis, and inhibition of miR-32 function in cell culture resulted in increased viral replication. Furthermore the viral protein *tas* was demonstrated to suppress miRNA-mediated translational inhibition, supporting the role of cellular miRNAs against the virus infection.

The cellular mechanisms do not always inhibit viral production. In the case of Hepatitis C virus (HCV), a liver-specific miRNA (miR-122) interacts with the 5' non-coding region of the HCV RNA, which in turn enhances virus replication (Jopling et al. 2005).

1.1.2.3. High-throughput sequencing in the search for vsRNA in mammalian cells

The development of high throughput technologies made it possible to detect and sequence small RNAs (sRNAs) which are in low abundance routinely. The first, and so far, only comprehensive study on vsRNAs produced in mammalian cells was conducted

on six RNA viruses by Parameswaran et al (2010). The study used Illumina and Roche 454 sequencing technologies to detect vsRNAs in infected invertebrate and mammalian cells. They have shown that vsRNA is present in some mammalian cells in an extremely low abundance. This has been shown to be dependent on the type of cell and virus studied (e.g. mouse embryonic fibroblast (MEF) and baby hamster kidney (BHK) cells produced a relatively large amount of vsRNAs, while dendritic cells (DC) and macrophages (MF) did not produce any detectable vsRNAs). The detected vsRNA reads may originate from two sources: they are either products of random degradation or Dicer activity. RNA degradation is usually characterised by a high diversity in the size of the resulting reads i.e. a lack of specificity for one size class is observed. The ratios of detected svRNAs mapping to the sense and antisense strands were different from the strand ratios observed in full-length virus genomes. While the full length genomic ratios can be from 30:1 to 100:1 (positive:negative strand) in the case of Polio, West Nile Virus and Vesicular stomatitis virus the observed ratios were closer to 1:1, 1:2, suggesting that not all of the fragments were products of random degradation.

Dicer knockout MEF cells used in the same study showed that while the amount of miRNA drops over 100 fold, the abundance of vsRNA only decreased by 2.1 fold, which suggests that some of this RNA is produced in a Dicer independent manner.

AGO2 knockout MEF cell lines showed an increase in vsRNA abundance relative to miRNA abundance; a possible explanation could be the increased stability of the vsRNA duplex due to the lack of AGO2, which unwinds it and discards the passenger strand.

In cells where the IFN-α/β receptor was inoperable the abundance of vsRNA also increased relative to the miRNA abundances, suggesting a crosstalk between the IFN

response and the RNAi. It is really difficult to judge if the detected svRNA sequences are abundant enough to be biologically relevant. Some sequences were more abundant than some functional miRNAs, which at least suggests that they may be functional. AGO pulldowns showed enrichment of vsRNA, which demonstrated that these sequences are loaded onto RISC.

The study also proposed that few miRNAs consistently change in different samples e.g. miR-17-5p, miR-125b levels show a decrease upon virus infection, and miR-21 level increased in immune cells. This result and findings in previous studies (B. Berkhout & K. T. Jeang 2007; Bryan R Cullen 2006; Ghosh et al. 2009) support the idea that the virus interacts with the host cell at RNAi level.

1.2. Mammalian antiviral innate immunity

The last ten years saw a tremendous progress in understanding how the innate immune system reacts to pathogens, and how it senses infection via pattern recognition receptors (PPR). In mammals the first line of defence against viruses is the innate immunity which detects either viral proteins or the genome of the invading pathogens. The recognition of "foreign" is based on unique molecular structures that are not associated with the host, called pathogen associated molecular patterns (PAMPs), such as single stranded DNA or RNA in the cytosol (Kawai & Shizuo Akira 2007; Koyama et al. 2008).

Double stranded RNA (dsRNA) is a very important PAMP as it is produced during the life cycle of all RNA viruses either as a replication intermediate or a self-complementing single stranded RNA. dsRNA is detected by several PRRs: Protein Kinase R (PKR), which causes translational inhibition and the enhanced transcription of interferon stimulated genes (ISGs) (B. R. Williams 1999), cytosolic RIG-I-like receptor

(RLR) family, which triggers the type I interferon response (J. Zou et al. 2009) (Nakhaei et al. 2009). The membrane-bound Toll-like receptor (TLR) 3, 7 and 8, are also important, which upon activating IRF3 NFκB and ATF2-c-Jun, trigger the type I interferon response (M. S. Jin & J.-O. Lee 2008). 2'-5' oligoadenylate synthetase (OAS) family activates RNase L leading to translational inhibition and apotosis (Levy & Garcia-Sastre 2001).

The function of these receptors is redundant and overlapping with additional feedback loops built into the signalling cascades. The result of activation is the triggering of type I interferon response, pro-inflammatory cytokine production, translational shutoff, a general antiviral state in both infected and neighbouring cells and apoptosis and trigger the adaptive immune system (Koyama et al. 2008; Ishii et al. 2008; PERRY et al. 2005; Haller et al. 2006)

1.2.1. Recognition of viruses by DExD/H box helicase RLRs

Most cells in the body use the so-called classical (or TLR independent) pathway for interferon signalling, which involves RLRs instead of TLRs. The intercellular sensors involved in this pathway detect viral signals upon infection (replication dependent detection), and activate the main interferon regulatory factors, IRF3 and NF-κB. This results in IFN-β production as an initial response, then switches to IFN-α during the subsequent amplification phase through IRF7.

One of the most important intracellular viral sensor families is the RIG-I-like helicase family. RIG-I (retinoic acid-inducible gene-I) and MDA-5 (melanoma differentiation-associated gene-5) are closely related cytoplasmic proteins, and they both belong to the DExD/H box helicase family. Their domain structure is similar: they consist of two N-terminal CARD domains (Caspase recruitment domains), which are responsible for signalling. A central ATPase, helicase domain serves to bind and

possibly unwind RNA (it is a DExD/H-box RNA helicase domain, similar to the one found in Dicer), and a C-terminal domain with an embedded repressor domain, which functions in autoregulation of the receptor molecule, and might be involved in target recognition (Yoneyama et al. 2004; Yoneyama et al. 2005) (**Figure 1.2**). LGP2 (Laboratory of genetics and physiology) closely resembles RIG-I and MDA-5, but it lacks the CARD domains of the latter. It was initially thought to function as a negative regulator of the host's defence based on in vitro studies (Rothenfusser et al. 2005). Mice knockout models demonstrated however that depending on the infecting virus, and possibly the cell type, LGP2 can serve as positive regulator/co-receptor as well (Venkataraman et al. 2007).

Knockout models have demonstrated that RLRs are essential for type-I IFN response in most non-immune cell types, and that despite of being closely related, their functions are not redundant (Hiroki Kato et al. 2006). RIG-I and MDA-5 recognize distinct and different viruses. RIG-I is important in recognizing hepatitis C (HCV), Sendai virus (SeV), influenza virus, vesicular stomatitis virus (VSV), Newcastle disease virus (NDV), rabies, Japanese encephalitis virus (JeV), and short polyI:C molecules. MDA-5 plays a role in detecting picoronaviruses, and long polyI:C molecules (Hiroki Kato et al. 2006; Gitlin et al. 2006).

RIG-I recognition is dependent on the presence of trisphosphate groups on the 5' end of the RNA, a characteristic of viral RNA synthesis, and not found in capped or processed cellular RNA (Schmidt et al. 2009). The A-form of dsRNA is also recognized by the receptor, irrespective of the sequence or end-modifications. Cellular RNAs, such as tRNAs and rRNAs are extensively modified to avoid RIG-I recognition. The RNA ligands recognized were characterized by Schmidt et al (2009) and Schlee et al. (2009).

They have found that the 5'-triphosphate end is not sufficient on its own. A blunt ended region of dsRNA adjacent to the 5'triphosphate group is also needed (Schmidt et al. 2009; Schlee et al. 2009). Hantaan virus, Borna virus, and Crimean-Congo hemorrhagic fever virus are able to avoid RIG-I recognition by modifying their 5' triphosphate groups (Habjan et al. 2008). Short dsRNA chains (about 31bp) with a minimum of single phosphate group on either ends can also trigger RIG-I recognition (Bürckstümmer et al. 2009; Baum et al. 2010). RIG-I also recognizes particular sequences within the RNA; uridine and adenosine-rich regions were shown to be preferentially bound by RIG-I, and these regions are found within the PAMP structure of a number of viruses (Saito et al. 2008; Uzri & Gehrke 2009). RIG-I also can recognize RNase L cleavage products which might serve as an amplifying mechanism for RLR signal transduction (Malathi et al. 2007).

MDA-5 was initially thought to detect long linear dsRNA. Long dsRNA (longer than 1kb) is indeed capable of induce MDA-5-dependent type-I IFN response, but at the present the accepted model is the recognition of higher-order RNA structures containing both ssRNA and dsRNA. These mesh-like structures are generated during the viral life cycle, and thought to be the primary ligands of MDA5 (A. Pichlmair et al. 2009).
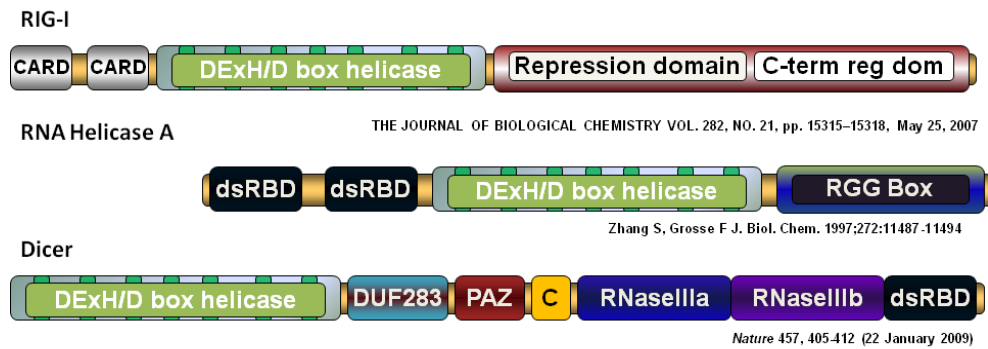
Figure 1.2 Domain Structure of selected DExH/D box helicases. RIG-I: tandem CARD domains, which are responsible for signalling, a central DExH/D box helicase domain, which has ATPase activity, and binds (possibly unwinds) the RNA ligand, and a C-terminal domain with a repression domain embedded, which is responsible for autoregulation and for target recognition**. RNA Helicase A:** two N-terminal dsRNA binding domains (dsRBD) amd a C-terminal domain are flanking the central DExH/D box helicase domain. The C-terminal domain has an RGG box (often found in RNA binding proteins, and contains repeats of Arg—Gly—Gly) The C-terminal also has a bidirection nuclear transport domain. **Dicer**: DExH/D helicase domain which has the possible functions of unwinding RNA, translocating Dicer, or facilitating handoff of products. DUF domain is of unknown function. PAZ (Piwi-Argonaute-Zwille) domain binds the end of the substrate dsRNA. Connector helix sets the length of the RNA fragment by placing the PAZ domain and the RNaseIII domains 65 Å from each other. Tandem RNaseIIIa domains are responsible for the cleavage of the substrate dsRNA. dsRBD domain presumed to participate in pri-micro-RNA recognition and sub cellular localization of Dicer.

1.2.2. The RLR signalling pathway

Signalling through RIG-I is tightly regulated by its C-terminal domain. Without ligands to bind, the molecule is in a "closed" formation, and only undergoes a conformational change upon ligand binding. This opens up the molecule, and the freed-up CARD domains appear to bind to free ubiquitin chains, which, in turn, induces the multimerization of RIG-I. These higher-order complexes of RIG-I and ubiquitin are strong inducers of type I interferons. They interact with the CARD domains of MAVS/Cardiff/IPS-1, and induce a signalling cascade which will trigger the transcription of interferons and ISGs. Although the activation of MDA5 is not as well studied as RIG-I, it is known that both MDA5 and RIG-I signal through mitochondrial/ peroxisomal MAVS via their CARD domains. MAVS is a critical anti-viral protein in the signalling pathway (Seth et al. 2005; Sabbah et al. 2009). It consists of an N-terminal CARD domain, a proline-rich region and a C-terminal hydrophobic transmembrane region that anchors it to the peroxisomal and outer mitochondrial membrane (Dixit et al. 2010). (The membrane attachment is crucial for the function of the protein; deletion mutants fail to induce the interferon response. HCV specifically targets the C terminal domain of MAVS for cleavage, further pointing to the importance of membrane attachment.) The exact mechanisms of how MAVS signals to downstream kinases are not fully understood yet. The binding of dsRNA to RIG-I induces a conformation change, and enables it to bind to MAVS via the CARD domains. MAVS, in turn, signals to both NF-κB and IRF3 signalling pathways by activating the IKK and TBK-1/IKKϵ kinase complexes. IRF3 is constitutively expressed in the cell, while IRF7 is induced by type-I IFNs. NF-κB and IRF3 translocate into the nucleus and turn on the expression of inflammatory cytokines, IFN-β, and other ISGs. The central function of IRF3 is underlined by the fact that many viral IFN inhibitors target it as the type-I IFN

response is impossible without it (Seth et al.; O. Takeuchi & S. Akira 2009) (**Figure 1.4**).

IFN-β acts in an autocrine and paracrine manner, and activates the second round of IFN signalling, which –among other proteins- turns IRF7 production on, amplifying the interferon response. ISGs are activated by both IFN-dependent and independent manner. IFN-dependent ISGs are induced through the JAK/STAT pathway. Some ISGs can be up regulated without IFNs; this was shown to be mediated by peroxisome-bound MAVS, while the IFN-dependent ISGs had a delayed activation through the mitochondria-bound MAVS signalling pathway (Schoggins & Charles M Rice 2011; Dixit et al. 2010). There are hundreds of ISGs with very diverse functions: some act as a negative or positive regulator of the IFN response, some target viral replication acting at every step of the virus life cycle collectively. It seems that many have overlapping functions, which builds redundancy into the defence system. Most ISGs have relatively moderate inhibiting effects on virus replication; it appears that many, moderately inhibitory ISGs are safer for the cells, than a selected few with strong inhibitory effects (Schoggins & Rice 2011)(**Figure 1.4**).
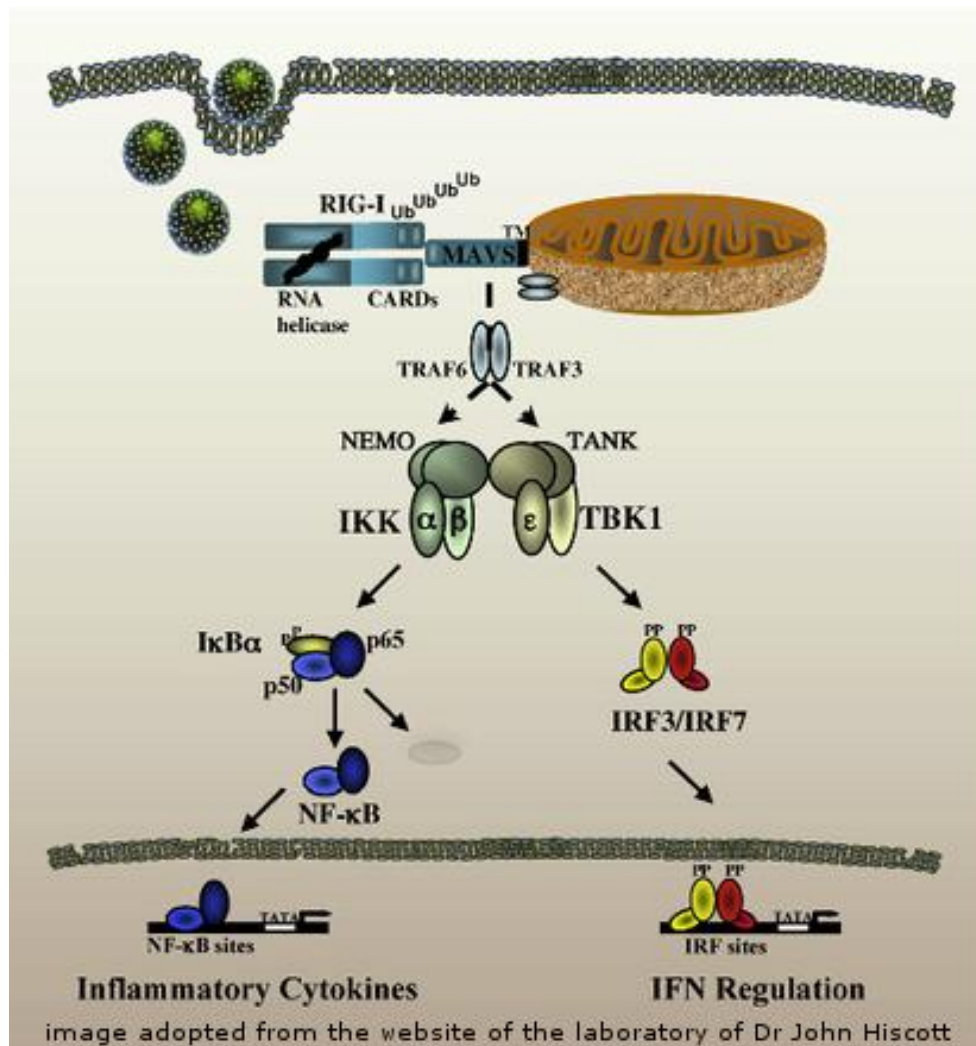
Figure 1.3 Signalling pathway of the RIG-I like helicases induces interferon and inflammatory cytokine production. Upon detecting viral RNA the inactive ("closed") RIG-I activates ("opens"), and the CARD domains bind to ubiquitin (Ub)chains resulting in the multimerization of RIG-I. This activated molecule can interact with the CARD domains of MAVS, which, in turn, activate the NF- κB and the IRF3 pathways through TBK1/IKK kinase complexes. NF- κB and IRF3 migrate into the nucleus where they trigger the transcription of inflammatory cytokines and type I IFNs, respectively.

Schoggins & Charles M Rice 2011
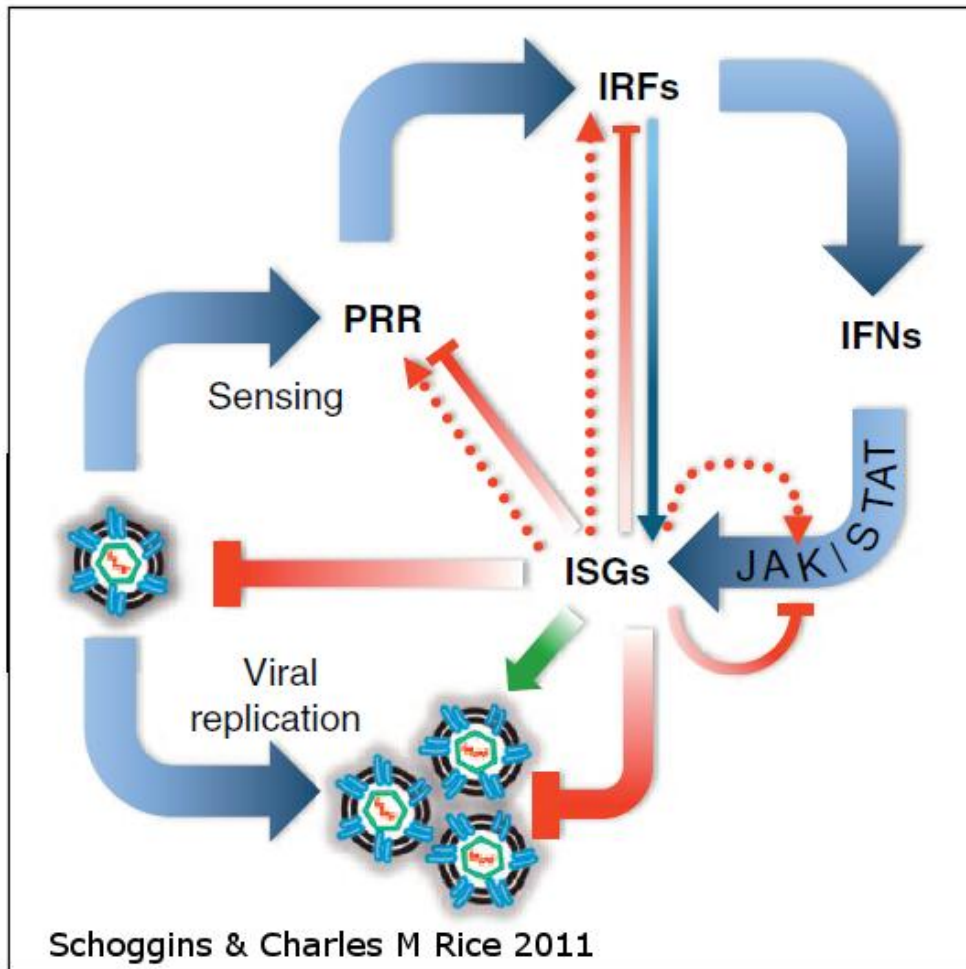
Figure 1.4. Activation of interferon induced antiviral state by virus replication Incoming viruses are sensed by several PRRs (Viral RNA is sensed by TLR-3 in endosomes, PKR/RIG-I receptors in the cytoplasm), which, in turn, starts a signalling cascade in the cell to produce and secrete type I IFNs. Type I IFNs induce the synthesis of ISGs through the JAK/STAT pathway. Some ISGs are induced via an interferon-independent pathway (thin blue arrow). ISGs are involved in inhibition of viral reproduction (thick red bar), but some can enhance virus replication (green arrow). In addition, several ISGs target parts of the innate immune response (PRRs, IFRs, etc) as a negative feedback loop.

1.3. Sindbis virus

1.3.1. Classification and structure

Sindbis virus (SINV) is a well-established laboratory model for alphavirus infection. It belongs to the Togaviridae family, and alphavirus genus. There are three subgroups in the genus: Semliki Forest virus subgroup (Semliki Forest, O'nyong-nyong and Ross River viruses); the eastern equine encephalitis virus subgroup (eastern equine encephalitis and Venezuelan equine encephalitis viruses) and the Sindbis virus subgroup.

The hosts of SINV are small mammals and birds; humans are considered dead-end hosts. In humans SINV causes arthralgia syndrome, high-titre viremia, and mild to severe fever.

The virus is an enveloped virus of about 65-70 nm in diameter, with an icosahedral nucleocapsid (NC). (**Figure 1.5A-B**.) It has a single stranded RNA of positive polarity of 11.5kb length, which is capped and polyadenylated, and serves as an mRNA molecule. (**Figure 1.5C**.) The virus encodes four nonstructural proteins (nsp1-4), which are important in virus replication, and five structural proteins (capsid, E1, E2, E3, 6K) translated from the subgenomic 26S RNA. (Flint 2004) The viral envelope is a host-derived lipid bilayer, in which 240 copies of E1 and E2 transmembrane glycoproteins are embedded. (**Figure 1.5 B**.) The virus envelope also contains small amounts of 6K viral protein.
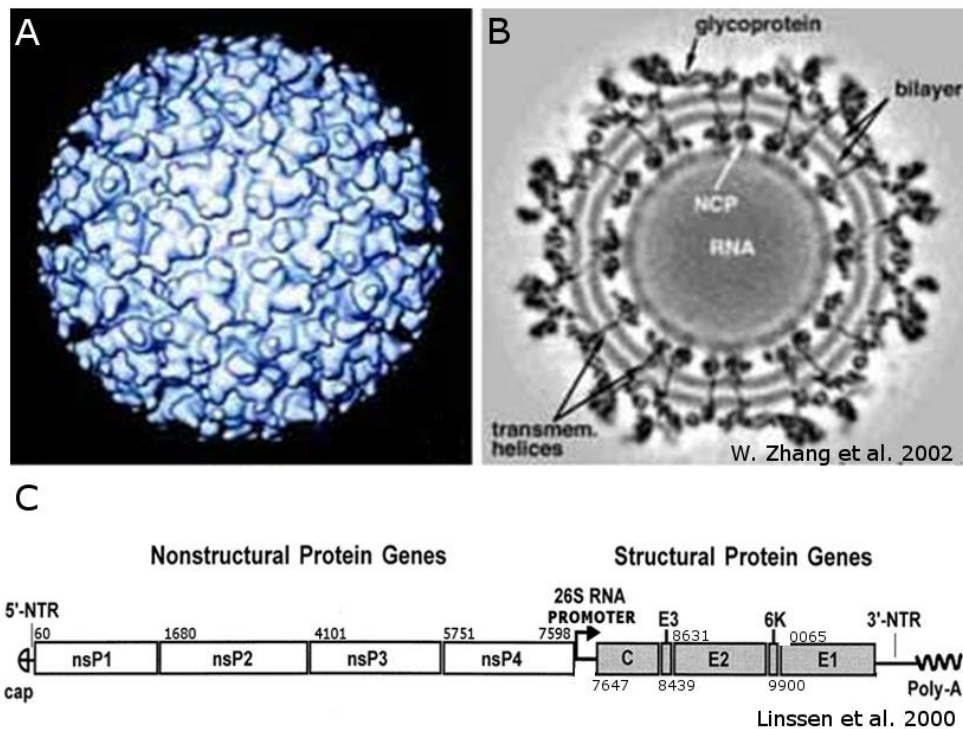
Figure 1.5. Structure of Sindbis virus. A.) Structure of Sindbis virus at 20Å resolution determined by X ray crystallography and 3D image reconstruction techniques. **B.)** Cross section of Sindbis virus at 11 Å resolution showing the glycoproteins (E1 and E2), the lipid bilayer, and the viral capsid (NCP) by cryo-EM **C.)** Schematic drawing of Sindbis virus genome organization. The virus genome is a single stranded RNA molecule with positive polarity. It is capped and has a polyA tail, which enables it to function as an mRNA molecule. The non-structural proteins are translated from the 49S full length genomic RNA as *nsp123* and *nsp1234* polyproteins which undergo cleavage during maturation by snP2. nsP4 is responsible for the RdRP activity of the SINV replication complex. The structural proteins are transcribed from the 26S RNA promoter as a polyprotein, and undergo processing and cleavage in the cytosol/Golgi apparatus. Numbers above or below the proteins show their positions on the genome. (Image adopted from (**Linssen et al. 2000**))

1.3.2. SINV replication

Virus entry is facilitated by a wide range of cell surface receptors (**Figure 1.6.**). E2 glycoprotein is responsible for virus-receptor interactions. The exact nature of receptors is still not known; what is clear is that the virus entry is a two-step, receptor mediated process. The first step is a highly dynamic binding process, while the second is a high-affinity binding and attachment, with reduced viral mobility, followed by viral endocytosis (Gu et al. 2011). Alphaviruses are capable to infect a wide range of hosts, and one hypothesis is that they use a conserved cell-surface receptor (e.g. laminin) to gain entry to the cell. Others argue that the virus is able to interact with multiple cellular receptors, or a combination of the two hypotheses (J H Strauss and E G Strauss n.d.).

As soon as the virus engages with its receptor the, E2 and E1 glycoproteins undergo conformational changes, and the virus is endocytosed. As the pH inside the endosome drops, the E1-E2 heterodimer is destabilizes, and exposes a fusion peptide in E1. This peptide inserts itself into the endosome membrane and forms trimers. This causes membrane fusion, and the nucleocapsid (NC) is deposited in to the cytoplasm of the cell. The NC is quickly disassembled and the transcription from the viral genome can proceed from this point on.

The non-structural viral proteins are translated from the full-length RNA, and can be detected as early as 1.5hpi. SINV -as most Alphaviruses- produce two non-structural polyproteins: nsp123 (1902 amino acids) and a small amount of nsp1234 (2512 amino acids). This latter, longer polyprotein is the result of a translational read-through of an opal termination codon after codon 1897 of the open reading frame, which occurs with about 10% efficiency. The polyproteins undergo sequential proteolytic steps during the course of virus reproduction.

Nsp1 (540 amino acids) possesses both a guaninine-7-methyltransferase and guanyltransferase enzymatic activities which are important for the capping and cap

methylation of newly synthesized viral genomic and subgenomic RNA. It is also a membrane associated protein, and serves as an anchor for the virus replication complex fixing it to cellular membranes.

Nsp2 (807 amino acids) is a multifunctional protein, which has several roles during virus replication. The N-terminal domain contains the helicase activity required for RNA replication and transcription and also responsible for the RNA triphosphatase and nucleoside triphosphatase activity. The C-terminal domain contains a cysteine protease domain, and an enzymatically inactive methyltransferase domain, which was shown to be important in regulating negative-strand synthesis. The protease domain is responsible for processing the viral non-structural proteins into their mature forms. The nsp2 protein also contains nuclear localization signals, and about 50% of all proteins are in the nucleus during infection, where they initiate host transcriptional shutoff. The abolishment of this signal results in attenuated virus phenotype.

Nsp3 (555 amino acids) is required for minus-strand and subgenomic RNA synthesis, but very little is known about the protein and its function.

Nsp4 (610 amino acids) is responsible for the RNA-dependent RNA polymerase (RdRP) activity.

Replication takes place in cytoplasmic vacuoles which are of endosomal and lysosomal origin. The nonstructural proteins form dynamic replication complexes anchored to these membranes. The nsp1234 polyprotein undergoes a *cis*-cleavage by nsp2 at the nsp3/4 junction, which yields nsp123 and nsp4. All other cleavage happens in *trans*-position. The next cleavage happens at nsp123 between nsp1 and nsp2, resulting nsp1 and nsp23. These polyproteins then are able to perform the final cleavage at the nsp2/3 bond. It has long been accepted that the differential processing of non-structural proteins is responsible for the changes in the activity of the virus replication

complexes, such as the switch from minus-strand synthesis to plus strand synthesis. Minus strand synthesis requires nsp123 and nsp4 in the replication complex. Nsp4 is rapidly degraded in the cell, and is only present in high concentration in the beginning of the infection. As the infection proceeds nsp123 is processed in *trans* into its individual proteins. At this point the virus switches from predominantly minus strand synthesis to plus strand synthesis. Plus strands are synthesized from both genomic and subgenomic promoter in approximately 1:3 ratios. It is not known if there are different replication complexes responsible for the production of the two different plus strands.

The structural proteins are encoded in the subgenomic RNA as a structural polyprotein (1245 amino acids) containing CP-E3-E2-6k-E1 structural proteins (it is also called p130).

The capsid protein (CP) has an autocatalytic function which enables it to undergo a cleavage from the nascent viral structural polyprotein. It binds to the full-length RNA encoding the viral genome, and assembles into icosaedric core particles, forming the nucleocapsid. The NC assembles in the cytosol from 240 copies of core proteins associated with a single plus strand genome. The mature NC interacts with the cytoplasmic domain of E2 and this interaction leads to budding and formation of mature virions.

The autocatalytic cleavage of the capsid protein from the rest of the structural polyprotein chain frees up a signal sequence on pE2 which directs the rest of the polypeptide into the ER, where E1 and pE2 undergoes a complex conformational change, maturation and oligomerization.

The function of the E3 protein is unknown.

E2 is responsible for the attachment of viral particle to the host cell. It is synthesised as a p62 precursor, which is processed by furin before it embeds itself into the cell membrane, and forms a heterodimer with E1.

6K is a membrane protein which is involved in viral glycoprotein processing, cell permeabilization and budding of viral particles. It is only present in a very low amount in mature virions.

E1 structural protein is a virus fusion protein. The protein is inactive as long as it forms a heterodimer with E2. After the endocytosis of the virion, the drop in pH destabilizes the E1-E2 heterodimer, and allows E1 to form trimers, which activates membrane fusion between the virus and the endosomal membrane.
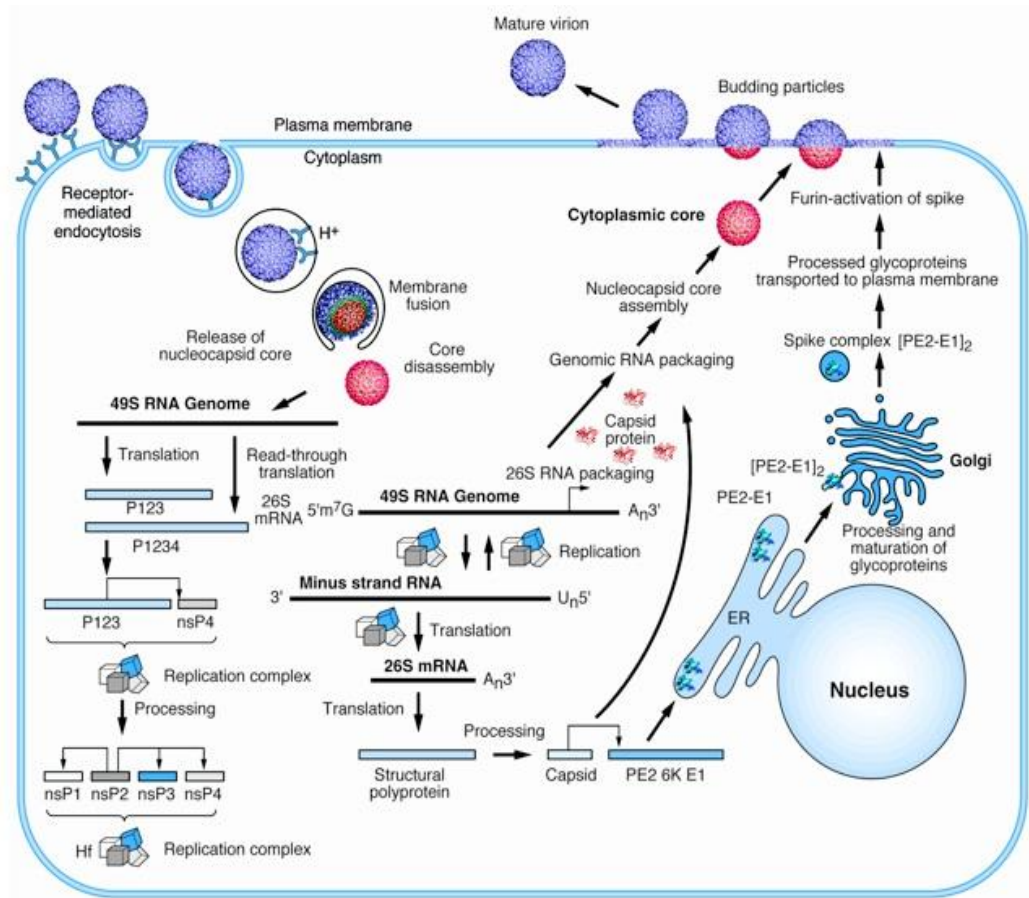
Figure 1.6 Alphavirus replication. The virion binds to its receptors on the cell membrane, and is endocytosed. As the pH drops in the endosome, the virus membrane fuses with the endosomal membrane, and the virus capsid is released into the cytoplasm, where it is disassembled. The full length virus genome serves as an mRNA molecule. First the non-structural proteins are transcribed as two polyproteins: p123 and p1234 using an opal codon readthrough. The non-structural proteins form the replication complex, which undergoes several proteolytic cleavage steps by nsp2. At the early stage of infection full length minus strand genome is produced by the replication complex, which is used as a template for the replication of genome and synthesis of the 26S subgenomic RNA encoding the structural proteins. These proteins are transcribed as a polyprotein as well. First the capsid protein is cleaved, which will form the nucleocapsid by interacting with the 49S SINV RNA. Meanwhile polyprotein carrying the rest of the structural proteins is directed to the ER and Golgi for processing and maturation, and end up embedded into the plasma membrane as E1-E2 dimers. E2 processed by furin just before virus budding with makes it able to interact with the NC proteins. The NC interacts with the E1-E2 glycoproteins, and this triggers the budding process, resulting in the release of virions. (Image source: Richard J. Kuhn)

1.3.3. SINV infection and innate immunity

Sindbis virus, as all alphaviruses, is an insect-borne virus, which means it has to be adapted to the immune system of both its host and its insect vector. It readily infects both mosquitoes and Drosophila, and the immune response of both insects to the SINV infections were studied in great detail in the last decades. It is important to point out that the virus needs to establish a persistent, non-pathologic infection in the vector, even though it usually causes an acute infection in its host organism. The difference between the immune systems of insects and mammals may be the main deciding factor about the different outcomes of infection in the different organisms.

In insects the major immune pathway against viruses is the RNAi pathway, which does not lead to an acquired immune response. The insect immunity is capable of suppressing virus replication without the death of the infected cells. In mammals the primary antiviral pathway is the type-I interferon response, which triggers a signalling pathway leading to an antiviral state in the infected cell and the host organism itself, the activation of adaptive immunity, and often leads to the apoptosis of the infected cells. Both insect and mammalian systems sense the same PAMP: viral dsRNA. (Double stranded RNA is not the only virus associated PAMP, but it is a very important one.)

In Drosophila the long exogenous dsRNA is detected by Dicer-2, and it processes it into 20-22nt long siRNA fragments. With the help of R2D2, Dicer-2 and siRNA are loaded onto a RISC complex carrying Ago2, and used in sequence specific cleavage of complementary, long mRNA sequences (Aravin et al. 2004; Qinghua Liu et al. 2003). This silencing process effectively inhibits viral replication.

There are several pieces of evidence demonstrating that RNAi is the major antiviral pathway in Drosophila. First, RNAi deficient flies are hypersensitive to viral infection, and have increased viral titers. Second, viruses encode RNAi suppressors. Third, vsRNAs have been discovered and characterized in insects (Kemp & J.-L. Imler 2009).

Systemic RNAi spread has been demonstrated to be active in Drosophila (Saleh et al. 2009). The rapid evolution of RNAi pathway genes compared to the miRNA pathway genes also suggests an on-going "arms race" between host and viruses (Obbard et al. 2006).

Although not as well studied, the mosquito immune system is very likely to be similar to the Drosophila innate immunity (Carol D. 2011; Fragkoudis et al. 2009). The ortholouges of Drosophila innate immunity genes have been identified in mosquitoes (M. Keene & E. Olson 2004). Injection of long viral dsRNA inhibits virus replication in mosquito cells, and knockdown of RNAi genes increased the viral titre (Campbell et al. 2008; M. Keene & E. Olson 2004; Sanchez-Vargas et al. 2004). Even though the nature of the viral dsRNA Dicer-2 substrate is unknown, high-throughput sequencing technologies detected vsRNA in mosquito cell lines, and were confirmed using northern blotting (Myles et al. 2009; Cirimotich et al. 2009; Sanchez-Vargas et al. 2004).

Most plant and insect viruses encode proteins that block one or more steps of RNAi to suppress the host immune response. These viral suppressors of RNAi (VSR) are very important in the replication of viruses (S. W. Ding & Voinnet 2007; Gordon & Waterhouse 2006; Feng Li & S.-W. Ding 2006). Several studies attempted to identify similar proteins in arboviruses, although their biology is different from insect-only viruses (H.-W. Li & S.-W. Ding 2005) indicated that there are no proteins encoded by DENG which can act as VSR. Other studies came to similar conclusions (Attarzadeh-Yazdi et al. 2009). Inserting VSRs into arbovirus genomes showed that there is a significant increase of virus replication in ticks and mosquitoes (Blakqori et al. 2007; Garcia et al. 2006). Transgenic SINV expressing the flock house virus (FHV) VSR (dsRNA-binding protein B2) showed significant reduction in vsRNA and increase in virus RNA synthesis, virus growth, which, in turn, lead to the decreased survival rate of

its mosquito vector (Cirimotich et al. 2009; Myles et al. 2009). These findings suggest that the evolution of VSRs were not selected in arboviruses, probably to maintain the fitness of its vector organism.

Evasion mechanisms of RNAi, however, seem to have been developed in arboviruses (Campbell et al. 2008). The sequerestation of replication complexes into membrane vesicles in the alphavirus family is probably one strategy to avoid RNAi (Sánchez-Vargas et al. 2009). In the case of FHV infection, (Flynt et al. 2009) found that hot-spot derived vsRNA sequences have low biological activity (probably because of the low accessibility for the RISC complex to secondary structures on the RNA molecule), which may be a way for the virus to avoid an effective RNAi response by overwhelming the RNAi machinery with inactive vsRNA fragments. They also found that many of the vsRNA molecules were not loaded onto RISC, which also could account for the low biological activity. Similar evasion strategy was described in plants (Itaya et al. 2007), and could be a way for arboviruses to evade RNAi.

1.4. Solexa/Illumina High-Throughput Sequencing Technology

Solexa sequencing was developed based on sequencing by synthesis (SBS) method. It is one of the next-generation, high-throughput sequencing technologies, which superseded the automated Sanger sequencing method in the last decade (Mardis 2008; Metzker 2009). It enables the detection of single bases as they are incorporated into growing DNA strands. The DNA strands first are attached to a solid surface, and amplified to form clusters. Four types of fluorescently labelled reversible dye-terminators are added and imaged as each base is built into the grown DNA chain. These terminators are then cleaved to allow the incorporation of the next base, and the process is repeated (**Figure 1.7**).

1.4.1. cDNA library preparation

Sample preparation starts with isolation of small RNA, and the ligation of special 3' and 5' adapters to the RNA chains using Illumina's kit (Illumina - Sequencing Technology) (**Figure A**). The 3' adapter is necessary for binding to the surface-bound primer in the flow cell of the sequencer, and the 5' adapter is necessary for the reverse transcription and amplification of the template. After the RT-PCR and purification steps, the library is ready for sequencing.

1.4.2. Cluster generation by bridge amplification

Illumina utilizes a unique "bridged" amplification reaction that occurs on the surface of the flow cell. The single-stranded, adapter-ligated sample is added to the cell, where the 3' end binds to the single stranded oligonucleotides immobilized on the surface (**Figure B**). The free end of the ligated fragment "bridges" to the complementary oligo on the surface, and is exposed to repeated denaturation and extension. This way single molecules form millions of clusters of the same sequence on the surface of the flow cell.

1.4.3. Sequencing by synthesis

Solexa technology is based on cyclic reversible termination: this method comprises nucleotide incorporation, fluorescent imaging and cleavage of fluorescent group from the incorporated nucleotides (**Figure 1.7C**). The first cycle starts with the incorporation of the first fluorescent nucleotide, followed by high resolution imaging of the flow cell. The signal itself identifies the location of any given cluster on the cell surface, and the fluorescent emission identifies which of the four bases was incorporated. The nucleotides have a chemically blocked 3'-OH group, making sure that in each cycle only one nucleotide gets incorporated into any molecule. The next step is to cleave the terminating group and the fluorescent dye, and the cycle is repeated one base at a time.

It generates a series of images representing the order of nucleotides in the sequence.

Presently the useful Illumina reads range from 26 to 100 bases.
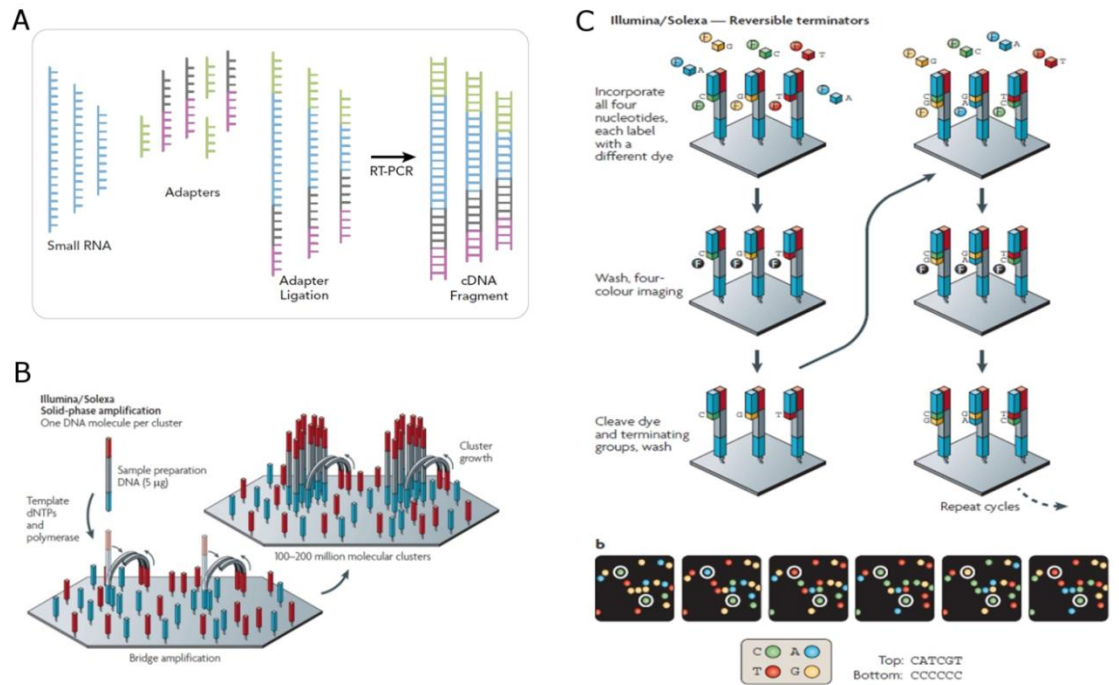
Figure 1.7 Overview of Solexa/Illumina sequencing **(A)**adapter ligation and preparation of the cDNA library **(B)** Solid-phase amplification of the cDNA library **(C)** Sequencing by synthesis. For explanation see text (source: A: Illumina v1.5 protocol manual, B, C: **(Metzker 2009)**)

2. Specific Aims

The main aim of this study was to discover what role RNAi plays in mammalian antiviral innate defence. Whether RNAi is a part of the innate immune system in mammals is not yet clear and this study attempts to answer a few key questions. Are viral small RNAs produced by Dicer in mammalian cells infected with viruses? How does the cellular miRNA expression profile change during virus infection? Does RNAi have any effect on virus replication? Our main approach was the use of state-of-the-art, high-throughput sequencing technology (Solexa/Illumina) to investigate the presence of viral small RNAs (vsRNAs), and to monitor the expression profile changes of cellular microRNAs (miRNAs).

The model system chosen was the alphavirus Sindbis virus, a single-stranded RNA virus, which is an arbovirus with a tropism for insect and mammalian cells. It has been previously shown that the primary mode of defence in the insect vector is RNAi, and vsRNA sequences mapping to the SINV genome were successfully isolated from insect cells. SINV is convenient for use in the lab as a class 2 virus which has no pathological effects on humans. Virulent non-attenuated SINV effectively suppresses the type 1 interferon response after infection in several cell lines, an important factor to investigate the RNAi response in the early stages of viral infection without the modulation of an anti-viral response by interferon, which induces translational inhibition and apoptosis.

In this thesis, the question of RNAi as antiviral defence in mammalian cells will be addressed by:

1. Characterizing the innate immune response to SINV infection in HEK293C cell line. I also studied the type I interferon response of HEK293C cells to several strains of SINV, and the apoptotic response to SINV strains to establish the time-frame of

apoptosis, as knowing the viral growth characteristics, effects on cell innate immunity and apoptotic processes are important for the sequencing experiments described in chapter 4. Since having accurate and fast virus titration was important to understand how host factors influence virus replication, I have developed an immunocytochemistry-based virus titration method that utilizes batch image-processing technology.

2. To investigate the effect of host factors on viral replication. We have chosen host factors that are important in innate immunity and in RNA interference. We have chosen to investigate IRF3 because it fulfils a central role in the type I interferon response. RNA helicase A was chosen because it was implicated in both antiviral defence, and as a factor important in the replication of several viruses, and it has been shown to be important in RNAi as well. Dicer was chosen because of its central role in RNAi; since mammals have only one Dicer gene, a knockout means the complete inhibition of the miRNA pathway, and partial inhibition of the siRNA pathway. (External siRNA fragments can be loaded onto RISC even in the absence of Dicer, however double stranded RNA will not be processed into small RNA.)

3. To find and characterize viral small RNA fragments in SINV infected mammalian cells using high-throughput sequencing technology (Solexa/Illumina), and to elucidate the changes in cellular miRNA expression profile of the cells during the early stages of virus infection. Should RNAi act as an antiviral mechanism in mammals in a similar manner as it does in plants and invertebrates, we expect to find large number of Dicer-produced vsRNA sequences mapping to the SINV genome. We also expect the abundance of several cellular miRNAs change in response to virus infection. We have chosen early time points because we were interested in how the cell reacts to the

invading virus while it is establishing itself, and before the innate immune response starts, inducing an antiviral state, translational shutdown and finally apoptosis in infected cells.

4. The results of the sequencing experiments showed that there are no SINV-specific svRNAs produced, and the miRNA expression profile of the infected cells does not change. Does RNAi work in virus infected cells? Exogenously added siRNAs have been shown to work efficiently to silence genes when added to human cells, demonstrating there is an intact RNAi machinery in humans. It is well known that gene expression is modulated by miRNAs in mammalian cells during development and tissue differentiation. Human cells express a single version of Dicer, which is responsible for biogenesis of both siRNAs and miRNAs. Despite of these reasons, my results demonstrate that RNAi does not act as an antiviral defence in human cells, unlike plants and invertebrates. I have set up a GAPDH knock down assay using GAPDH specific siRNA. This system was used to test several factors which might influence siRNA knock-downs. A pestiviral IFN inhibitor (N^{pro}), a dsRNA homologue (polyI:C), type I IFN, arsenate, RHA and SINV infection were used to test the activity of the RNAi system.

3. Materials and methods

3.1. Cells and Viruses

All cells were maintained at 37°C in 5% CO_2. HEK293C, DY8 cells (derived from human embryonic kidney isolate) were grown in DMEM-Glutamax (Invitrogen, Dulbecco/Vogt modified Eagle's medium) with 5% non-essential amino acids, 10% FCS and penicillin-streptomycin. BHK cells (derived from hamster embryonic kidney cells) were maintained in DMEM/F-12 (Invitrogen) with 5% non-essential amino acids, 10% FCS and penicillin-streptomycin. DLD-1 Wild Type and DLD-1 Dicer-/- cells (colorectal adenocarcinoma cell lines) were purchased from Horizon Discovery. They were cultured in DMEM/F-12 + Glutamax (Gibco, 31331), supplemented with 10% FBS and 1% Penicillin-Streptomycin. Four different SINV strains were used in this study (**Table 3.1**). AR339: the original SINV isolate. (C M Rice 1987) Sindbis Virus strain AR339 was acquired from Professor Diane Griffen, John Hopkins University via John Fazakerly, University of Edinburgh. Sindbis Virus infectious clones TR339 was a gift from William Klimstra, University of Pittsburgh, TR339-GFP was a gift from Raul Andino, University of California, San Francisco, Capsid-mCherry tagged strains was a gift from Beth Levine, UT Southwestern. TR339 is a consensus "wild-type" sequence, possessing no or minimal cell culture adaptations, representative of the original AR339 strain; more virulent than laboratory SINV strains (McKnight et al. 1996). TR339-mCherry strain is a TR339 strain with a mCherry tagged Capsid protein (**Figure 3.1A.**). TR339-GPF strain is a TR339 strain that has a GFP encoding gene inserted into the genome; this gene is controlled by the second subgenomic (26S RNA) promoter of the double subgenomic SINV vector pTE3′2J, and is not fused to any viral proteins (**Figure 3.1B.**). Rabbit anti-Sindbis polyclonal antibody was a gift from Sondra Schlessinger,

Washington University Medical School St Louis. This polyclonal antibody is an anti-E2

antibody, but it detects E1 and capsid proteins as well.

Table 3.1. SINV strains used in this study

Virus strain name	GENOME
SINV-AR339	Original Sindbis isolate, cell culture adapted strain. (C M Rice 1987) (McKnight et al. 1996, p.339; Attarzadeh-Yazdi et al. 2009)
SINV-TR339	Infectious clone of AR339 with tissue culture adaptations reverse engineered to resemble the original SINV isolate. (W. B Klimstra et al. 1999)
SINV-TR339-GFP	Same as TR339 with a GFP-encoding gene cloned into the genome (Saleh et al. 2009)
SINV-TR339-mCherry capsid	Same as TR339 with an mCherry tag fused to the Capsid protein (Orvedahl et al. 2010)
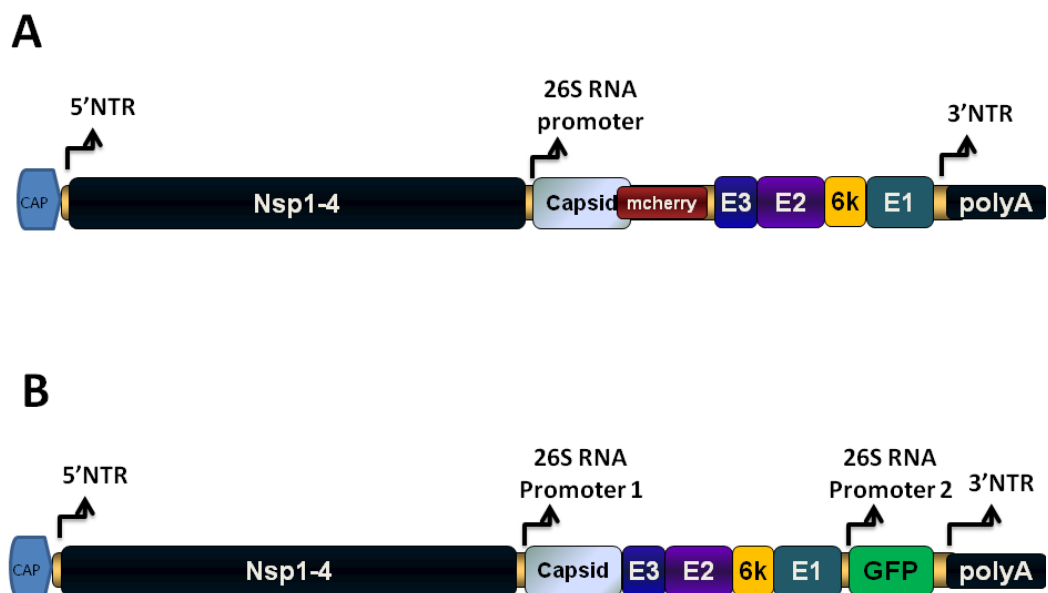
Figure 3.1. Structure of SINV TR339-mCherry and TR339-GFP. **A.)** SINV TR339-mCherry infectious clone carries an mCherry tag fused to the Capsid protein. **B.)** SINV TR339-GFP infectious clone encodes a GFP gene controlled by a second subgenomic (26S RNA) promoter.

3.1.2. Sindbis virus (SINV) production

All RNA and DNA samples were quantified using a NanoDrop instrument (Thermo Scientific). Plasmids containing the full length genome of different strains of Sindbis virus (TR339, TR339-GFP, TR339-mCherry) were grown in bacterial culture, plasmid isolated by standard technique using Plasmid Midi kit (Qiagen), and linearized with XhoI (New England Biolabs) (See **table 3.1.**). Infectious mRNA was transcribed *in vitro* using the mMessage Machine SP6 kit (Ambion). The mRNA was transfected into BHK cells using Lipofectamine 2000 (Invitrogen). The media was changed after 4 hours, and the cells were incubated for 48 hours (by the time all the cells displayed cytopathic effects and cell death). After incubation the tissue culture flasks were frozen to lyse cells, and the contents centrifuged at 3000RPM on a bench centrifuge to remove cell debris. The media containing virions was passaged on HEK293C cells repeatedly to adapt the virus to the cell line. AR339 strain was received as frozen virus stocks. Virions were detected by Western blot and immunostaining using an anti SINV antibody, or by using RT-PCR using SINV specific primers (see below).

3.1.3. Preparation of concentrated SINV stocks

SINV was concentrated by either ultracentrifugation, or polyethylene glycol (PEG-it; System Biosciences) precipitation. First the media containing the virus was centrifuged at 3000 RPM in a bench top centrifuge to remove the cell debris. The samples were pooled, and 35ml/tube were purified with centrifugation at 50 000g in an Optima XL-100k ultracentrifuge (Beckman) with a SW28 rotor for 4 hrs. The virion-containing pellets were resuspended in 0.5ml OPTIMEM media (1:50 concentration), and aliquots were frozen in -80ºC. Alternatively after removing the cell debris PEG-it was added to the media in a 1 to 5 dilution and the mixture was incubated at 4ºC overnight, then the precipitate collected by centrifugation with 3000g for 30 minutes.

3.2. Immunoflurescence

BHK and HEK293C cells were grown on 13mm coverslips, and infected with the various Sindbis virus SINV strains. The cells were fixed with 4% PFA at 2, 4, 8, 24 hpi, permeabilized in 0.1% Triton X-100, and blocked in 4% BSA. The cells were stained with anti-Sindbis virus antibody (dilution 1:500) for 60 min, and Alexa Fluor 488- or Alexa 594-conjugated secondary antibody (1:1000 dilution) for 60 min before being stained for 5 min with 4', 6'-diamidino-2-phenylindole (DAPI) (Sigma).

3.3. Virus Titration

BHK cells were grown on flat bottomed, black 96 well plates used for fluorescent imaging, and infected with a dilution series of the virus samples. After 8hpi the cells were fixed with 4% PFA for 10 mins at 2, 4, 8, 24 hpi, then permeabilized in 0.1% Triton X-100, and blocked in 4% BSA. The cells were stained with anti-Sindbis antibody (dilution 1:500) for 60 min, and Alexa Fluor 488- or Alexa 594-conjugated secondary antibody (1:1000 dilution) for 60 min before being stained for 5 min with 4', 6'-diamidino-2-phenylindole (DAPI) (Sigma).

Five random field of each well was imaged using an inverted microscope (Zeiss). The images were saved in .zvi format in Axiovision, and exported into 8bit grayscale TIFF files. These files were loaded into Cell Profiler for batch image analysis. Cell Profiler and Cell Profiler Analyst is open source software package for batch image processing and analysis. First the cells (their nuclei) were identified and counted using the DAPI channel images. To identify cell nuclei from debris and/or imaging artefacts, the software uses the pre-set size, shape and intensity values. The next step was to detect the presence of viral infection in cells, for which the signal intensity in the green channel was measured. The area used for measurement was defined as a diameter two pixels larger than the nuclei's. This was chosen because this way closely packed cells

would not give false positives should a SINV infected cell's cytoplasm be close to a SINV negative cell's nucleus. Additionally, for titration purposes the actual cell shape or the signal intensity is irrelevant –the protocol detects positive and negative cells. Because only a binary measurement was needed (positive/negative), background correction and further image processing before analysis was not necessary. (See pipeline in supplementary material.) The data was loaded into Cell Profiler Analyst, where the cells were sorted using machine learning. In short, randomly picked cells were sorted manually into positive and negative categories, and the program established the sorting rules. After repeated testing, the whole dataset was analysed, and exported into a .csv file. Alternatively, black 96 well plates were used, and integrated intensity of the fluorescence/well was measured using a FLUOstar Omega plate reader. The data in both cases was sorted and analysed using Excel. The TCID 50/ml values were determined using non-linear regression fit with Graphpad Prism 6.0.

3.4. One-Step Growth Experiments

One-step growth experiments were carried out as previously described.(Flint 2004) Cells were infected at high MOI (8<MOI) with Sindbis virus in a low volume. The cells were incubated for 30 minutes at 37°C, washed with PBS and cell culture medium, and incubated with fresh medium at 37°C. At regular intervals samples from the cell culture medium were collected to assess the biological activity of SINV over time. A dilution series was prepared from each sample, which was used to infect BHK cells plated in 96 well plates. At 8hpi the cells were fixed and stained for SINV, and the cells imaged using an inverted fluorescent microscope. The cells were counted and analysed as described in the previous section (Virus Titration).

3.5. Western Blots

Cells were purified by centrifugation, and lysed in hot SDS lysis buffer (1% SDS 10mM Tris pH 6.8 at 94˚C), The lysate was stored on -20°C. The samples were sonicated with 3 pulses lasting 10 seconds. The lysate was purified by centrifugation at 4°C for 10 min at 15 000 g in a table top centrifuge to remove cell debris. The protein concentration was determined using the BCA protein assay kit (Thermo Scientific). 50µg of protein per sample was mixed with loading buffer, denatured for 5 minutes at 95°C, cooled on ice, and loaded onto an SDS-PAGE gel (12%). Protein separation with gel electrophoresis was carried out for 2.5hrs at 100V. The proteins were transferred to FL PVDF membrane (Immobilon, IPFL00010) using the Bio-Rad Trans Blot Semi Dry Transfer Cell. The membrane was incubated with rabbit-anti SINV antibody (dilution 1:15000), and HRP conjugated goat anti-rabbit secondary antibody. The proteins were visualized using the Thermo Scientific SuperSignal West Pico Chemiluminsecent Substrate kit. Alternatively fluorescent tagged secondary antibodies were used with Odyssey reader (Li-Cor Biosciences).

3.6. RNA isolation

Trizol (Invitrogen) was used for routine RNA extraction for SINV and N^{pro} screening, total RNA isolation and small RNA isolation. Trizol was used according to the manufacturer's instructions. Cells were washed with PBS and lysed directly in the tissue culture dish with 1ml Trizol, and collected into 1.5 ml Eppendorf tubes. After 5 minutes of incubation 0.2ml chloroform was added, and the samples were vigorously mixed. After 3 minutes of incubation the mixture was separated using a table top centrifuge at maximum speed at 4°C for 15 minutes, and the aqueous phase containing RNA (top clear layer) carefully removed, and placed into a fresh tube. The RNA was precipitated using isopropyl alcohol (0.5ml/1ml Trizol used). The samples were incubated at room temperature for 10 minutes (for small RNA the samples were

incubated at -20°C in isopropanol overnight), and the precipitated RNA purified using a centrifuge at 12 000g for 10minutes at 4°C. The RNA pellet was washed once with 1ml 75% ethanol, and mixed by pipetting. The RNA precipitate is purified with centrifugation at 7.500g for 5 minutes at 4°C, the solution removed from the pellet, and dried for 10 minutes. The RNA was dissolved using 10-15µl RNase-free water.

The GenElute (Sigma-Aldrich) kit was used in applications where high purity RNA samples were needed, such as RT-PCR, northern blotting. The mirVana (Ambion) kit was used for isolating total RNA for the Illumina sequencing of small RNA, because the mirVana kit is ideal for the isolation of small RNAs.

3.7. RT-PCR, one-step RT-PCR

Primers for several targets were designed using the PerlPrimer software (Marshall 2004). (

Table 3.2) For RT-PCR reactions Superscript II (Invitrogen) and GoTaq (Promega) were used, following the manufacturers' instructions. The starting material was 1µg of RNA in all cases. For the screening for Sindbis and N^{pro} expression a One-step RT PCR kit (Qiagen) was used. A Veriti Thermal Cycler (Applied Biosystems) was used for all RT-PCR reactions. Verification of primers was done by sequencing of amplification products (TGAC BBSRC).

Table 3.2 **List of PCR primers**

Name		Sequence	Annealing Temperature (°C)
Sindbis (-) Strand	Forward	GGAAGTGCTTCTCGGAGCTT	60
	Reverse	CCCTGCGTACAACACCAACT	
Sindbis (+) Strand	Forward	TCAGCCTCCAATTAGATACAGAC	60
	Reverse	CTTTCAACAAGTGCCTTATACGG	
β-Actin	Forward	CACCACACCTTCTACAATGAG	55

(ACTB)			
	Reverse	GTGATCTCCTTCTGCATCCTG	
GAPDH	Forward	TGTTCCAATATGATTCCACC	50
	Reverse	CTGTAGCCAAATTCGTTGTC	
N^{pro} mCherry	Forward	ATGGAGTTGAATCATTTTGAACTTTTATC	60
	Reverse	GCAACTGGTAACCCACAATGGACA	
18S RNA	Forward	TGAGAAACGGCTACCACATC	60
	Reverse	TTACAGGGCCTCGAAAGAGT	

3.8. Nucleic acid transfections

Dharmafect 4.0 (Dharmacom), Lipofectamine 2000 (Invitrogen) and JetPrime (PolyPlus transfection) were all used according to the manufacturers' instructions. In brief, cells were plated at a plating density of 5.0×10^4 cells/ml a day before using antibiotic-free tissue culture medium.

In two separate tubes appropriate amounts (depending on the size of the tissue culture dish used) of siRNA and Dharmafect 4.0 was diluted in serum-free medium, and gently mixed with pipetting. After 5 minutes of incubation the contents of the tubes were mixed and incubated for an additional 20 minutes at room temperature. Sufficient amount of antibody-free medium was added to the tube. The medium was removed from the cells, and the transfection mixture was added. The cells were incubated for 24 hrs at 37°C.

Appropriate amounts (depending on the size of the tissue culture dish used) of Lipofectamine 2000 and DNA/RNA/siRNA was diluted in Opti-MEM medium in two separate tubes. The two tubes were mixed after 5 minutes of incubation in a 1:1 ration, incubated for a further 5 minute, and the DNA-reagent complex added to the cells. After 4hrs of incubation the medium was changed to antibody-free medium, to avoid the cytotoxic effects of Lipofectamine.

JetPrime, JetPrime buffer and nucleic acid (siRNA and/or polyI:C) was mixed according to the volume of the tissue culture plate used (values were from the JetPrime protocol), incubated for 15 minutes and then added to the tissue culture medium. Cells were incubated for 24hrs. Optimal siRNA and plasmid concentrations were determined experimentally. PolyI:C (Sigma, Roche) was used in a 50μg/ml final concentration.

3.9 Interferon Assays

Interferon assays were conducted using the luciferase expressing DY8 cell line, a gift from K. Fitgerald, U Mass, Worcester, MA. DY8 cells are HEK293C cells transfected with the luciferase gene under the control of three Interferon-Sensitive Response Elements (ISREs), which ensures that type I interferon signal leads to the production of luciferase in a dose dependent manner.

Supernatant from cell treated with SINV or polyI:C was heat inactivated at 50°C or UV inactivated (to inactivate SINV virions present in the tissue culture medium), and added to DY8 cells. The cells were incubated for 8hrs the supernatant. Over this time the type I IFNs released by cells treated with SINV/polyI:C activate luciferase expression controlled by ISRE present in the DY8 cells. After the incubation period DY8 cells were lysed, and the lysate was stored in -20°C until use. The luciferase assay was performed using 30μl of lysate with 30μl of luciferin substrate in a 96 well white plate. The luminescent signal was read using an EnVision 2103 multi-label plate reader (Perkin Elmer) at 590nm.

3.10. High Throughput Solexa sequencing

High-throughput sequencing was carried out as previously described (Szittya et al. 2008). Total RNA was isolated from the samples using the miRvana™ miRNA isolation kit (Invitrogen). The kit is formulated to isolate the small RNA population along with

total RNA combining the advantages of organic extraction with solid-phase extraction. The next step was the ligation of adapters of the Illumina kit on both the 3' and 5' end of the small RNA molecules using Illumina Small RNA Sample Preparation Protocol v1.5. This modified protocol was developed by Illumina to specifically enrich the library in miRNA and siRNA. The v1.5 small RNA 3' adapter is specifically modified to target microRNAs and other small RNAs that have a 3' hydroxyl group resulting from enzymatic cleavage by Dicer. Following this step the samples were amplified by an RT-PCR step with the adaptor-specific primers provided in the Illumina kit. The PCR product was separated on a native 8% PAGE gel, and stained with Ethidium Bromide. The bands corresponding to the adapter-ligated product (21-31 bp small RNA + 75bp both adaptors) were excised at the 100bp band of the ladder, and purified from the gel. This small RNA library was sent for sequencing to BaseClear, The Netherlands. Isolated small RNA populations were sequenced with the Illumina/Solexa Genome analyser (Mardis 2008; Metzker 2009; Illumina - Sequencing Technology).

3.11. Data analysis

Data analysis was performed by Dr Irina Mohorianu (Dept. of Computational Biology). The preliminary analysis of the sequenced libraries was conducted using the UEA sRNA Workbench (Stocks et al. 2012). The adaptor removal, quality check and genome matching were conducted as described by Irina Mohorianu et al. (2011). The accepted reads were mapped full length, with no mis-matches against the human genome, or full length with up to 2 mis-matches against the SINV genome. The normalization was conducted using the proportional scaling approach, "reads per million" (RPM) (Mortazavi et al. 2008). The identification of miRNAs was conducted using miRCat (S. Moxon et al. 2008), with standard parameters for human samples and miRprof using as input all mature and precursor sequences of miRNAs deposited in

mirBase (Griffiths-Jones et al. 2008). The statistical analysis of the properties of sRNAs was conducted in R using the standard *stats* package.

3.12. Northern Blotting

3.12.1. Total RNA blots

Total RNA was isolated from samples using either Trizol (Invitrogen), or the GenElute (Sigma-Aldrich). Electrophoresis, transfer and blotting were performed as previously described (Sambrook 2001). In short 5 micrograms of each RNA sample was resolved in a 1% denaturing agarose gel, and transferred to a nylon membrane (BioRad) overnight. After UV crosslinking the membranes were hybridised overnight in ULTRAhyb hybridisation buffer (Ambion) with ɣ-ATP labelled primer probes (incubated at 42°C), and imaged using Fuji phosphorimaging screen. Densitometric analysis of the northern blot images was carried out using QuantityOne (Bio-Rad) (**Table 3.3**).

Radioisotopes were purchased from Amersham, UK.

3.12.2. Small RNA blots

RNA from samples was isolated using either Trizol (Invitrogen), or the mirVana kit (Ambion). Electrophoresis, transfer and blotting were performed as previously described (Pilcher et al. 2007). In short 10 micrograms of each RNA sample was resolved in 15% denaturing PAGE gel, and transferred using the semi-dry method onto nylon membranes (BioRad). After chemical crosslinking the membranes were hybridised overnight in ULTRAhyb-Oligo hybridisation buffer (Ambion) either with ɣ-ATP labelled primer or LNA probes (incubated at 37°C) or with α-CTP labelled riboprobes (incubated at 64°C), and imaged using Fuji phosphorimaging screen (**Table 3.4.**).

Table 3.3. List of primer probes used for total RNA northern blotting

Probe name	Sequence
GAPDH probe	GGCATGGACTGTGGTCATGAG
SINV genomic and subgenomic primer probe sequence (position7568-7631):	GTATTAGTCAGATGAAATGTACTATGCTGACTATTTAGGACCACCGTAGAGATGCTTTATTTCC
18S RNA probe	TTACAGGGCCTCGAAAGAGT

Table 3.4. List of miRNA primer probes used for northern blotting

let7	AACTATACAATCTACTACCTCA
miR182	GTGTGAGTTCTACCATTGCCAAA
miR100	ACAAGTTCGGATCTACGGGTT
miR92	GGAGGCCGGGACGAGTGCAATA
miR378	GCCTTCTGACTCCAAGTCCAGT
miR424	TCAAAACATGAATTGCTGCTG
miR19	TCAGTTTTGCATGGATTTGCACA
miR34	ACAACCAGCTAAGACACTGCCA
MiR196	CCCAACAACATGAAACTACCTA
miR769	GCTCAGAACCCAGAGGTCTCA
miR197	GCTGGGTGGAGAAGGTGGTGAA
miR10	ACAAATTCGGTTCTACAGGGTA
miR378	GCCTTCTGACTCCAAGTCCAGT
miR29a	TAACCGATTTCAGATGGTGCTA
miR155	ACCCCTATCACGATTAGCATTAA
U6	TCATCCTTGCGCAGGGGCCA

4. Host Factors Involved in SINV Reproduction

4.1. Overview

The interaction between host and virus is crucial for successful replication. Host factors may be beneficial or detrimental for virus infectivity and replication. The expression or absence of host factors in cells governs whether the virus survives. This chapter describes the establishment of the virus infection model using Sindbis virus. Two immunocytochemistry-based virus titration methods were used to quantitate the virus. One is an imaging-based method that utilizes batch processing and machine learning, and the other is a fluorometric method based on multiwell-plate readers. I have used the titration methods I developed to investigate whether important cellular factors including Dicer, interferon regulatory transcription factor IRF3 and RNA helicase A (RHA) influence the replication and survival of SINV in HEK293C cells. Interestingly I have discovered important novel results which show that s that Dicer and RHA activity, but not IRF3 modulate the efficiency of SINV replication in mammalian cells.

4.2. Introduction

Sindbis virus is a widely used model system of virus-host interaction due to its wide host-specificity, simplicity of production and use. We have chosen it to study viral host interactions on the level or RNA interference, as it has been shown not to encode VSRs in mosquitoes, and as a single-stranded RNA virus, it offered the highest probability for production of vsRNAs.

4.2.1. Preparation and characterization of SINV stocks

In order to able to reproducibly infect cells with SINV at a consistently high titre in replica experiments, and to monitor the kinetics of virus replication, a fast and non-biased method for the characterization of SINV stocks was needed. In these experiments

different SINV strains were used, including AR339, TR339, and fluorescently tagged infectious clones SINV TR339 GFP and SINV TR339 Cherry Capsid (See **Table 3.1**), it was also important to determine if these strains had similar growth characteristics.

RT-PCR, immunocytochemistry and western blotting were used as sensitive methods to detect viral nucleic acids and replication in cells and viral proteins, respectively. SINV-GFP strain was used as a simpler method to detect viral infection, than immunofluorescence with an anti-viral antibody, as the fluorescent tag makes it possible to identify virally infected cells by observation under a fluorescent microscope. An advantage of SINVTR339-GFP over SINV TR339-mCherry was that the GFP is inserted into the infectious clone under the control of a second subgenomic promoter. Fusing fluorescent tags to viral structural proteins can have a negative effect on viral replication (**Figure 3.1**.). In the case of SINV TR339-mCherry infectious clone, the tag is fused to the capsid protein. This strain has a decreased replication rate, due to impeded capsid protein folding and assembly of virions. We have observed that this strain grows slowly, has a delayed response in apoptosis, and it also loses the mCherry tag with increased passage number in tissue culture.

4.2.2. Imaging-Based Virus Titration methods

The measurement of viral growth kinetics required a sensitive titration method. Because virus preparations contain imperfectly formed virions, called defective interfering particles (DI's), methods that measure the amount of viral RNA or protein (qRT-PCR, northern blotting, ELISA, western blotting) do not correspond with the infectious dose of virus (measured as TDIC 50). Biological activity is measured with plaque assays and endpoint dilution assays, both of which are expensive and time consuming, or not possible with non-plaque forming viruses, or viruses not causing cytopathic effects in their host cells.

Based on previous biological assays with the use of anti-SINV antibody, I developed two different methods to allow for a faster, easier quantitation of virus samples. Also, due to the use of computer-based batch processing, the observer bias has been reduced in these methods.

4.2.3. Virus-host interactions

To characterize some aspects of virus-host interactions, we have investigated the innate immune response to a positive stranded RNA virus (SINV) infection, and the effects of several host factors on virus replication.

4.2.3.1. SINV and Innate immunity

The main focus of this study is the way SINV interacts with the RNAi machinery, because it is not yet clear what role mammalian RNAi plays in antiviral defences. One hypothesis is that the evolutionary newer innate and adaptive immunity replaced RNAi, and it has only gene-expression regulatory roles in mammalian cells. To be able to assess how cell-autonomous innate immunity (the type I IFN response) works in mammalian cells in response to SINV infection, I have used luciferase interferon assay. It was important to understand the dynamics of host-SINV interaction for this study. I needed to make sure the cells were not in antiviral state at the time point when we assessed the activity of the RNAi system. The antiviral state, induced by interferons, is a complete translational inhibition in the cell, along with the induction of apoptotic pathways. It has also been reported that Dicer is down regulated in response to IFN stimulation (Wiesen & Tomasi 2009), pointing to the possibility that genes important in RNAi are down regulated, and RNAi is inactive in cells in antiviral state.

4.2.3.2. Role of Cellular Factors in virus replication

In order to understand factors that affect SINV replication and secretion, and which antiviral pathways may be inhibiting different aspects of the SINV life cycle, I have used

1.) a Dicer knockout adenocarcinoma cell line (DLD-1) because it was of special interest to find out how the virus replication kinetics changes if the cells have no Dicer present, as Dicer is a central part of the RNAi system.

2.) a viral protein, Npro, to deplete cells of IRF3, to suppress the IFN response and study the effects on SINV replication

3.) and siRNA to deplete cells (knock down) of RHA, to assess if it acts as an antiviral factor, or the opposite, a viral replication factor in SINV replication. (Both cases have been reported previously.) RHA is also important in RNAi, as it is an essential factor in RISC loading.

4.3. Results

4.3.1. Generation and characterization of Sindbis virus

4.3.1.1. Generation of Sindbis virus

An overview of the SINV generation can be found on **figure 4.1**. The plasmid encoding the infectious clones SINV-TR339, TR339-GFP and TR339-mCherry were linearized using XhoI (Rice et al), and transcribed using Ambion's mMessageMachine SP6 RNA polymerase kit (**Figure 4.2A**). The product mRNA (1µg) was separated on a native agarose gel to check for integrity (**Figure 4.2B**). BHK cells were transfected with 0.5 µg mRNA using Lipofectamine 2000 in a six well plate. The transfection reagent was removed after four hours, and the cells were incubated until the first cytopathic effects (cells rounded up and detaching) were observed. AR339 strain was received as

viral stock, and was used to infect BHK cells in a six well plate. In both cases after 48hpi the cell culture medium was collected, and cellular debris was removed by centrifugation at 3000rpm at 4°C. The virus was concentrated using one of two methods. Initially ultracentrifugation was used, and later concentration was performed using a polyethylene glycol system (PegIt) by SBI for cost effectiveness and simplicity. The protocol greatly simplifies virus concentration. The virus-containing medium is incubated overnight in a 1:5 ratio with PegIt at 4°C. This follows a centrifugation step using a table top centrifuge to achieve effective virus concentration. Both methods gave satisfactory results for virus concentration, but ultracentrifugation is more time consuming and there is a higher chance of contamination of the virus samples due to handling. PEG-It was developed by SBI to concentrate lentivirus stocks, but tests showed that it worked equally well with Sindbis virus.

4.3.1.2. Detection of Sindbis virus

SINV containing supernatant collected from BHK cells was subjected to serial passage through HEK293C cells to adapt the virus to efficiently replicate in a human cell line. It was important because high level of infection was needed in subsequent experiments. One-step RT-PCR, northern blot analysis, western blot analysis and immunocytochemistry were also used to monitor the accumulation of viral nucleic acids and proteins in infected cell samples for screening purposes (**Figure 4.2C, Figure 4.3, Figure 4.4, Figure 4.5**).

Northern blotting was carried out using the following protocol. HEK293C cells were infected with Sindbis virus at MOI=8.0 for 30 minutes. After the incubation period the cells were washed with PBS twice, and the medium replaced. The cells were collected at different time points post-infection, the RNA isolated and quantified with a Nanodrop instrument. The concentrations and the quality of samples were verified by

checking the intensities of the 18S and 26S RNA bands on a native agarose gel. For Northern blotting, 3µg from each time point was loaded onto a denaturing formaldehyde agarose gel, and blotted onto a nitrocellulose nylon membrane. After UV crosslinking the membranes were blotted using P^{32}- ATP radioactive labelled virus specific probes. **Figure 4.3** shows a positive strand specific probe labelled membrane. The probe is specific to the 26S subgenomic region of the genome, and detects both the subgenomic and full length genomes (position7568-7631). The double band on the blot represents the full length (49S) and the subgenomic RNA (26S). The time course shows that the virus has established an efficient replication by 4hpi, and the rate of replication increased dramatically by 8hpi.

The accumulation of viral proteins were monitored using Western blotting (**Figure 4.4**) and microscopy (**Figure 4.5**) (**Figure 4.6**) with the use of polyclonal antibody against the viral structural proteins.

GFP tagged Sindbis virus is readily detectable directly under a fluorescent microscope, simplifying screening, while non-tagged virus strains need to be stained using anti-SINV antibodies.
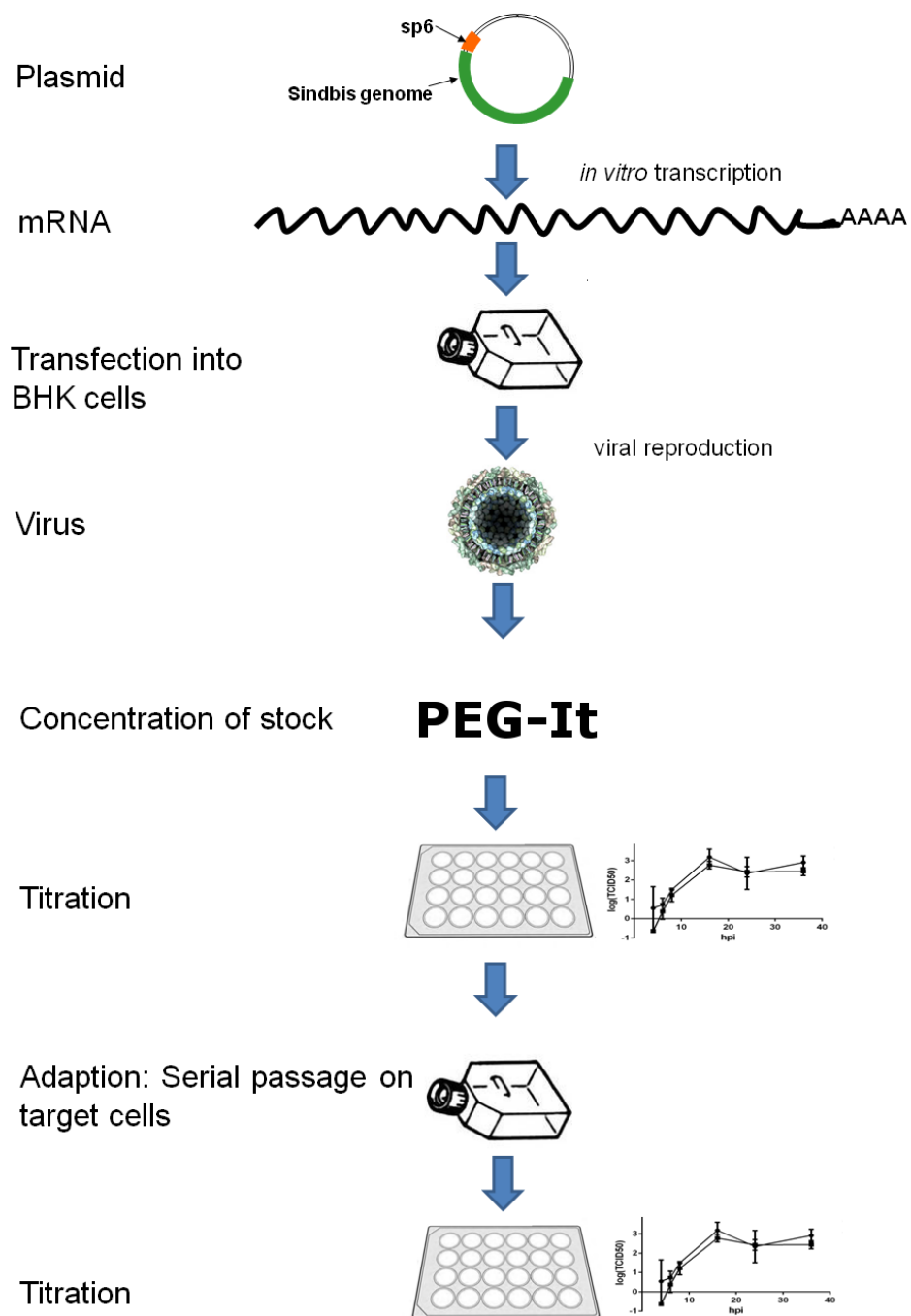
Figure 4.1 Overview of SINV generation using infectious clones. The plasmid carrying the DNA copy of the viral genome is linearized with a restriction endonuclease (XhoI), and the linear plasmid is used to transcribe mRNA. The mRNA is transfected into BHK cells, which translate the genome, and start producing virions. The virions are concentrated from the medium, and the biological activity of the stock is assessed using virus titration. The virus then is adapted to the target cell using serial passages until the virus reaches high enough titre, and the TCID50 (tissue culture infectious dose) is monitored.
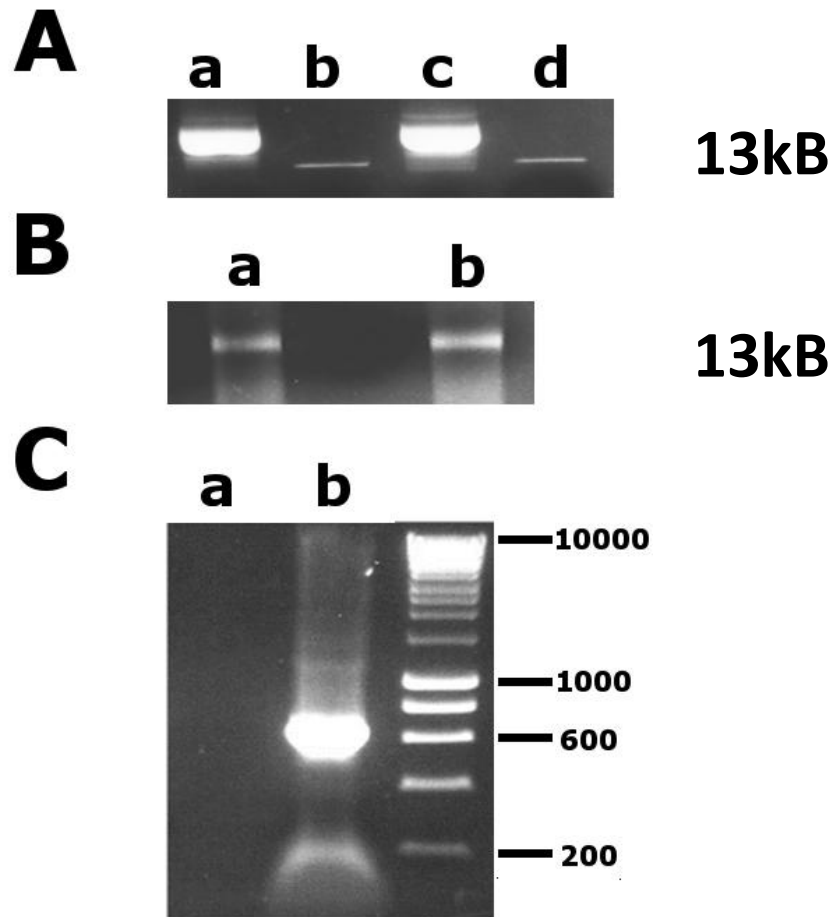
Figure 4.2 Production of SINV genome using infectious clones. A.) SINV infectious clone is linearized using XhoI restriction endonuclease. **a.)** SINV-TR339 plasmid, suprecoiled **b.)** SINV-TR339 plasmid, linearized with XhoI **c.)** SINV-TR339-GFP plasmid, supercoiled **d.)** SINV-TR339-GFP plasmid, linearized with XhoI. **B.)** SINV cRNA is transcribed from linearized plasmid encoding the SINV genome using the bacteriophage SP6 promoter. The resulting RNA was separated on a native agarose gel for quality check. **a.)** SINV-TR339 RNA product **b.)** SINV-TR339-GFP RNA product. **C.)** SINV virus detected in BHK cells after a passage of viruses, showing effective virus production. **a.)** RNA isolated from mock infected BHK cells **b.)** RNA isolated from SINV-infected BHK cells. The virus is detected using one-step RT-PCR and custom SINV primers (product size 600bp).
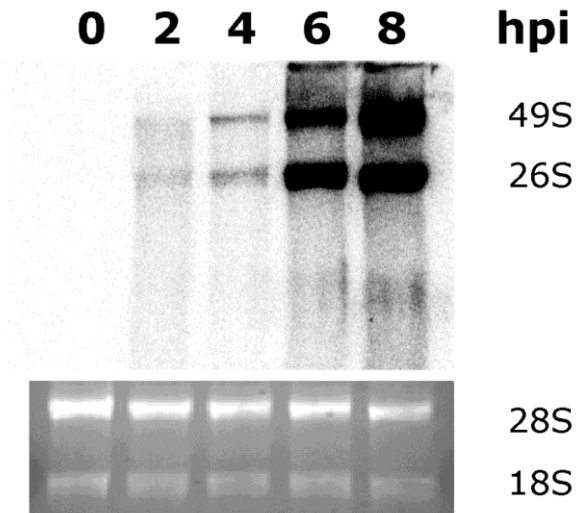
Figure 4.3 Time course of SINV replication in HEK293C cells. HEK293C cells were infected with SINV-GFP for 30 minutes at MOI >8 and the accumulation of SINV genome monitored using northern blotting. The upper band shows the full-length RNA (49S), while the lower band shows the subgenomic RNA (26S). The lower image is of the denaturing agarose gel prior to transfer, with the 28S and 18S ribosomal RNA bands, to show equal loading.
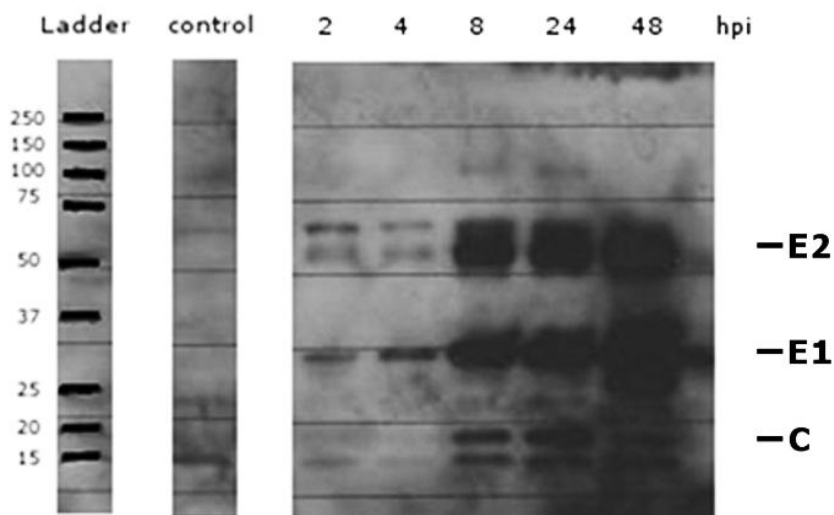
Figure 4.4 SINV replication over a time course of 48hrs in HEK293C cell. Western blotting with polyclonal anti- SINV antibody shows that the concentration of SINV proteins increase over time. The antibody detects E2 at 60kDa, E1 at 35kDa and C (capsid) at 20kDa.
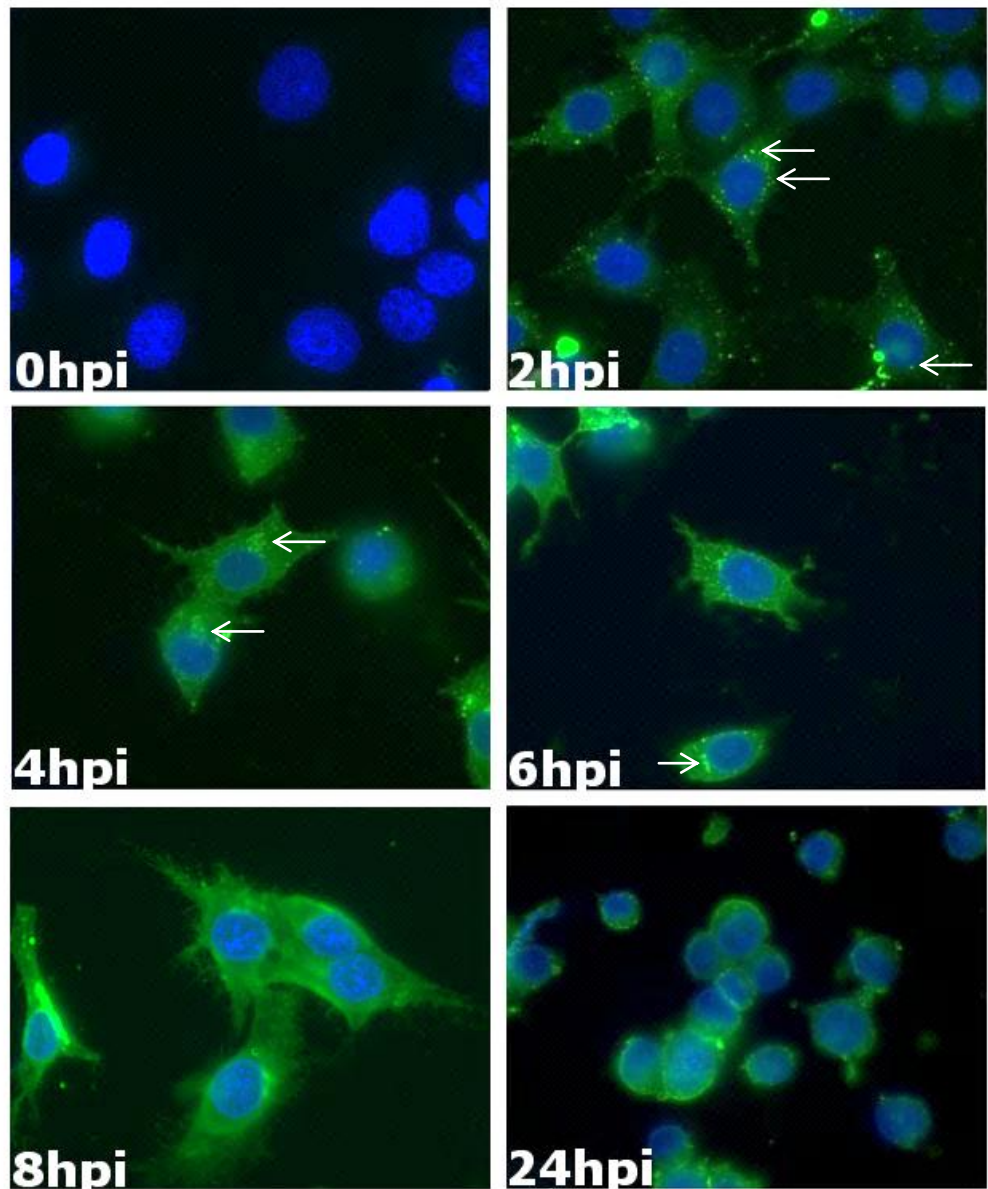
Figure 4.5. SINV effectively infects BHK cells, and cells die by apoptosis by 24hpi. BHK cells were infected and stained with anti-SINV antibody. (Blue: DAPI, green: anti-SINV antibody.) The first viral proteins appear at 2hpi, forming small puncta (arrows), and by 4hpi the replication centres are fully formed (arrows). The first burst occurs at 8hpi (as measured by one-step growth curve experiments, which corresponds to the literature as well), and the cells are rounded by 24hpi indicating cell death. By 36hpi all cells are detached.
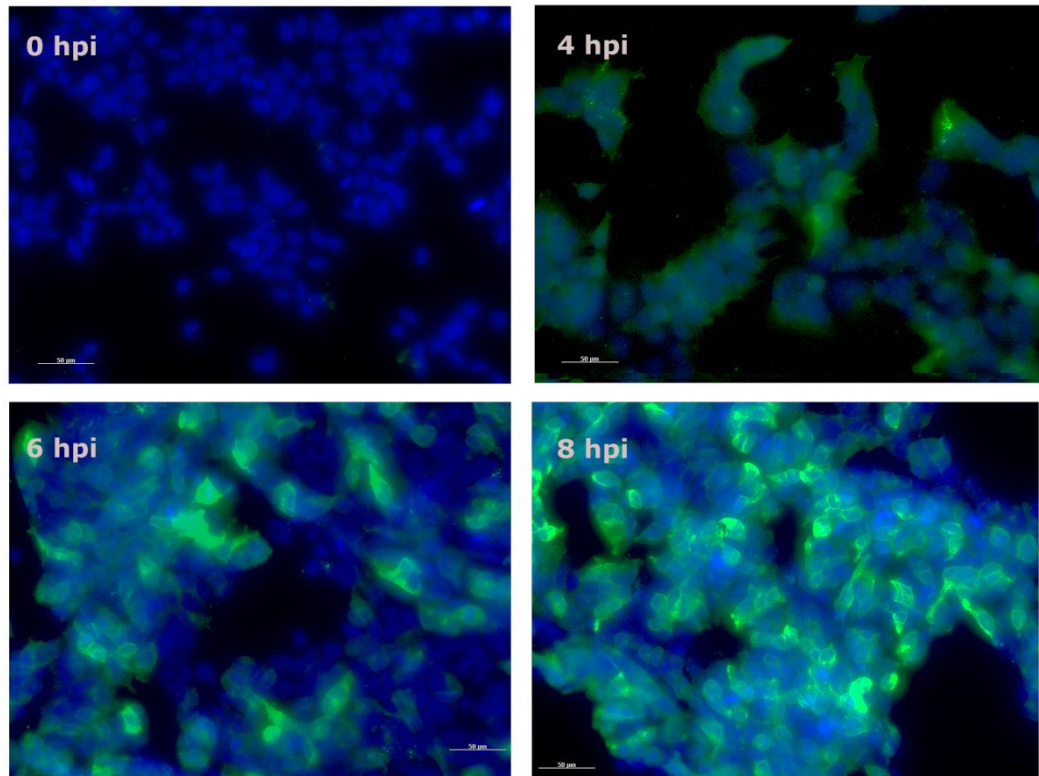
Figure 4.6. SINV passaged from BHK cells onto HEK293C cells replicate efficiently. SINV
AR339 was propagated on HEK293C cells for 3 passages. Cells infected with the adapted AR339 strain
were stained with anti-SINV antibody. (Blue: DAPI, green: anti-SINV antibody.) Virus replication is
already well established by 4hpi, but the apparent apoptotic effects only appear around 60hpi (not shown),
demonstrating that the dynamics of viral reproduction is different in different cell lines.

4.3.1.1. Titration of virus stocks

Recent advances in batch image processing made it possible to accurately count and quantify cells in large number of micrographs without human interference. I have utilized a freely available software package, Cell Profiler and Cell Profiler Analyst, to count and measure SINV stained cells in dilution series, and Graphpad Prism to calculate the TCID50/ml of the virus stock (A. Carpenter et al. 2006; CellProfiler Project; T. R. Jones et al. 2009).

The BHK cells were plated in 96 well plates and infected with SINV. Due to the low magnification used it was possible to use standard tissue-culture treated plates, instead of plating the cells onto individual cover slips. Black or white, flat bottomed plates provide better images of better quality, as they are designed for fluorescent microscopy. These plates, however, are significantly more expensive than plain tissue culture treated plates. The cells are infected with a dilution series of SINV stock / cell culture medium containing SINV, and incubated (**Figure 4.8-1.**). After eight hours of incubation the cells are fixed, stained using SINV specific polyclonal antibody and counterstained with DAPI. (8 hpi as was chosen because of practical reasons: viral proteins are already present in high abundance, and the virus has undergone only one round of infection at that time point.) The immunostaining steps can be automated using pipetting stations, reducing both the workload and the time necessary for the experiment. Using an inverted microscope (Zeiss Axiovert 135) at 10X magnification micrographs of 5 randomly selected fields of views (FOVs) were taken (**Figure 4.8.-2A**). To avoid bias the FOVs were chosen using the blue (DAPI) channel. This step can also be automated using a motorized stage and autofocus to take images from pre-programmed areas of the plate, which considerably reduces the workload. The individual channels in each of the resulting digital image files were exported into greyscale 8bit TIFF format (**Figure 4.8.-2B**). These images were analysed by Cell Profiler using a pipeline of actions that was

performed in the whole image set automatically (**4.8.-2C**). The threshold between background and nuclei on the blue channel images needs to be set for each batch of images analysed; hence high contrast images are desirable. Cell Profiler has modules that can perform background correction and other image processing steps should the quality of images require these, but ideally the image quality should be such that they can be omitted. Because cells can be tightly packed and their cytoplasm can be partially overlapping, it is sufficient and necessary to define cells as an area around the nuclei with a radius of the nuclei plus two pixels.

The software first identifies cell nuclei using the blue channel, and then measures the integrated fluorescence value on the green channel in the area defined as cells (radius of the nucleus plus two pixels). This data is fed into Cell Profiler Analyst where the cells are scored using a machine learning algorithm which can be "trained" using the actual image set. The training consists of manually sorting randomly selected cells into positive and negative categories, and instructing the software to set up the selection rules. Repeating this process several times will refine these rules. The accuracy of the selection criteria is verified by retrieving positive and negative cells from the image sets and checking them manually. Once the computer is able to accurately sort cells into positive and negative categories, the analysis is performed on the whole image set. The cells are sorted into positive and negative categories, and the data is exported in a .csv file (**Figure 4.8.-2D**). Finally Microsoft Excel is used to determine the percentage of infected cells per dilution, and Graphpad Prism 5.0 is used to calculate the EC50/ml value (which is the same as TCID50/ml in case of virus infection of cells) using non-linear regression fit.

4.3.1.1.1. Comparison of image processing methods with plate reader results

The quantitation of fluorescently labelled infected cells can also be performed using multiwell plate readers. For this method opaque (black or white) 96 well plates are needed with flat and clear bottom, as these plates are optimized for fluorescent microscopy. BHK cells were plated and infected similarly to the previous method, labelled with anti-SINV antibody, and the plates were read using a FLUOstar Omega multiwell plate reader (BMG labtech). The integrated intensity values of the dilution series were used to calculate the EC50 and the TCID50/ml value with Graphpad Prism. This method is considerably faster and requires less manual labour, however it is costly in equipment and consumables, as the specialized plates and plate reader are expensive. The results are similar with both methods when applied to the same samples (**Figure 4.9**).

1

control

non-diluted stock

1/10

1/100

1/1000

1/10000

2

A

merged image

B

blue channel

green channel

C

analysed images

D

Image Number	Total Cell Count	Positive Cell Count	Negative Cell Count
1	379	349	30
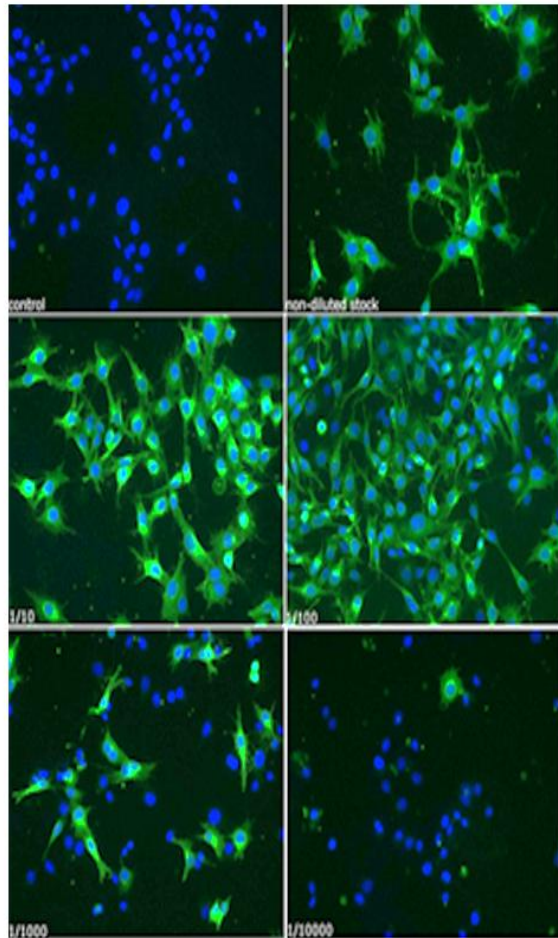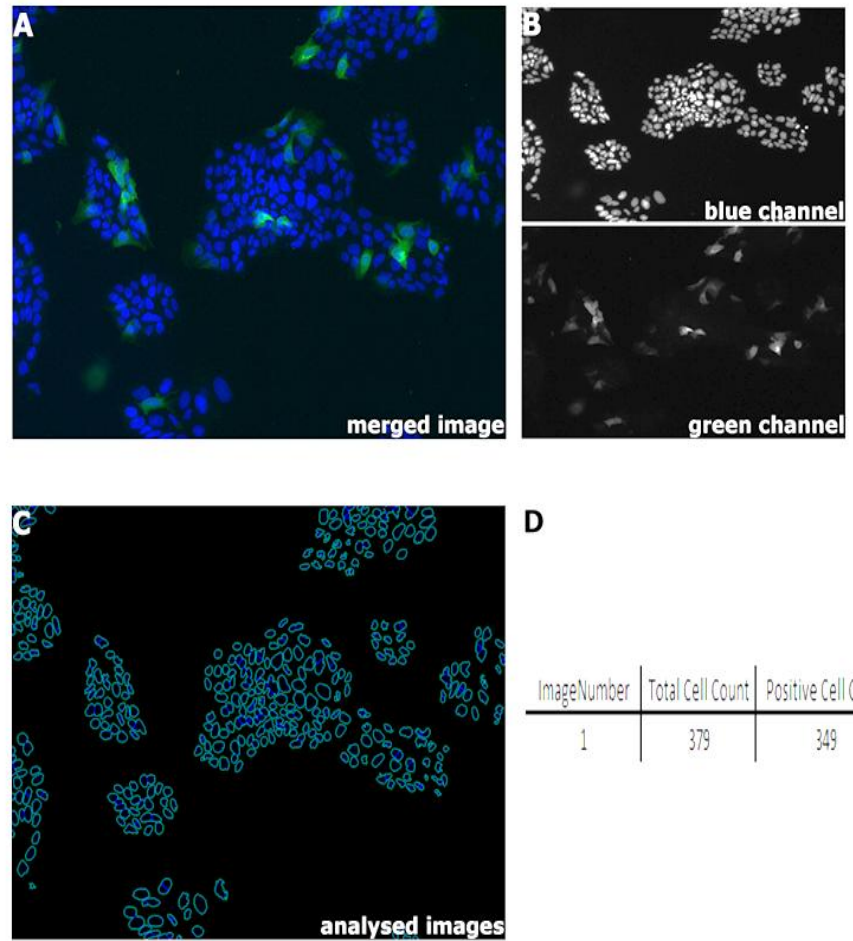
Figure 4.8 Titration of SINV AR339 infected HEK293C cells by automated image analysis with Cell Profiler. 1.) A dilution series is prepared from the medium of infected cells / viral stock, and used to infect BHK cells. 8hpi the cells are fixed and stained for SINV using anti-SINV antibody (blue: DAPI, green: anti-SINV antibody.) **2.A**) Images are taken of five random fields in each dilution using DAPI and GFP filters **2B**) the blue and green channels are loaded separately onto Cell Profiler, which identifies the nuclei using the blue channel and determines level of fluorescence in the green channels. **2C**) shows the processed images with the contours of the nuclei and the cytoplasm which is defined as the diameter of nuclei +2 pixels. **2D**) Data along with the fluorescent integrated intensity of the green channel is fed into Cell Profiler Analyst, which can sort the positive and negative cells after training (machine learning).
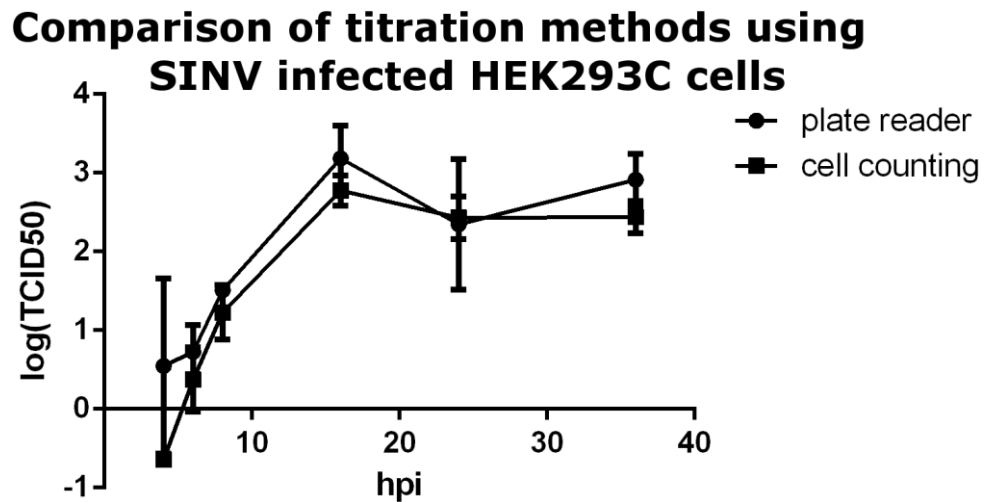
Figure 4.9 Comparison of one step growth curve experiments using imaging based virus titration and intensity measurement-based titration using multiwell plate reader. The same biological replicates were measured with imaging based titration and intensity measurements using mulitwell plate reader, and the results graphed. Both methods show the same result using the same sample which indicated good degree of reproducibility with either method.

4.3.2. Characterization of interferon response to SINV infection in mammalian cells

4.3.2.1. Sindbis virus does not induce type I interferon response in the first 24hrs after infection in HEK293C cells

The HEK293C cell line is permissible for SINV infection, and after adaptation high virus titre can be achieved which was deemed crucial for finding vsRNA sequences in the high-throughput sequencing experiments, which was an important selection factor for choosing it for the high-throughput sequencing experiments. SINV does not replicate well in DLD-1 cell lines, making this cell line a poor candidate for svRNA detection. DLD-1 cells were used for establishing the role of Dicer in viral replication because of the availability of Dicer -/- strain.

As a positive control for IFN induction I have used polyI:C. PolyI:C is a synthetic double stranded RNA homologue, and is detected by the innate immunity as dsRNA. Because dsRNA is a danger signal indicating viral replication (dsRNA is a viral replication intermediate, and it is a pathogen associated molecular pattern, or PAMP), polyI:C is used widely. The detection of polyI:C leads to the stimulation of the IFN pathway in most cell types. Cells expressing TLR3 can be stimulated with polyI:C exogenously; HEK293C cells lack TLR3 and polyI:C has to be transfected into cells.

Cell culture medium (supernatant) from HEK293C cells were collected 24hrs after transfection with a concentration series of polyI:C, and from cells inoculated with two different SINV strains (SINV AR339, TR339) in a time course experiment. After heat/UV inactivation of SINV present in the supernatant, it was added to DY8 cells for 8hrs, the cells were lysed and luciferase assays were carried out. Heat inactivation renders the virus incapable of replication, and it would not be able to infect the DY8 cells. It is important that the assay detects the IFNs present in the supernatant, and not

the IFN response of activated DY8 cells. Viral proteins and RNA were still present in the heat inactivated supernatant added to the DY8 cells.

DY8 cells are stably transfected with a luciferase gene under the control of three IFN-β promoters (ISREs), which act as a reporter gene for IFR-stimulation. Results obtained with the virus infected samples showed that while polyI:C effectively up regulates the expression of type I IFNs in a dose dependent manner after 24hrs, none of the SINV strains used triggered the type I IFN response at any time points (**Figure 4.9A-B**).

These results show that the production of type I IFNs is suppressed in SINV infected HEK293C cells at the early stages of the virus infection, and these findings are in line with previous studies (Frolov et al. 2012).

4.3.2.2. Sindbis virus induces apoptosis at 60hpi in HEK293C cells

SINV infection has been reported to trigger apoptosis in most mammalian cell lines through both extrinsic and intrinsic apoptotic pathways. One major apoptotic pathway activated by SINV is the caspase pathway (Nava et al. 1998). BHK cells show cytopathic effects (rounding and detachment) by 24, and by 32hpi most cell are detached. HEK293C cells show similar reaction after 3-4 days. Using the Promega Caspase-Glow 3/7 assay Caspase-dependent apoptosis was detected by 72hpi in HEK293C cells, these findings are in line with the observation that HEK293C cells will undergo apoptosis days later than BHK cells (**Figure 4.10**). These data shows that at early stages of SINV infection the apoptotic machinery is not activated, and degradation of RNA by apoptotic processes would not occur at 4 and 6hpi. Non-specific RNA degradation products would interfere with the high throughput sequencing of Dicer-generated sRNA population of infected cells. This was one of the main reasons to choose the 4 and 6hpi time points for high-throughput sequencing.

It is interesting to note the differences between two transgenic SINV strains. The SINV TR339 strain generated higher Caspase3/7 activity than the SINV TR339-mCherry strain. The mCherry tag interferes with the assembly of the virus capsid. The SINV TR339 and SINV TR339-GFP strains have similar characteristics as the GFP tag is not fused to any viral protein (data not shown). We have observed that over several passages the the mCherry tag is lost in the mCherry-TR339 strain, which also points to it being detrimental for viral replication.
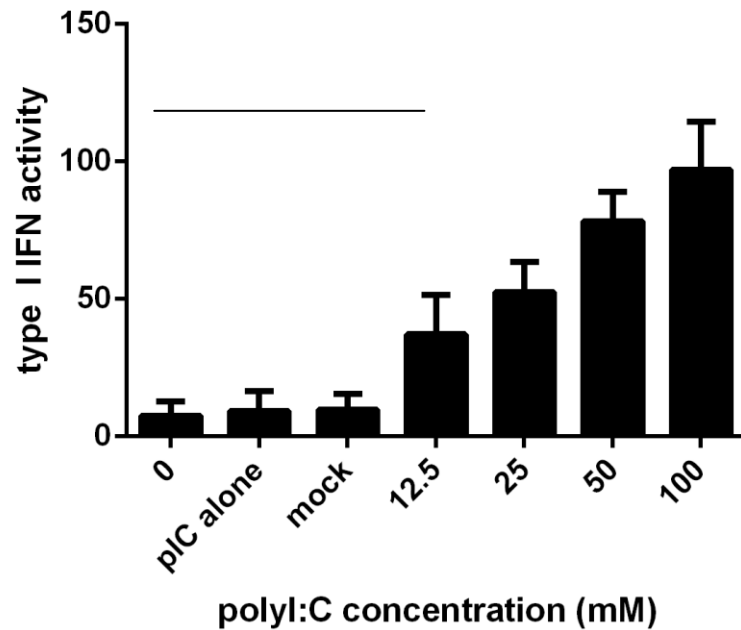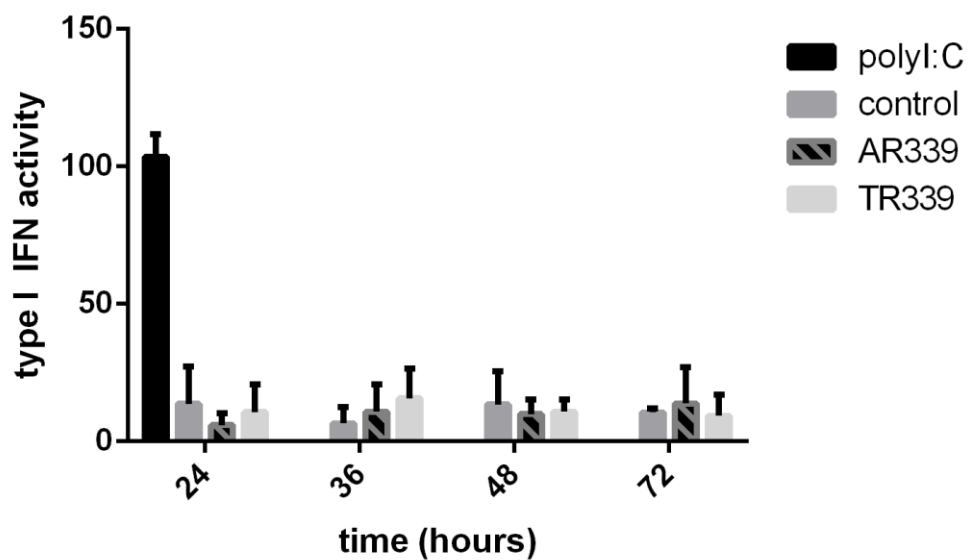
Figure 4.9 Type I interferons are induced in HEK293C cells by polyI:C, but not by SINV AR339 or TR339. A.) Double stranded RNA (polyI:C) effectively induces type I IFN expression in HEK293C in a dose dependent manner. Cells were transfected with polyI:C using lipofectamine and the IFN activity in the supernatant was measured with luciferase assay. The line above bars indicate groups which were not significantly different (Student's two tailed t-test) **B.)** Sindbis virus trains AR339 and TR339 do not activate IFN production in HEK293C cells. HEK293C cells were infected with SINV

AR339 and TR339 in a time-course experiment, and the IFN activity of supernatant measured by

luciferase assay.
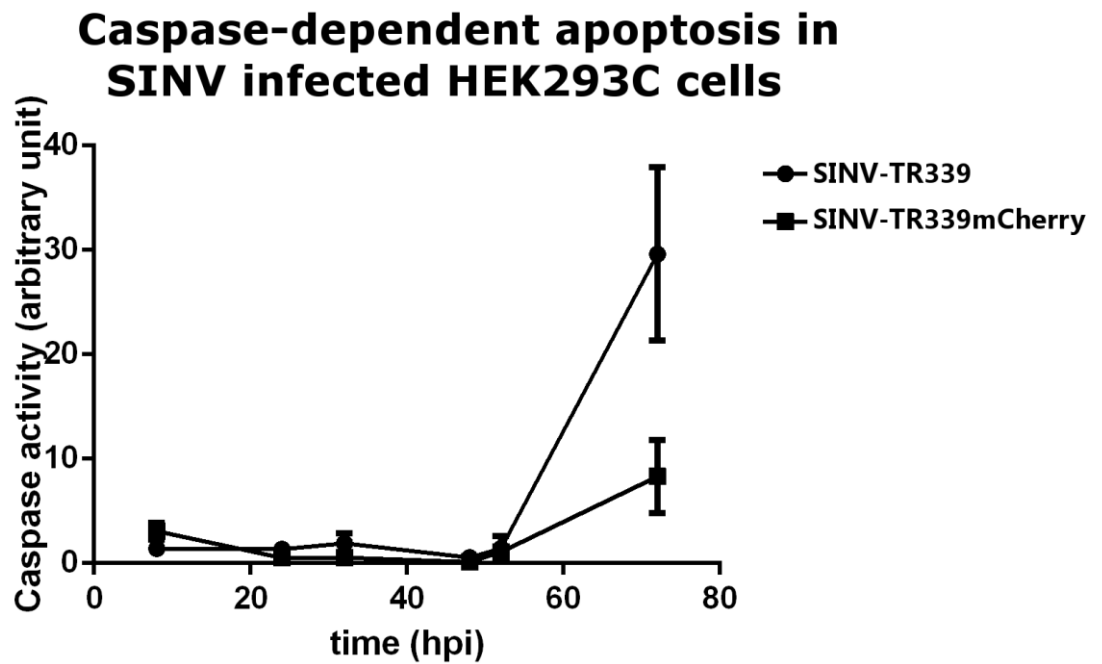
Figure 4.10 Sindbis virus triggers apoptosis in HEK293C cells in a 72hr period. HEK293C cells

were infected with SINV-TR339 and SINV-TR339-mCherry strains, and collected at 8, 24, 32, 48 and

52hpi. Caspase3/7 activity was measured using the Promega Caspase Glow3/7 assay, and the signal from

virus infected samples was normalized to the control and plotted against time.

4.3.3. Host factors involved in SINV replication

4.3.3.1. Dicer -/- cells are more permissive to SINV replication than the wild type control

Several cellular factors have been identified as potentially important in virus replication with a wide range of functions: signal transduction factors in innate immunity, cell cycle regulation, apoptosis, cell differentiation, as viral replication factors, etc. Because of the focus of this study, components of the RNAi system were of special interest. It was an important question to investigate if Dicer, one of the main effector proteins of RNAi, has any effect on SINV replication. Cells depleted of Dicer have been reported to be more permissive to viral replication, producing viruses in a higher yield than wild-type cells (Triboulet et al. 2007, p.-1). Dicer was also shown to be down regulated by several cellular stress signals and type I IFNs, demonstrating a connection between innate immunity and RNAi (Wiesen & Tomasi 2009). It was, therefore, a great interest to find out if Dicer has an antiviral role in mammals.

4.3.3.1.1. DLD-1 Dicer -/- cells have decreased miRNA expression profile

The DLD-1 colon cancer cell line which has a considerably reduced Dicer activity due to a mutation induced in exon 5 of the Dicer gene. Complete Dicer knockout usually confers a lethal phenotype in both cell lines and animals; the DLD-1 Dicer -/- cell line has a very low Dicer activity, which is under the detection limit of northern blotting (**Figure 4.11**).

4.3.3.1.2. DLD-1 Dicer -/- cells show increased viral RNA and protein accumulation

A time-course experiment showed between two and three fold increase of viral RNA accumulating in Dicer KO cells compared to their wild-type counterparts (**Figure 4.12**) using northern blotting on total RNA from a time-course experiment. The densitometric analysis of SINV-specific northern blot signals confirmed this result. Similar trend was

seen using microscopy: Dicer knockout cells were more permissible to virus infection in time course experiments. Using the same virus stock in control and Dicer -/- cell, twice as many Dicer -/- cells were infected with SINV virus over a 24 hour period (**Figure 4.13**).

4.3.3.1.3. Effective SINV replication is hindered in DLD-1 cells

To assess the dynamics of virus replication one-step growth curve experiments were performed on DLD-1 wt and Dicer -/- cell lines infected with SINV. The level of infectivity of the media collected from the two cell lines did not differ from each other significantly, indicating that the cells produced similar quantities of virions (**Figure 4.14**). This apparent discrepancy between these results and the results of previous experiments is not surprising looking at the graph of the one-step growth curve experiment. The curve is repressed, showing limited virus release; compared to other cell lines, the burst size is very small. (Burst size is the difference in TCID50/ml values between the eclipse phase, the first part of the virus replication, and the plateau phase, release of virus particles.) This result points to the possibility that while SINV can infect and replicate in DLD-1 cells, virus assembly and/or release is severely impeded in this cell line, which can indicate lack of essential cellular viral replication factors, or an effective immune response on behalf of the cell. The northern blotting and the microscopy results, however, suggest that SINV replicate better in the absence of Dicer.
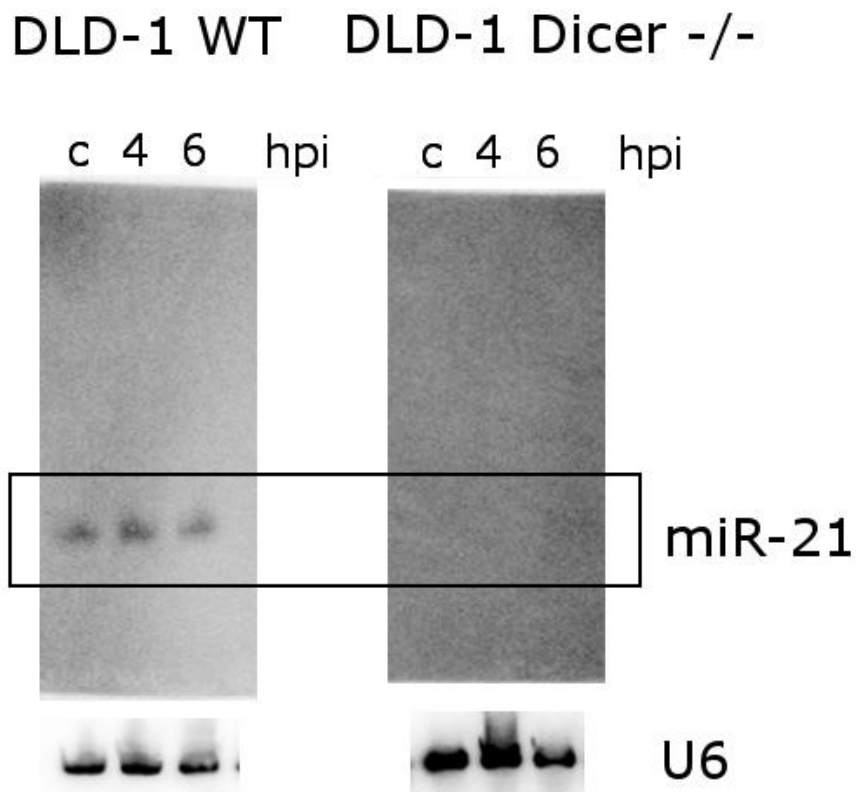
Figure 4.11 DLD-1 Dicer -/- cells have no detectable Dicer activity and do not express detectable amount of miRNAs. A SINV-infection time-course was prepared with both DLD-1 WT and Dicer -/- cell lines. The Northern blot hybridization of miR-21 specific primer probe shows that the level of miR-21 is under the detection limit in case of Dicer -/- cell lines. U6 blot is shown for equal loading.
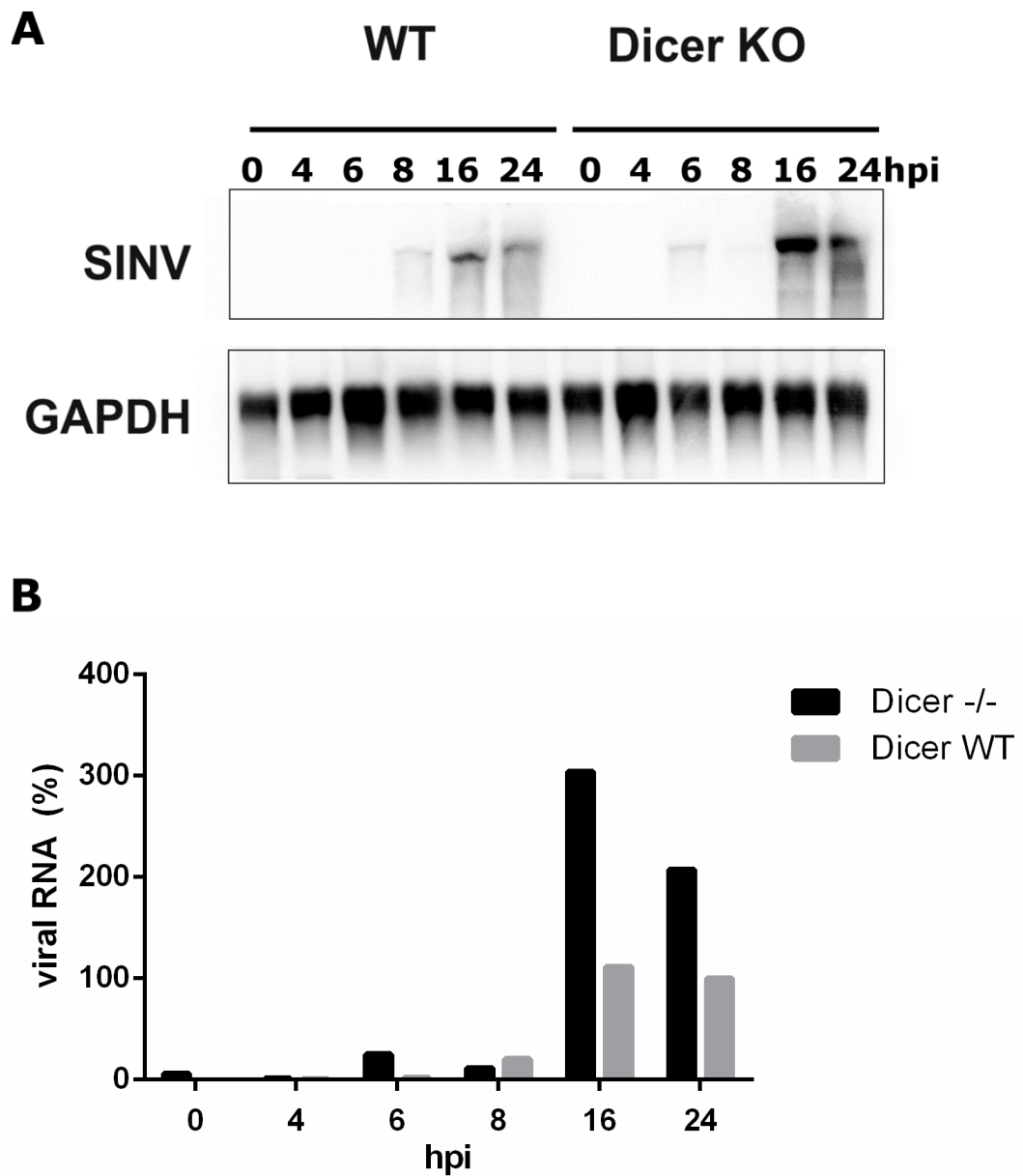
Figure 4.12 Effect of Dicer on the accumulation of SINV mRNA. A). SINV RNA accumulation in Dicer knockout and wild type cells over time. The Northern blotting experiment was performed using a positive strand specific probe. It shows higher levels of Sindbis RNA in Dicer knockout cells. **Lane 1-6** Dicer WT, **lane 7-12** Dicer -/- cells. GAPDH blot is shown for equal loading. **B**). Quantitation of the northern blot demonstrates that the level of Sindbis genomic RNA is 3x as high in Dicer knockout than in wild type cells. (WT sample at 24hpi was used as a 100% for comparison purposes.)

A

DLD-1 WT — 0hpi · 4 hpi · 6 hpi

DLD-1 Dicer KO

DLD-1 WT — 8 hpi · 16 hpi · 24 hpi

DLD-1 Dicer KO

B

Dicer -/- cells are more premissive to SINV infection

Legend: ■ DLD-1 WT, ▨ DLD-1 KO

Y-axis: % of infected cells

X-axis: time (hpi) — 0, 4, 6, 8, 16, 24
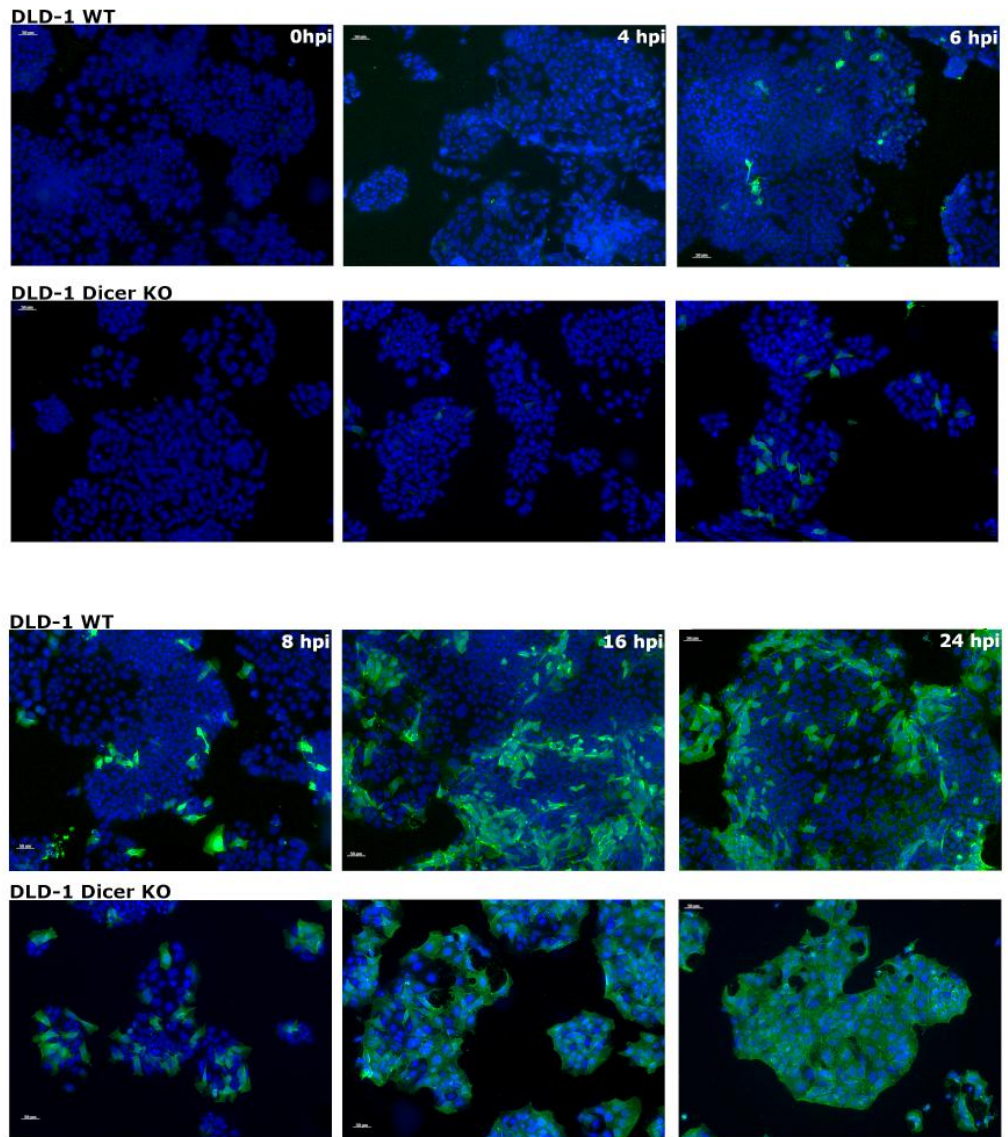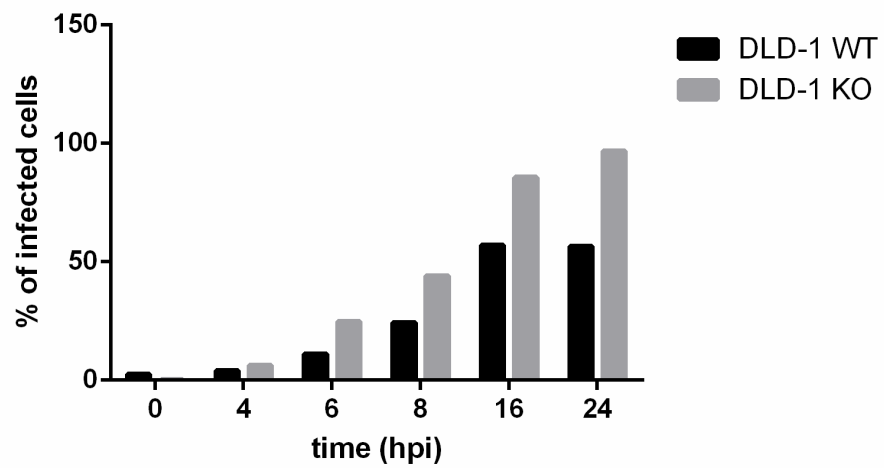
Figure 4.13 DLD-1 Dicer knockout cell are more permissive to SINV infection. **A.)** DLD-1 WT and Dicer KO cells were infected with SINV-GFP at high MOI, and fixed at different time points. Microscope images were taken at random locations. (Blue: DAPI, green: anti-SINV antibody.) **B.)** The cells were counted using automated cell counting; the ratio of infected cells was plotted over time. The accumulation of GFP (and virus proteins) was almost two-fold in Dicer knockout cells than in wild type. By the end of the 24hr time course all DLD-1 Dicer Knockout cells were infected, while only 54% of wild type cells were positive for SINV.
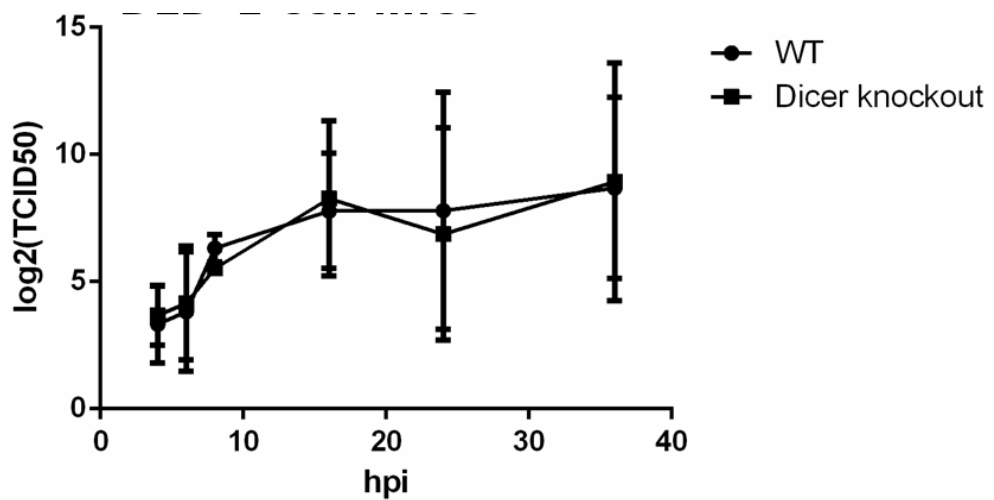
Figure 4.14 Effective SINV replication is hindered in DLD-1 cells. The one step growth curve shows SINV virus replicating in wild type and Dicer knockout cells. The suppressed exponential phase suggests that SINV virus replication is hindered in the DLD-1 cell line, as the amount of released, biologically active virions is very low.

4.3.3.2. The inhibition of IRF3 does not have an effect on SINV replication

Interferon Regulatory Factor (IRF3) plays a key role in the type one interferon response (**Figure 1.4**), and the absence of IRF3 should completely block IFN induction, thus we should observe an increased viral replication. IRF3 is also essential for apoptosis; cells lacking IRF3 have a decreased apoptotic response. Viruses are routinely propagated in cells that have deficient IFN response (e.g. Vero cells), and viral IFN inhibitors are also used to remove IRF3 or other IFN signalling components to make cells more permissible to viral replication (Hopps et al. 1963). These techniques are used to culture exotic viruses in cell culture environment. Transgenic animals lacking IRF3 or TBK are hypersensitive to virus infection due to the inactivity of the IFN response (Menachery et al. 2010).

Sindbis virus has been reported to suppress the interferon response early in the infection in many cell lines by unknown mechanism (J H Strauss and E G Strauss 2009; Byrnes et al. 2000; Klimstra et al. 1999; Nava et al. 1998; Ryman et al. 2007). Studies conducted using mice demonstrated the presence of type I interferons in the blood of the animals, indicating that the suppression of the interferon response is not complete and systemic (Nava et al. 1998; Ryman et al. 2007).

4.3.3.2.1. HEK293C cells are expressing N^{pro} when using transient expression system

N^{pro}, the N-terminal protease of the Pestivirus family, is a known IRF3 inhibitor (La Rocca et al. 2005). It induces the degradation of IRF3 in mammalian cells, and thus blocks the type I interferon response. I have used it to deplete cells of IRF3 and inhibit their type-I interferon response.

A plasmid carrying the mCherry tagged version of this viral protein was transiently transfected into HEK293C cells (**Figure 4.15A-B**.), and the effect of the absence of IRF3 on Sindbis virus reproduction was determined. Because N^{pro} is toxic for the cells,

it was important to determine the optimal amount of plasmid that can be transfected without killing them, and still achieving high degree of expression in this transient system. The mCherry tag offers a quick and easy way to observe the level of expression and the efficiency of transfection. One-step RT PCR was also used to monitor N^{pro} mRNA expression in the transfected cells (**Figure 4.15A**), and Western blotting made it possible to monitor the protein levels of N^{pro} and IRF3 (**Figure 4.15B**). As expected, the level of IRF3 decreased by the expression of N^{pro}.

4.3.3.2.2. IRF3 suppression has no effect on SINV replication in HEK293C cells

Wild type and mCherry-N^{pro} expressing HEK293C cells were infected with SINV-GFP, and the produced viruses were titrated using one-step growth curve experiments. The results show that the virus replication is not affected by N^{pro} (**Figure 4.16**). This finding suggests that Sindbis virus suppresses the type I interferon response in non-immune cell lines, in line with my previous results. By blocking the IFN response with the removal of IRF3, the additional suppression did not cause synergistic effects on viral replication. At this stage it is difficult to determine the role of IRF3 in antiviral defence against SINV. The lack of effect upon IRF3 inhibition suggests that if IRF3 is a host factor against SINV infection, it (or other signalling molecules in the IRF3 signalling pathway) may already be suppressed by SINV. This possibility will have to be explored in future research.
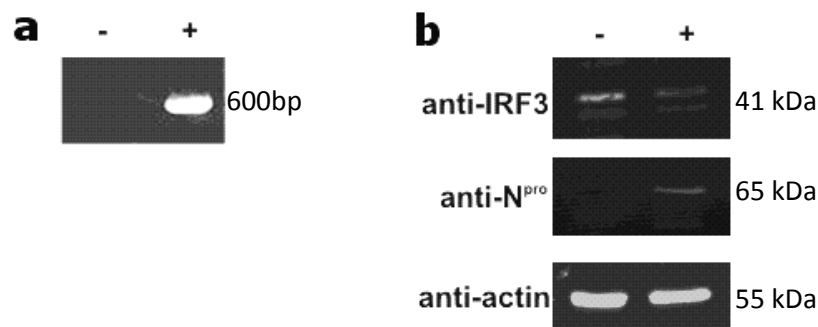
Figure 4.15 N^{pro} is present in HEK293C cells transfected with N^{pro} -mCherry plasmid. A.) mCherry-N^{pro} is present in transfected cells. The mCherry-N^{pro} plasmid was transfected into HEK293C cells, after 24rs the cells were collected, and the RNA was extracted using Trizol. One step RT-PCR was performed using N^{pro} primers. **B.)** N^{pro} mCherry suppresses IRF3 levels in HEK293C cells. HEK293C cells were transfected with mCherry- N^{pro} plasmid. After 24 hrs the cells were collected, washed in PBS and lysed with hot SDS buffer. The protein samples were ran on a 12% SDS-PAGE gel and probed with IRF3, N^{pro} and β-Actin antibodies. β-Actin is shown for equal loading.
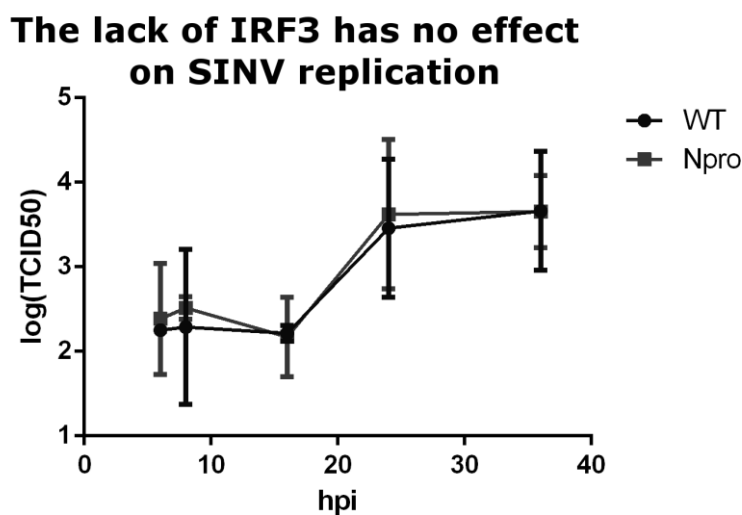
Figure 4.16 N^{pro} -therefore decreased levels of IRF3- has no effect on SINV replication in HEK293C cells. One step growth curve experiment was conducted on wild type and mCherry- N^{pro} expressing HEK293C cells. There was no difference in virus replication between the samples.

4.3.3.3. RNA Helicase A has antiviral effects during SINV infection

RHA is a multifunctional protein, part of the DExD/H box helicase family (along with Dicer and RLRs; **Figure 1.2**), that has diverse roles in transcription, translation, antiviral immunity (L. Lin et al. 2012), but also in RNA interference, as a factor important in RISC loading (Robb & Rana 2007a).

RHA shown to be a dsRNA sensor in myeloid cells, and the C-terminal domain was shown to interact with MAVS, suggesting that RHA links into the RLR pathway (Z. Zhang et al. 2011, p.9). It is an ISG and it has been shown to be phosphorilated by the dsRNA-binding kinase PKR, demonstrating the connection between RHA and antiviral immunity. (Sadler et al. 2009) It is interesting to note, however, that many virus use RHA as a replication factor; for example, RHA plays an essential role in the replication of foot-and-mouth virus (Lawrence & Rieder 2009), and it enhances influenza A virus replication (L. Lin et al. 2012, p.1). Our laboratory has demonstrated that RHA binds to N^{pro} (unpublished results), but the nature of the interaction is not yet clear. It was, therefore, of great interest to see what effect RHA has on SINV replication. RHA specific siRNA was used to deplete cells of RHA, to find out if it plays any role in the viral life cycle.

4.3.3.3.1. RHA levels can be successfully decreased with RHA-specific siRNA

HEK293C cells were depleted of RHA using RHA specific siRNA, and the knock-down was verified after 24hrs with western blotting with an anti-DHX9 antibody (**Figure 4.17**).

4.3.3.3.2. RHA has a negative effect on SINV replication

One-step growth curve experiment showed that SINV replication is significantly higher in RHA knockdown cells (**Figure 4.18**). This observed effect may be the result of an antiviral function of RHA, but another possibility is that it is due to the role of

RHA in RISC loading. RHA knock-down cells have impeded RNA interference response (Robb & Rana 2007a), which may help the virus replicate. Virus replication may be enhanced if no svRNA molecules are produced by the cell, and/or the cells are unable to alter their miRNA expression patterns in response to the virus infection. However my own findings (Chapter 6) suggest that the RNAi machinery is functional in RHA knockout cells, hence the observed difference in virus replication in RHA knockdown and wild-type cells is probably not due to suppressed RNA interference system. These novel results points to potential antiviral roles of RNA helicase A during SINV infection.
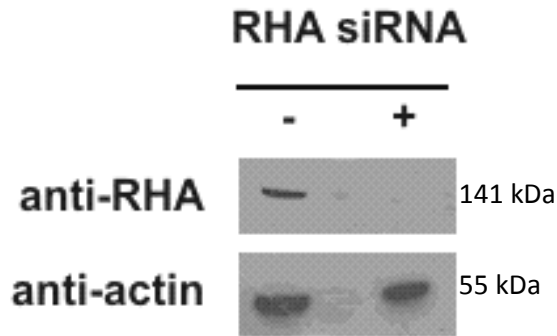
Figure 4.17 RHA protein levels decrease using RHA siRNA (western blot). RHA-specific siRNA was transfected into HeLa cells, and the cells lysed 24hrs post transfection. RHA was detected with Western blotting using anti-RHA antibody.
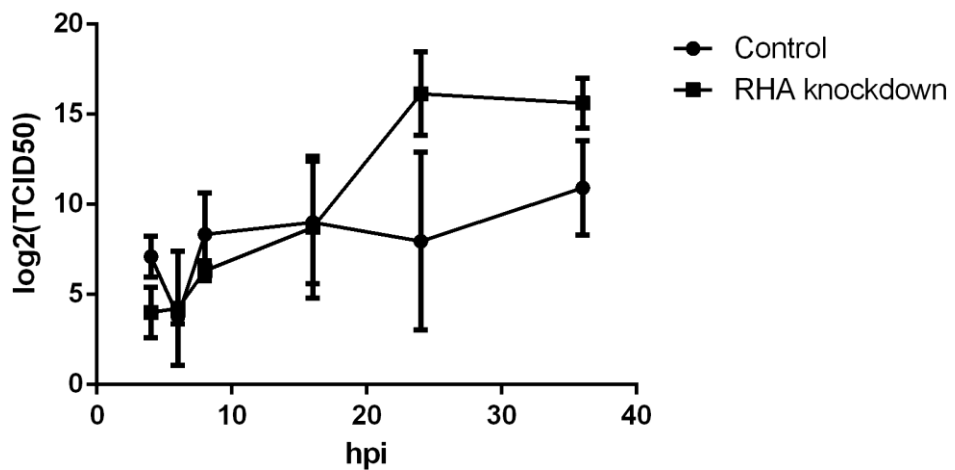
Figure 4.18 RHA has a negative effect on SINV replication. One step growth curve experiment was conducted in both wild type and RHA knockdown HEK293C cells. After 16hpi the knockdown samples had significantly higher levels of virus present in the medium (student's two tailed t-test).

4.4. Discussion

4.4.1. Virus Titration

For the quantitation of viral particles produced in cells I have developed both an image-based titration method and a multiwell-plate reader based titration method. These methods offer several advantages over the traditional TCID50 and plaque assays currently in use. The main reason behind the development of these methods was that they do not require the virus to form plaques. This means they can be performed in a wider variety of viruses than the traditional assays would allow. The only requirement is the availability of specific antibodies.

These assays also require less time, as it is not necessary to wait for visible plaque or cytopathic effects to develop; as soon as the viral proteins are translated, the assay can be employed. They are highly automatable and reduce workload considerably. Since the computer does the counting according to pre-set criteria, the observer bias is greatly decreased. Bias is always an issue with the evaluation of TCID50 assays, as they depend on the person's judgment conducting the study. Automated systems, depending on the degree of automation used and the method chosen, are cost effective as well.

4.4.2. The relationship between Sindbis Virus and the Innate Immunity

The interferon assay based on cells expressing ISRE-controlled luciferase gene is a very sensitive assay to detect type I interferons from tissue culture medium. This assay showed that HEK293C cells are responding to double stranded RNA with production of interferons, while SINV infection did not trigger IFN production. Carrying on with this line of the investigation, Jasmine Buck and Stephen Lewis working in our laboratory demonstrated that while SINV infection does not up regulate type I IFN gene expression, several innate immunity genes (RLRs, interferon-independent cytokines) are up regulated (data not shown).

Sindbis virus causes an acute infection and triggers apoptosis is most mammalian cell lines, while it is a persistent chronic infection in its vector. The cytopathic effects were clearly observable on BHK cells after 24hpi, but HEK293C cells only underwent apoptosis at 60-72hpi as detected by a Caspase 3/7 activation assay, demonstrating that virus-cell interactions are dependent on both the virus and the host cell, and can be very different.

4.4.3. Cellular factors and SINV replication

The imaging based virus quantitation protocol made it possible to monitor the dynamics of virus replication using one-step growth curves. The cells were infected at MOI>8 at the same time point, and after 30 minutes of incubation the media was replaced, making sure that all cells are infected at the same time. The cell culture media was sampled at different time points, and the amount of viral particles determined in each sample. This method can detect when the first virus particles are released from the host cells, and how big the viral load is, giving an accurate picture of viral replication kinetics. Comparison of these values acquired from different experimental systems help us understand the potential effect of any cellular factor, mutations in either the host or viral genome, or any given treatment have on the replication of virus.

4.4.4. Effects of Dicer on viral replication

Dicer is one of the key members of the RNA interference machinery, and is responsible for producing the small 20-24 mer RNA duplexes (miRNAs) from their progenitors (pre-miRNAs), which are loaded onto the RISC complex and consequently used to target their complementary sequences. It is also responsible for processing dsRNA into siRNA fragments; in this, mammalian cells greatly differ from plants and invertebrates which usually have more than one Dicer homologue.

DLD-1 WT and Dicer -/- cells were infected with SINV-GFP, and subjected to several experiments. Time course northern blotting, time-course imaging and one-step growth curve experiments were performed to understand the effect Dicer has on the virus replication.

As the DLD-1 Dicer knockout cell line grows slower than the wild-type control, it needed to be seeded at a higher density (1.5X) a day prior to experiments. This ensured that the amount of cells in control and Dicer -/- groups were similar. First, a time-course of SINV infection was carried out. At different time points the cells were fixed with 4% PFA, and stained for SINV using a polyclonal anti-SINV antibody. With the help of batch image processing technology, an average of 70 000 cells/experiments were counted and sorted into positive and negative groups at different time points. The results show that infected with the same MOI<8, Dicer-/- are more permissive to virus infection; the virus protein translation starts earlier, and more cells are infected than in the control group.

RNA from similar time course experiments was used for northern blotting as described previously, and probed for SINV with SINV specific radio-labelled primer probes. The blots show a similar trend: the accumulation of viral genome in Dicer -/- cells is double than in the control. The one-step growth curve experiment, however, showed that the dynamics of virus production is not altered in Dicer -/- cells. The curves of the wild type and the Dicer -/- cells were indistinguishable from each other. As discussed previously, the curves also show that the virus is not replicating well in this cell line. The curve is depressed, and indicates that despite of the production of viral nucleic acids, as shown by the northern blot, and viral proteins, as shown by the imaging experiments, very few virus particles are actually released. While the nucleic acid and protein accumulation testifies that the absence of Dicer does have an effect on

virus replication, this does not translate into increased biological activity. The reason for this is most likely the cells are mounting an effective immune response against the infection.

There are several possibilities how Dicer can influence virus replication. The first possibility is that Dicer detects and processes virus replication intermediates into svRNA, and loads them onto RISC where they are used to repress the expression of the virus genome. This has been demonstrated in mosquitoes, the vector organisms of the virus. (Campbell et al. 2008) The second possibility is that the lack of Dicer changes the miRNA expression profile of the cell, and makes it more susceptible for virus infection; several microRNAs have been shown to possess antiviral capabilities (C. H. Lecellier et al. 2005; Muller & J. L. Imler 2007). Dicer, being a DExH/D helicase, may have hitherto unknown functions in the cell as well. It may have PRR functions, as it does in plants and invertebrates. Another possibility is that simply the lack of Dicer makes the cells less able to mount an effective antiviral response at the replication stage at the viral life cycle, due to their severely impaired cellular machinery, and decreased viability -to which their slower growth rate may be attributed to.

4.4.5. The inhibition of Interferon Response Factor 3 has no effect on virus replication

IRF3 is a central member of the type-I interferon response, and a very frequent target of viral IFN suppressors. The central role of IRF3 can be demonstrated by inhibiting it; the activation of IF-β transcription becomes repressed, suppressing the whole type-I IFN response.

I have used a viral inhibitor of IRF3, N-terminal protease (N[pro]) from the classical swine fever virus family, to deplete HEK293C cells of IRF3. N[pro] is a multifunctional cystein protease which has no known homologues in any other organism. By degrading

IRF3, it effectively blocks the IFN response, thereby aiding the viral reproduction (La Rocca et al. 2005; Bauhofer et al. 2007).

There are several possible approaches for generating N^{pro} expressing cell lines. I have used lentiviral vectors to incorporate the mCherry- N^{pro} expressing gene into the cellular genome. I have also used plasmids encoding N^{pro} to create a stably expressing cell line, with a selection agent added to the cell culture medium. I have found that over time cells down regulate N^{pro} expression, regardless of the manner of delivery of the gene, and hence the generation of stably expressing cell lines was met with difficulties. For reproducible results the cells need to express N^{pro} in a dependable fashion at high level. Because N^{pro} encoding plasmids are easy to generate in large quantity using bacterial culture, it was decided to use fresh, transient transfections 24 hrs before each experiment. Transient transfection thus ensured that the level of N^{pro} expression was always the highest possible, once the optimal plasmid concentration was determined. Because the results from repeated experiments were conclusive and similar, the possibility of slight changes in transfection efficiency in different experiments did not present any problems.

The ratio of successfully transfected cells was easily monitored by microscopy, as the mCherry tag is readily detectable in live cells, and western blotting demonstrated that the level of IRF3 is decreased in N^{pro} transfected cell lines, proving that the mCherry tag does not interfere with the function of N^{pro}.

The one-step growth curves, however, show that IRF3 (and N^{pro}) has no effect on Sindbis virus replication.

4.4.6. RNA Helicase A has a negative effect on SINV replication

RNA Helicase A is a member of the DExD/H box helicase family characterized by the conserved motif Asp-Glu-Ala-Asp (DEAD) motif; the same family Dicer and the

RIG-I like receptors are members of. It has been implicated in many cellular processes, including transcriptional regulation, embryogenesis, cell growth, innate immunity and RNA interference (Fuller-Pace 2006; Sadler et al. 2009; Robb & Rana 2007b).

Studies showed that RHA plays an essential part in RISC loading, and thus have a central role in RNA interference (Robb & Rana 2007b). RHA has been shown to be an important antiviral host factor (Fuller-Pace 2006), and also in case of certain viruses, a viral replication factor, including classical swine fever virus, influenza and foot and mouth disease (Sheng et al. 2013; Lawrence & Rieder 2009; L. Lin et al. 2012).

One-step growth curve experiments performed on RHA-depleted and wild-type HEK293C and HeLa cells have shown that RHA depleted cells are significantly more permissible to viral replication than the wild type controls. This novel result points to the possibility of RHA plays an antiviral role during SINV infection. An alternative explanation is that by inhibiting RISC loading, it renders the RNAi machinery inoperable, making it possible for the virus to replicate better in these cells. Chapter 5 and 6 will explore RNA interference in virus infected cells further, but the exact method of how RHA inhibits alphavirus replication needs to be examined in the future.

5. Detection of small viral RNA and miRNA profile changes in SINV infected mammalian cells

5.1. Overview

In this chapter I describe the use of next generation sequencing technology (Solexa/Illumina) to attempt to detect SINV originated vsRNA fragments, and to characterize the changes in the host miRNA expression profile. The chapter also describes the validation of sequencing data. Unexpectedly, Solexa sequencing showed only a very few number of potential vsRNA sequences mapping to the SINV genome, and further analysis suggested they were products of random degradation rather than Dicer products. The RNAi machinery is present in mammalian cells, and our hypothesis was that it would process viral replication intermediates in the cytoplasm; however, it does not seem to be the case. None of the detected vsRNA reads could be validated by northern blotting due to their extremely low abundance. The overall expression profile of cellular microRNAs did not change according to the bioinformatics analysis, which was verified by northern blotting on selected human miRNA sequences. The bioinformatics analysis was performed by and the results written with Dr Irina Mohorianu, RNA Computational Biology group at the University of East Anglia.

5.2. Introduction

The focus of this study is to elucidate the connection between the mammalian RNAi system and invading viruses. In other organisms where RNAi has been shown to be part of antiviral immunity, the presence of vsRNA fragments was demonstrated during virus infection (Carol D. 2011; Gordon & Waterhouse 2006; Z. Xie et al. 2004). While the mechanism can differ between plants and invertebrates, one thing is common in all cases: large amounts of virus-derived small RNA sequences are detected in virus

infected cells. If similar mechanism is active in mammalian cells we expect to see similar enrichment in vsRNA sequences over the course of virus infection. To date only one study attempted to systematically explore RNA virus and mammalian cell interactions using high-throughput sequencing (Parameswaran et al. 2010). We have adopted a similar approach using the 1.5 version of the Solexa/Illumina technology, and Sindbis virus, an arbovirus, as a candidate. SINV was chosen as it has been shown to trigger antiviral RNAi response in its vector organisms, the members of the Culex mosquito genus, and it has been shown not to encode RNAi suppressors in these organisms (Campbell et al. 2008). SINV also has very broad host specificity, making it easy to grow in a wide range of mammalian and insect cells.

Another possibility of interaction between viruses and their host cells is the modulation of the cellular miRNA expression profile by either the host or the virus itself. RNA viruses (aside from retroviruses) have to date not been shown to encode microRNA sequences (C. H. Lecellier et al. 2005; Muller & J. L. Imler 2007; Umbach & B. R. Cullen 2009; Saumet & C.-H. Lecellier 2006). There are several studies in many different organisms describing differentially regulated microRNAs which have antiviral activity (or activity that enhances virus replication). We were interested to see which known human microRNAs are differentially regulated over the course of infection between 0 to 6hpi, as these microRNAs may potentially possess antiviral activity, and also because nsp2 of SINV inhibits transcription in the nuclei of infected cells by blocking RNA polymerase I and II within 4-6hpi, which prevents the transcriptional activation of antiviral genes (Frolov et al. 2012).

5.3. Results

5.3.1. Sindbis virus is efficiently replicated in HEK293C cells

The role of RNAi in the context of mammalian innate immunity against RNA viruses is not yet established. SINV is a valuable research model of a positive stranded RNA virus not associated with human disease, and which can infect both mammalian and insect cells. SINV AR339 is an attenuated laboratory strain, first isolated from mosquitoes, but which has been adapted to replicate in a wide range of mammalian cells in culture (McKnight et al. 1996). The TR339 strain is a "reverse engineered" strain encoded on a DNA plasmid (infectious clone), in which most of the mutations responsible for the tissue culture adaptation of the virus were removed, and it is thought that this strains resembles best the original SINV isolate (C M Rice 1987, p.339).

In the initial experiment, SINV was adapted by serial passaging to efficiently replicate in human HEK293C cells with the aim of detecting sRNAs (either miRNA or svRNA from virally infected cells), and in the human DLD-1 cell line to study the role of Dicer, a component of RNAi machinery in regulating virus infection. SINV virus was serially passaged through HEK293C cells to obtain high titre virus prior to infecting these cells with SINV at a multiplicity of infection (moi) of 8. RNA was isolated at different time points (2, 4, 6, 8hpi) and virus replication was detected by Northern blotting with SINV specific probes. The presence of full length transcripts at 49S and the sub genomic transcript at 26S demonstrated efficient replication starting between 2 and 4hpi in HEK29C cells and increasing through 8hpi (**Figure 5.1A**). Total RNA was isolated at different time points (2, 4, 6, 8hpi) and virus replication was detected by northern blotting with SINV specific primer probes (**Figure 5.1B**). The presence of full length transcripts (49S) and the sub genomic transcript (26S) showed efficient replication starting between 2 and 4hpi in HEK29C cells and increasing through 8hpi, demonstrating that SINV effectively and rapidly infected and replicated in HEK293C cells. Based on this information the time points for sRNA sequencing were chosen at

4hpi and 6hpi as times when there would be sufficiently high concentration of double stranded RNA replication intermediates as substrates for Dicer. This is also the approximate time frame of the switch from predominantly negative strand synthesis to positive strand synthesis, and the shutoff of cellular transcription processes by SINV (Frolov et al. 2012). Previous experiments have shown that there is no IFN production and no apoptotic processes that the early stages of SINV infection. After 8phi the first newly synthesised virions are secreted into the media and the apoptotic process initiates after approximately 24 or 36hpi depending on the cell line. Therefore earlier time points, 4 and 6hpi, were chosen to avoid RNA degradation due to apoptosis and potentially active parts of the cellular antiviral innate immune responses.

5.3.2. Small RNAs from SINV infected HEK 293 cells: high-throughput sequencing shows viral RNA in very low abundance

RNA was isolated from control (mock infected) and SINV infected HEK293C cells at 4hpi and 6hpi. cDNA libraries were generated for the small RNA (sRNA) content of the cells using the version 1.5 of the Illumina protocol, and sequenced using Illumina GA II. The sequencing yielded between 29.1M and 30.5M reads per sample (**Figure 5.2**). The size class and complexity distributions for all reads for which the adapter sequence was identified (**Figure 5.3 A1-2**.) showed a preference for sequences of lengths 22-23nt. The reads in this size class are also characterised by a low complexity. Complexity is defined as the ratio of non-redundant to redundant reads, and low complexity characterises a low number of unique reads with high abundance (Irina Mohorianu et al. 2011)

Next, the sequences were mapped to the human and SINV genomes, respectively, using PatMaN (Prufer et al. 2008). More than 83% of sequences mapped to the Human genome (HUM reads), and 0.8% sequences mapped to the SINV genome (SINV reads).

The size class and complexity distributions of the Hum reads (**Figure 5.3 B1-2**) are similar to the overall distributions, preserving the properties of the 22-23nt reads, while the SINV reads (**Figure 5.3 C1-2**) showed an even distribution for all size classes, suggesting that the SINV reads may be degradation products. This hypothesis is also supported by the uniformity of the complexity index (i.e. the complexity was similar for all size classes in the 4hpi and 6hpi samples) (**Figure 5.3 C2**). No conclusion was based on the complexity distribution for the mock sample because of the extremely low number of SINV reads (20 reads total) present. These findings suggested that the viral mapping reads were probably not Dicer1 products. In addition the ratios of vsRNA mapping to positive and negative strand were 4:1 at 4hpi and 20:1 at 6hpi, supporting what would be expected at these time points for replicating virus. (*Fields virology* 5th ed)

To investigate the hypothesis, that the SINV reads are random degradation products, we analysed the distribution of expression (sum of abundances of SINV reads for all positions) for the whole genome (**Figure 5.4B**) and conducted a χ^2 analysis applied on the size class distribution compared to a random uniform distribution, for windows of length 100nt (**Figure 5.4A**). The purpose of identifying regions which show a preference for a size class is that these regions are likely to be excised in a precise manner through the RNAi pathway. In other words, the equal abundance of variants is an indication of random degradation. This analysis revealed highly significant regions (i.e. regions for which the size class distribution was significantly different from a random uniform distribution, the p Value was below 0.05 in both 4hpi and 6hpi samples), and regions for which the size class distribution was very similar to a random uniform distribution (p Value above 0.7, in both 4hpi and 6hpi samples). We attempted the validation of reads coming from the highly significant regions, but their abundance

was found to be below the detection limit using riboprobes, primer probes or LNA probes.

The validation of sequencing data was done using northern blotting, which offers a direct and sensitive detection method of RNA sequences. Primer probes and LNA probes were designed to be complimentary to the most abundant viral sequences. Riboprobes were generated using PCR products of different lengths (300-500-1500bp) from different parts of the SINV genome. These PCR products were generated using specially designed primers which had a T7 promoter sequence on the forward primers, and a SP6 promoter sequence on the reverse primers added. This way the same PCR products could be used to generate a positive strand specific probe (using SP6) or a negative strand specific probe (using T7). The length of PCR product decreases specificity, as more than one vsRNA sequence would be detected using the same riboprobe. However, because of the decreased specificity the sensitivity increases, as the same probe would bind to many different vsRNA, amplifying the signal detected. LNA and primer probes are typically end-labelled with radioisotopes (γ-(^{32}P) ATP), which means that each probe carries only one signal. Riboprobes, on the other hand, have multiple radioactively labelled (α-(^{32}P) CTP) incorporated during synthesis, which further amplifies the signal, increasing the sensitivity of the probe. Custom, SINV-specific LNA probes were unsuccessful to detect putative vsRNA sequences, and even the most sensitive method, using RNA probes, failed to detect any signal in the small RNA range (**Figure 5.5**). This suggested that the number of reads matching to the SINV genome is not sufficient for northern blot validations as they are below the detection limit. Increasing the number of mis-matches between the reads and the reference genome (0, 1, 2, 3 mis-matches) did not change the conclusions.

To better understand the interaction between the virus and the host, we computed the number of reads that could match to both the virus genome and the human genome. Only 5% of the SINV reads matched to both genomes. All of the sequences were low abundance and many variants were present on the SINV alignment, suggesting that the reads have a higher probability to be produced by the virus RNA, rather than the human genome. **Figure 5.4B** shows the lack of hotspots, which suggest the absence of specific cleavage of the viral genome and the lack of location specificity on the SINV genome. In addition, the uniform distribution of reads on both strands supports the hypothesis of random degradation.

5.3.3. SINV infection does not modulate the cellular miRNA expression

Since the majority of reads mapped to the human genome (>8M and >6M reads in the first two sample and in the third, respectively), we also investigated the changes induced by the virus infection in the cellular sRNAome. First, we identified miRNAs using miRCat (S. Moxon et al. 2008) and mirProf (Stocks et al. 2012); out of the 110 predicted miRNAs, 92 (including variants) were conserved and 18 were novel. These formed the majority of reads mapping to the human genome. To further investigate the sRNAome changes, other properties of miR loci (miR precursors) were analysed. First, using all human miRNAs from MirBase (Griffiths-Jones et al. 2008) for which we could identify at least 3 reads in the samples, the distribution of signal across the precursors was analysed. For all miRNAs more than 90% of the signal was consistently concentrated on the miRNA (5p sequence) and miRNA* (3p sequence), in all three samples. Next the size class distribution on the precursors was analysed using a χ^2 test (the approach was similar to the one used for the analysis of the whole SINV genome). The approach was applicable since the distribution of pre-miR lengths shows little variation around the 100nt mark, which was used for the SINV genome. Under the

assumption of random uniform distribution, all of the pre-miRs had significantly different size class distributions, biased on 22mers. The distributions for samples 4hpi and 6hpi were statistically the same as for the mock sample, suggesting no influence of the virus infection to modulate the miRNA expression (**Figure 5.6**). The scatterplot on annotated miRNAs shows that they display little variation between the 0 hpi, 4hpi and 6 hpi time points. Although the variation was small, we selected the miRNAs showing the most difference in expression as candidates. These results were confirmed by northern blots shown in **Figure 5.7**.

Twelve highly abundant and shown to be differentially expressed microRNAs were chosen for northern blot verification; most of these microRNAs were implicated in innate immunity (see **figure 5.7.** and below). HEK293C cells were infected with SINV AR339 and SINV TR339 in biological triplicates at MOI>8; total RNA was isolated at 0, 4, and 6. Three microRNAs (miR-155, -182, -496) were under detection limit, nine showed no changes in expression levels, corresponding to the result from sequencing.

MicroRNA 29a has already been linked to several defences against pathogens. It is shown to regulate the immune response to intracellular bacterial infection through IFNγ modulation (F. Ma et al. 2011); also the level of miR29 increases 50-fold in A549 cells in response to influenza infection, which leads to IFNλ and COX2 up-regulation (Fang et al. 2012). In addition, miR-29 down regulates the expression of Nef protein of HIV-1, and it interferes with HIV-1 replication (Ahluwalia et al. 2008). miR378 was also shown to be targeting HIV-1 genes (Hariharan et al. 2005). mir34 was shown to be an important modulator of innate immune response through the regulation of IFNβ expression (Witwer et al. 2010). Kaposi's sarcoma-associated herpesvirus (KSHV) and pseudorabies virus both encode miR10 homologues, which have an essential role in viral self-regulation (Y.-Q. Wu et al. 2012; Lei et al. 2010). miR19 and let7 are

important regulators of inflammatory responses as they upregulate NF-κB activity (Gantier et al. 2012). Let7 also modulates the innate immunity through the regulation of IFNβ expression (X. Ma et al. 2011). The miR17/92 cluster has been shown to regulate Epstein-Barr virus gene expression (Skalsky et al. 2012). miR196 can effectively repress hepatitis C virus gene expression and replication (Hou et al. 2010). miR197 targets the tumour suppressor protein FUS1 (L. Du et al. 2009).

These results confirmed the conclusions from sequencing. These results show that the Sindbis virus infection does not change miRNA expression in HEK293 cells at a time when miRNAs may regulate an innate immune response or affect viral replication (Campbell et al. 2008).
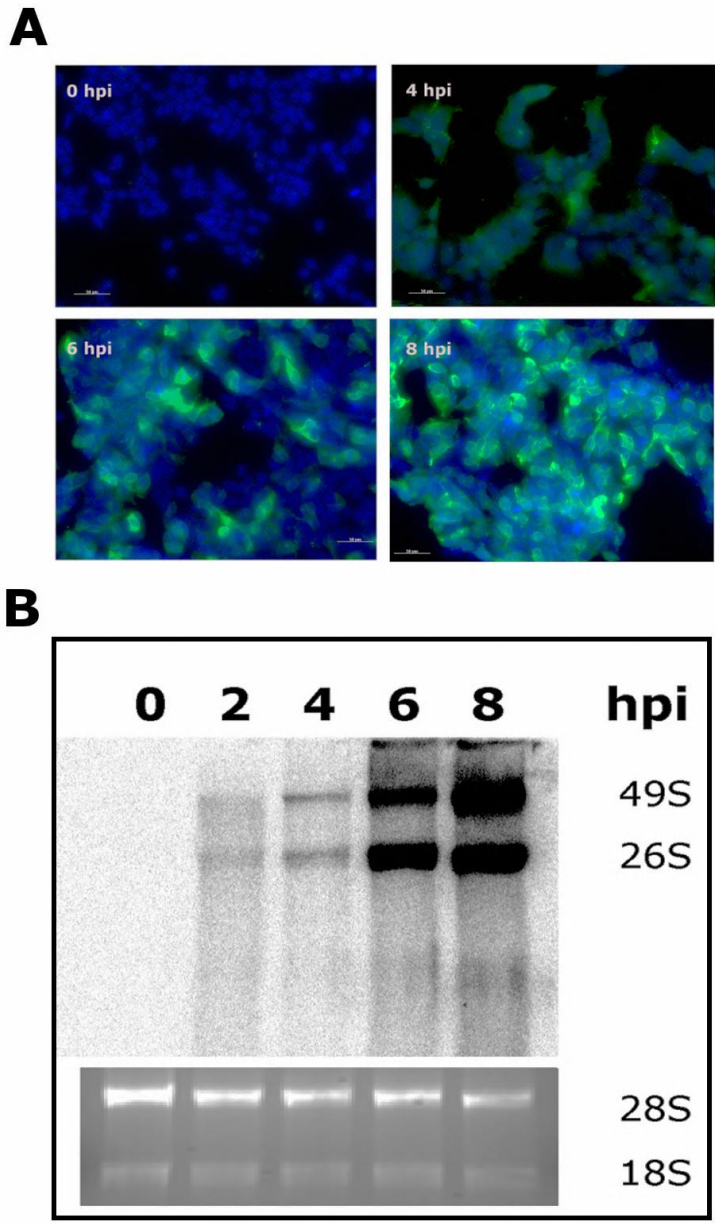
Figure 5.1. Preparation of SINV infected HEK293C cells. **A.)** Cells were infected with SINV for 2, 4, 6 hpi at high multiplicity of infection (MOI<8), and stained with anti-SINV antibody (Blue: DAPI nuclear stain, green: SINV). The immunostaining demonstrates that almost 100% of the cells are infected with SINV. **B.)** The northern blot shows the rapid accumulation of SINV RNA in HEK293C cells starting at 2hpi and increasing through 8 hpi. The end-labelled primer probe specific to the position 7568-7631 of the SINV genome detects full length (49S) and subgenomic (26S) (+) positive strand RNA. The 28S and 18S RNA bands stained with ethidum bromide are displayed to demonstrate equal loading. Both images show the actual samples used for Solexa/ Illumina sequencing
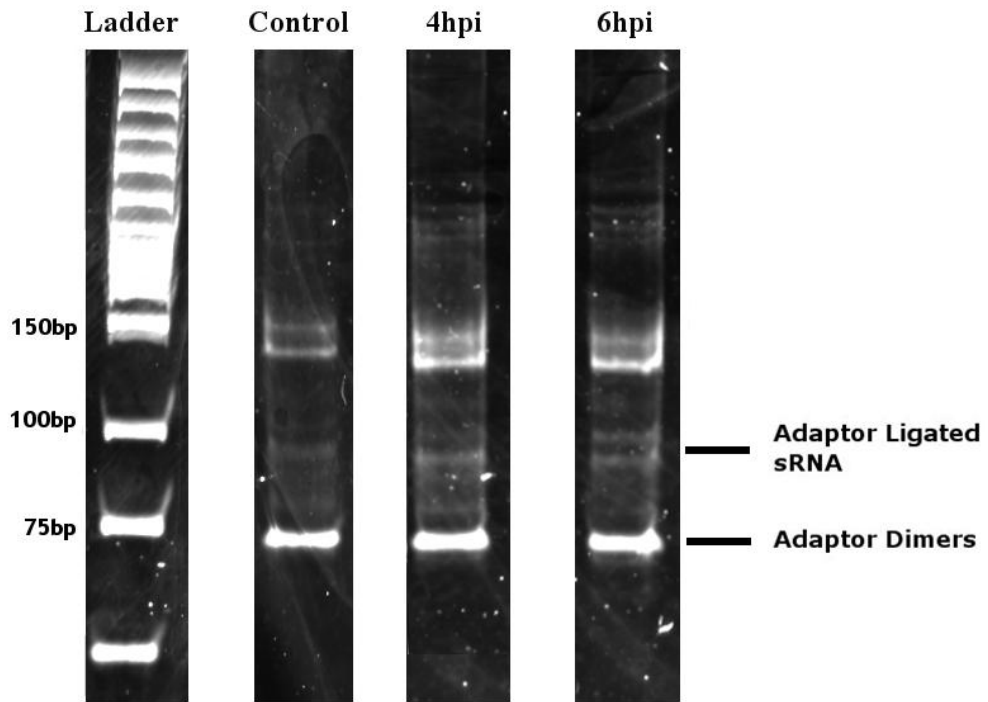
Figure 5.2 sRNA library of SINV infection time course at 0, 4, and 6 hpi. Based on northern blotting and immunocytochemistry experiments we have chosen 4 and 6hpi time points for further studies. 3 μg of RNA was used to prepare the Illumina library. After PCR amplification the resulting cDNA was ran on a PAGE gel, and the ~100bp band (75bp adapters + 20-25bp small RNA) excised and sent for sequencing.

A

1

Redundant Reads 21-24 mers (all)

2

Distribution of Complexity (all sizes)

B

1

Redundant Reads 21-24 mers (human)

2

Distribution of Complexity (human)

C

1

Redundant Reads 21-24 mers (SINV)

2

Distirbution of Complexity (SINV)
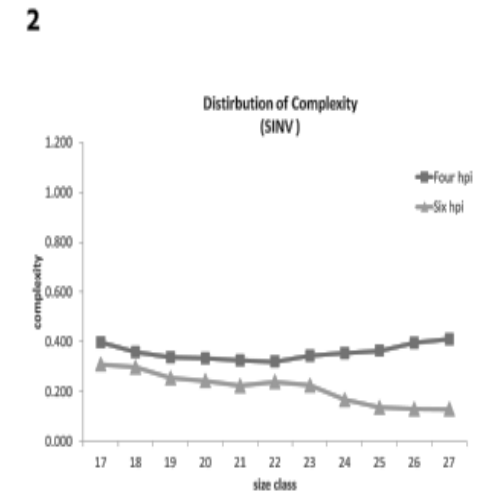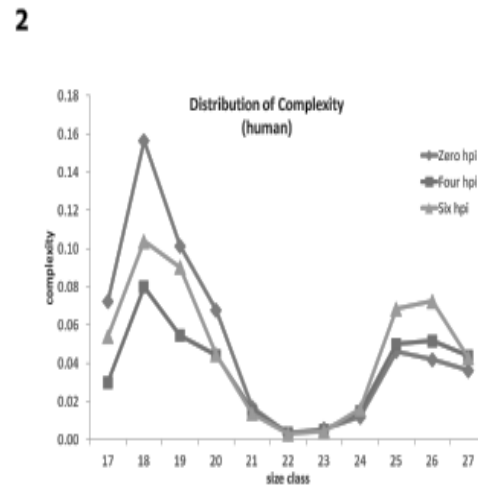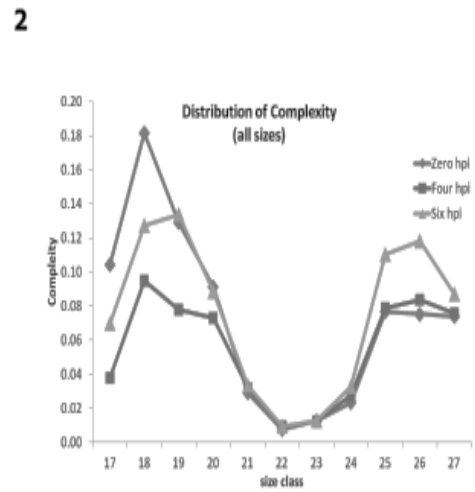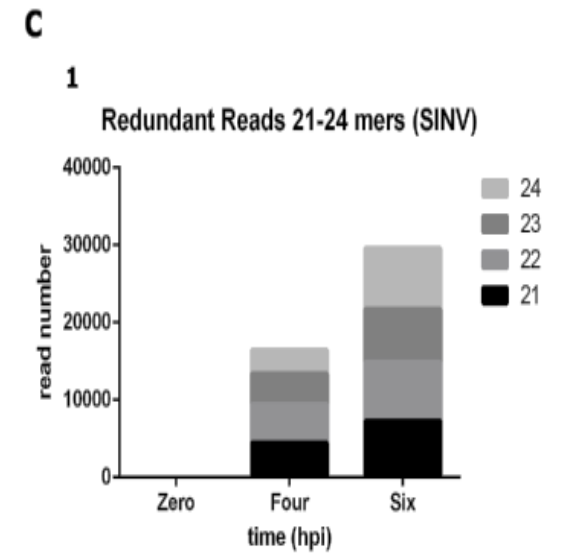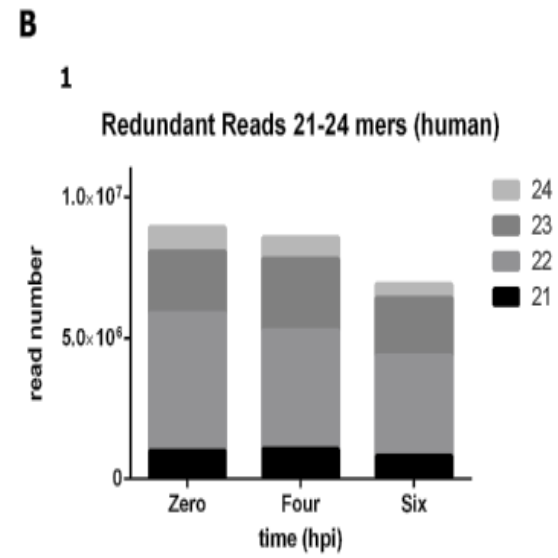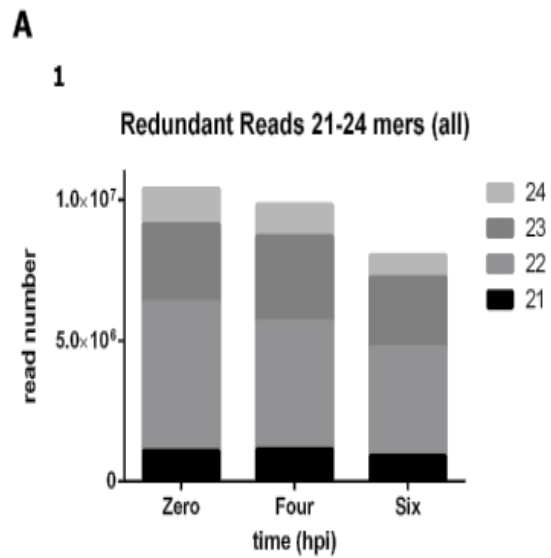
Figure 5.3 Size class distributions for (A1) all reads, **(B1)** reads mapping to the Human genome, **(C1)** reads mapping to the SINV genome. The total reads and the reads mapping to the human genome are enriched in 22-23 nt sequences. Sequences mapping to the SINV genome show even distribution suggesting random degradation. Complexity distribution for **(A2)** all reads, **(B2)** reads mapping to the Human genome, **(C2)** reads mapping to the SINV genome. Complexity of all sequences, and sequences mapping to the human genome show a decrease in the 22-23nt region, which indicates small RNA presence, while reads mapping to the SINV genome have an uniform complexity index, which also suggests degradation.
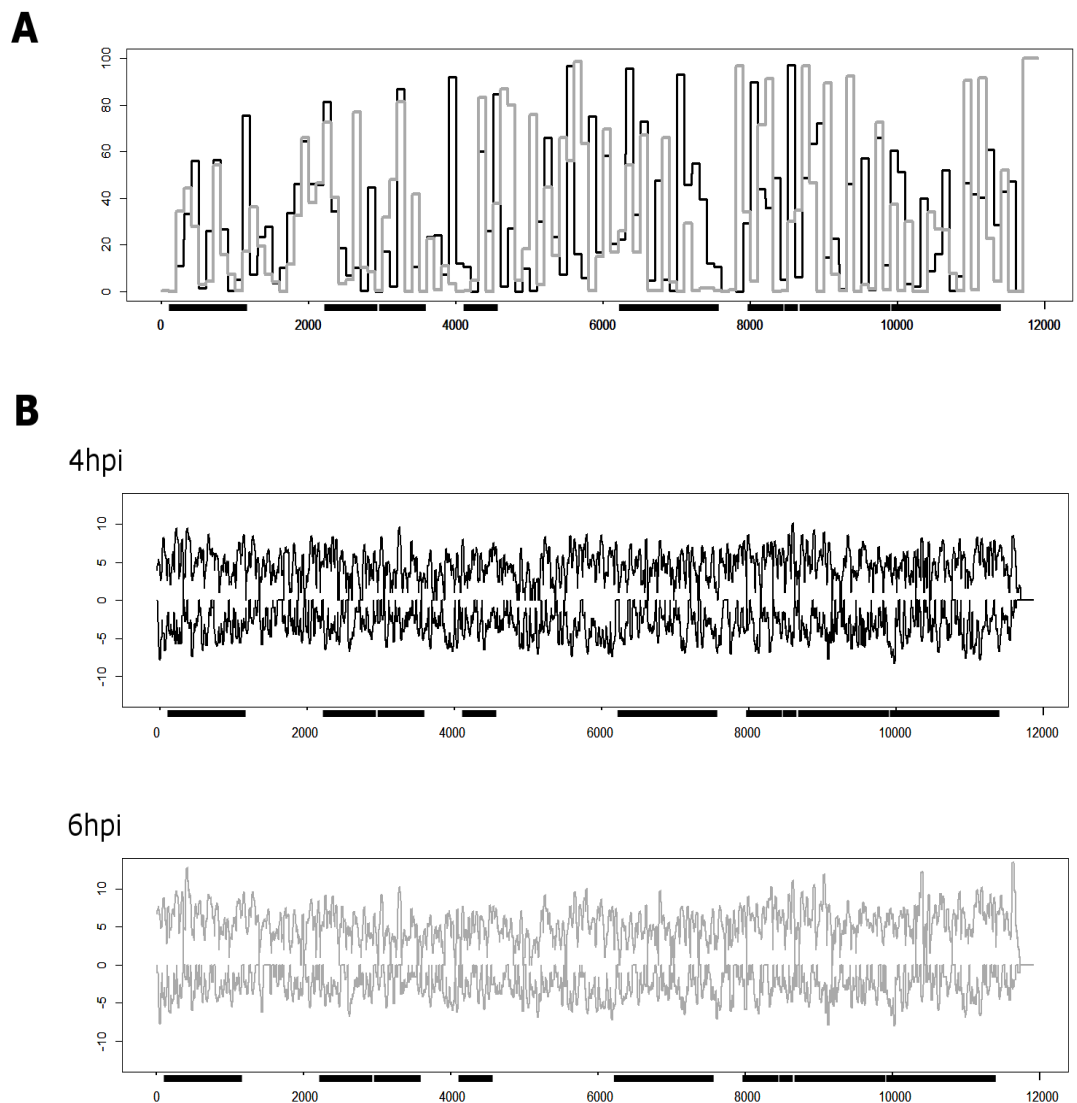
Figure 5.4 (A) variation of expression level for SINV reads. Reads mapping to the SINV genome are shown in relation of the full-lenght SINV genome (x axis). The size of peaks (y axis) shows the number of reads on that particular location; the orientation (positive or negative) shows which strand (positive or negative) of the SINV genome the reads map to. **Black**: samples from 4hpi, **gray**: samples from 6hpi. **(B)** Variation of p Value for a ChiSq significance test on the size class distribution compared to a random uniform distribution for windows of length 100 nt. The reads are mapped to the SINV genome as previous. Thick black line signifies the proteins encoded by the given part of the genome.
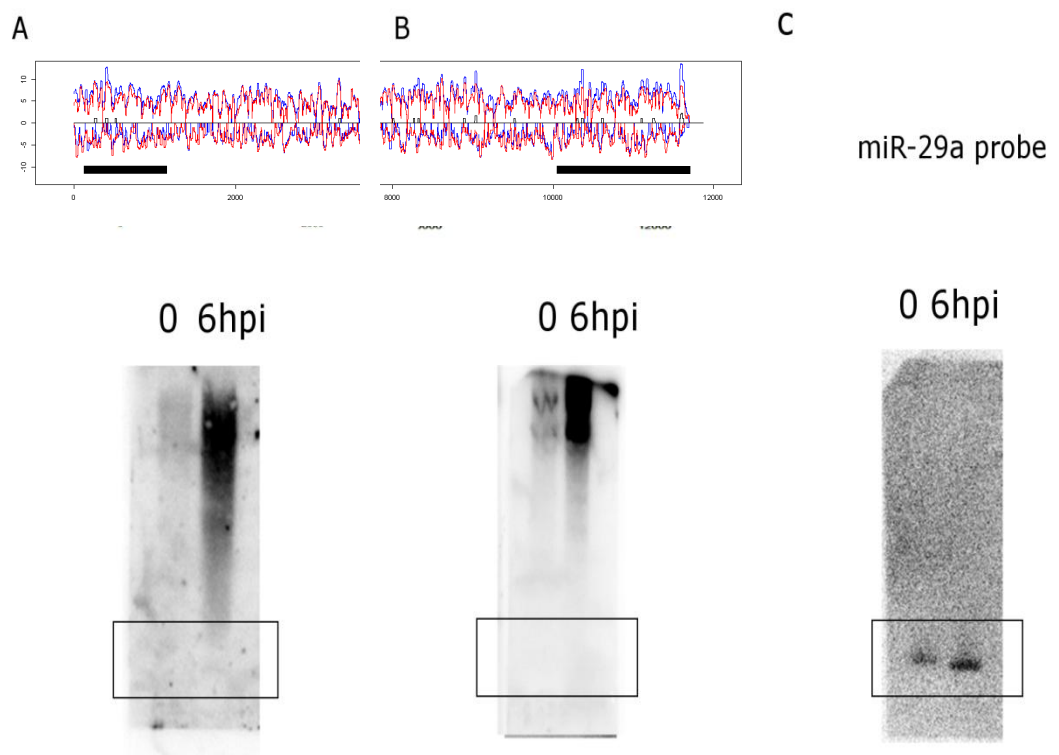
Figure 5.5 SINV specific riboprobes are unable to detect vsRNA. The graph depicts a part of the SINV genome with the abundance of SINV reads mapped to the genome (red: 4hpi, green: 6hpi). The blue line underneath shows the area of which the riboprobe is complementary to. The blot shows a smear at the high molecular weight range. There are no distinct bands detected, and no signal found at the expected 21-22mer range (lower 1/4th of the blot). (A) 500 pb long riboprobe specific to the beginning of the SINV genome. (B) 1500bp long riboprobe mapping to the end of SINV genome. (C) miR-29a probed membrane used as size marker for the expected 21mer ban

A
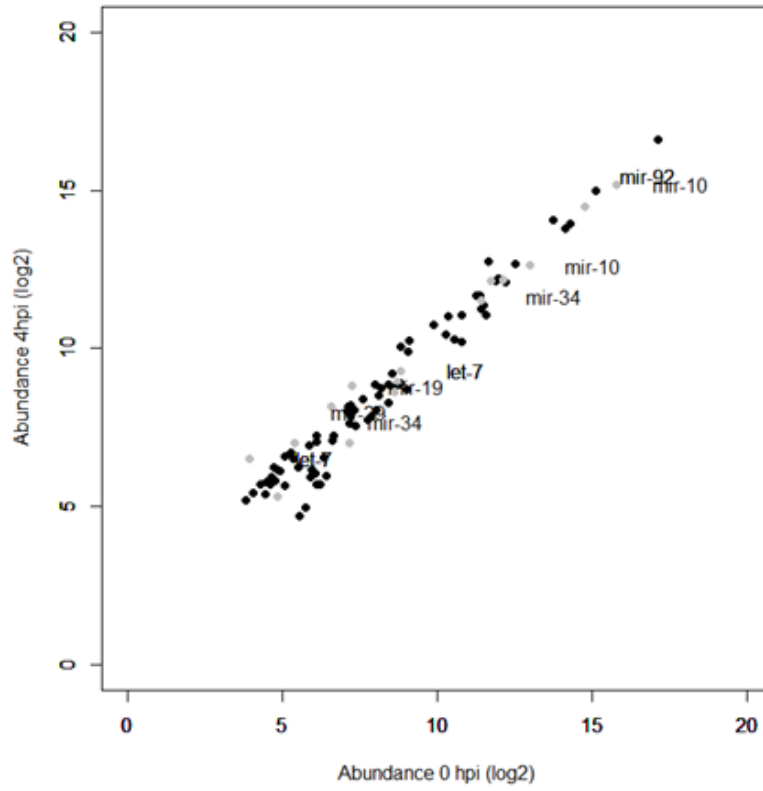
B
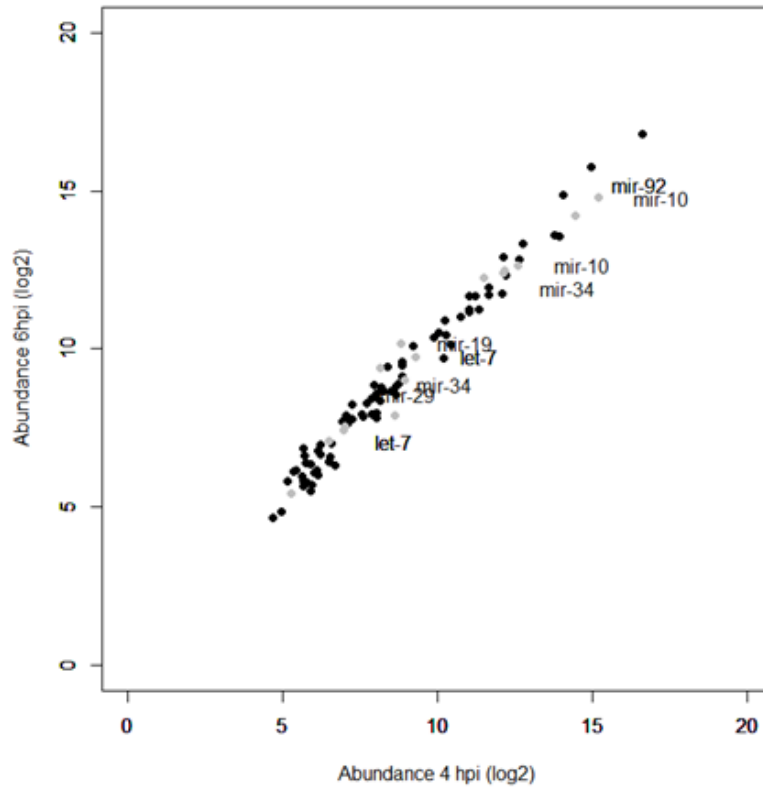
Figure 5.6 Sequencing results show human miRNA expression profiles remain unchanged during early SINV infection (0, 4 and 6phi). A.) miRNA profile changes in 0hpi sample vs 4 hpi sample. **B.)** miRNA profile changes in 4hpi sample vs 6 hpi sample. Scatter plots of miRNA expression levels indicate no significant change in expression in HEK293 cells. On both x and y axis we represent the normalised expression levels of the miRNAs at a given time point in log2 scale. MicroRNAs chosen for northern blot validation are shown on the plot.
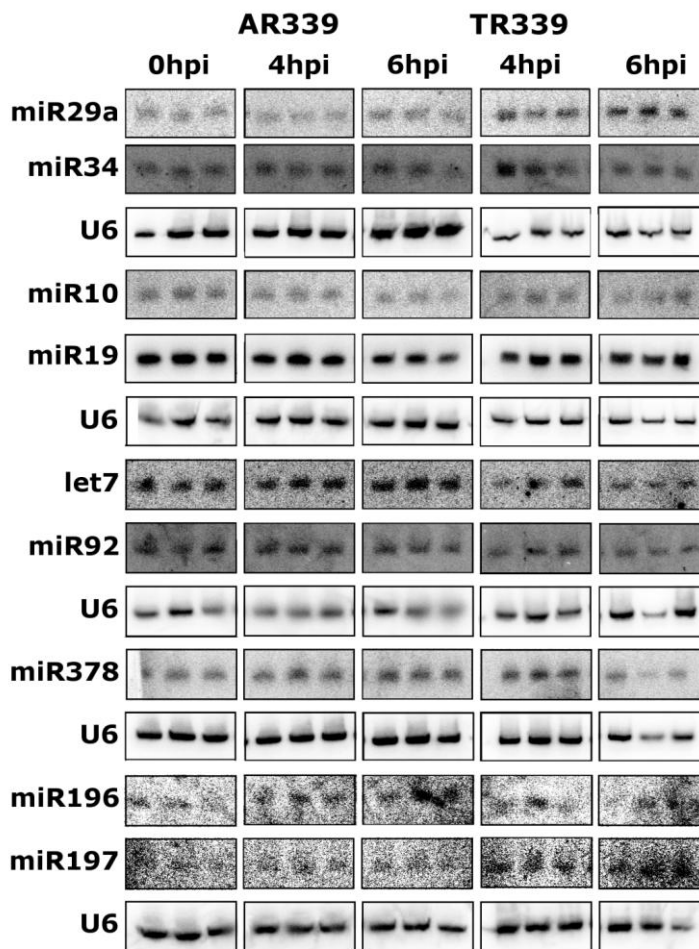
Figure 5.7 Northern blots confirm that Human miRNA expression profiles remain unchanged during early SINV infection (0, 4 and 6phi). Northern blot validation of candidate miRNAs in SINV AR339 and infectious clone TR339 also support the hypothesis of no change in expression. Twelve microRNAs (miR10, miR19, miR29a, miR34, etc) were chosen for validation based on the change in their expression profile according to the sequencing data. The northern blot validation was conducted in biological triplicates. Three microRNAs were under the detection limit (miR155, miR182, miR-496), the rest showed no change in expression between the 0-6hpi period. The equal loading is shown by U6.

5.4. Discussion

This study investigated whether there is a role for RNAi during SINV infection of mammalian cells in the light of the well-established role of RNAi in SINV infection in insect vectors (Myles et al. 2009; Campbell et al. 2008; Saleh et al. 2009). To date several modes of action of RNAi as response to viral infection have been proposed: 1) RNAi produces svRNAs that can target the generating transcript reducing virus genome, (2) the viral genome encodes miRNA-like regions that are processed by RNAi into miRNAs which can in turn target the genes of the host, (3) the host genome encodes miRNAs which can modulate viral replication through RNAi and (4) viral infection can influence the expression of cellular miRNAs. The effect of RNAi can therefore be antiviral (as in the cases (1) and (3)) or beneficial to the virus (as in (2) and (4)) (Saumet & C.-H. Lecellier 2006).

An example of the antiviral effect of the RNAi machinery which illustrates the first mode of action is the systemic RNAi response against SINV in Drosophila. (Saleh et al. 2009) The second mode of action is illustrated by the herpes virus family and other large DNA viruses which encode miRNAs that target cellular innate and acquired immunity factors (A Gupta et al. 2006); for example, miRNA encoded by EBV targets the pro-apoptotic factor PUMA, microRNA encoded by KSHV down regulates MyD88, and HCMV encode miRNAs that inhibit RANTES expression (Choy et al. 2008; Bryan R Cullen 2013; Y. Kim et al. 2012). The third mode of action is illustrated by Hepatitis C Virus, for which the liver-specific miR-122 has been shown to have a stimulating effect on viral replication (Jopling et al. 2005). EBV infection is an example of the fourth mode of action (viral infection modulates cellular miRNAs expression). EBV strongly induces miR155 in B cells to promote cell transformation (Gatto et al. 2008).

Therefore it was of interest if SINV infection of mammalian cells generated small RNAs to target the SINV genome, if SINV provides viral miRNA, or if the virus infection changes cellular miRNAs profiles during virus infection.

In this context, we studied sRNAs during SINV infection of mammalian cells to understand in which of these categories it is classified. Sequencing showed that there were no svRNAs in the 20-25nt range which could indicate the processing of the dsRNA virus replication intermediate by the RNAi machinery. This would suggest that there is no self targeting of viral RNA. This is in contrast to SINV infection in mosquito cells where SINV is a substrate for RNAi as SINV vsRNAs were readily detected and were shown to prevent viral spread between cells (Saleh et al. 2009). In mosquitos variations in levels of Ago2, DICER2 and other components of RISC were observed during virus infection, indicating that the virus can modulate the RNAi system. Our results support this finding also for mammalian cells where the lack of Dicer promotes viral replication, indicating a role for Dicer in sensing SINV infection. What this role may be is unclear. In Shapiro et al study the incorporation of a pri-miRNA into SINV led to the generation of a Dicer dependent mature miRNA (Shapiro et al. 2010) demonstrating the Dicer recognition during cytoplasmic replication of an engineered SINV.

In addition, the lack of 20-25 nt svRNAs indicated that there are no viral miRNAs in the genome that would affect gene expression in either host or virus. This finding is in line with other RNA viruses, where viral miRNAs have never been described, although they are well documented in DNA viruses, such as herpes viruses and adenoviruses (Gottwein & Bryan R. Cullen 2008).

The sequencing data showed that human miRNAs were not differentially expressed in SINV virus infected cells at the early stages of virus infection. This was confirmed by northern blot of nine of the most abundant miRNAs being unchanged over 6 hpi. However, this mode of action has been associated with some RNA viruses, for example the picornavirus enterovirus 71 (EV71) activates transcription of miR141, which in turn suppresses translation of the cap-binding protein eIF4E in order to inhibit cap dependent translation (B.-C. Ho et al. 2011). It has also been proposed that during infection with HIV-1, the expression of several micro RNAs is induced (Triboulet et al. 2007). Although SINV infection did not up-regulate host miRNAs, it does not preclude pre-existing cellular miRNAs influencing SINV replication, as in the case of the RNA virus HCV where the liver specific miR 122 stimulates viral translation (Henke et al. 2008).

It has been shown that the SINV itself does not activate interferon at early time points in non-immune cells (Burke et al. 2009), but many other interferon sensitive genes (ISGs) have been shown to be induced within 4-6 hpi, dependant on PKR and MDA5. These results indicate that for SINV infection of mammalian cells a more effective control may be the innate immunity (Dhanushkodi et al. 2011).

6. Suppressors of RNAi

6.1. Overview

In the last chapter, I have shown that SINV infection of HEK 293 C cells does not lead to the production of small viral RNAs and does not modulate the expression of host miRNAs. SINV, as all RNA viruses, generates a double stranded intermediate, but it is not recognised by RNAi. Why should this be the case, if we consider the following available evidence: Firstly, exogenously added siRNAs have been shown to work efficiently to silence genes when added to human cells, demonstrating the presence of intact RNAi machinery in humans. Secondly, it is well known that gene expression is modulated by miRNAs in mammalian cells during development and tissue differentiation (Goljanek-Whysall et al. 2012). Thirdly, human cells express a single Dicer, which is responsible for production of both siRNAs and miRNAs, and human cells contain Ago2 and the components of RISC. Despite of these reasons, my results demonstrate that RNAi does not act as an antiviral defence in human cells, unlike plants and invertebrates. In this chapter, I investigated possible reasons for this.

I have set up a gene silencing assay to measure the activity of the siRNA pathway in cells. The assay involves using siRNA against a housekeeping gene, GAPDH, followed by northern blot to check for RNA knockdown in HEK293C.

After optimising the knockdown of GAPDH RNA, using different transfection reagents and times after transfection of siRNAs, I used this assay to look for cellular and viral molecules that may be inhibitors of RNAi. These included RHA, which I previously showed inhibits viral replication (Chapter 4), and with SINV infection, or transfection with synthetic dsRNA (poly IC), and also cellular stress induced by sodium

arsenate. I have primed the cells with interferon, and finally I have used a viral inhibitor of the interferon pathway.

RNA helicase A has been shown to be involved in the RNAi pathway. A high profile report in the literature demonstrated that RHA knockdown can block the RNAi pathway, and showed RHA is important in RISC loading (Robb & Rana 2007b). In their study, gene expression knockdown using siRNA and shRNA against GFP in GFP-expressing HeLA cells was inhibited when RHA was depleted. As I have previously shown in Chapter 4, RHA is an important host factor in SINV replication, it was therefore reasonable to predict that there may be interaction between RHA and SINV through the RNAi pathway. When RHA is knocked down, SINV replication increased, suggesting that RHA modulation of RNAi may be an anti-viral defence. As cited in Chapter 4 discussion, RHA is an important host factor in the replication of several viruses (Q. S. He et al. 2008; Ranji & Boris-Lawrie 2010). In another study it was shown that there is an antiviral response directed by PKR phosphorylation of the RNA helicase A (Sadler et al. 2009).

SINV has been shown to induce stress granules after infection of mammalian cells (Venticinque & Meruelo 2010). Stress granules or P bodies play an important role in the generation of miRNAs, as they contain Dicer, RISC, Ago and contain translationally silenced mRNA (Beckham & Parker 2008; Paul Anderson & Kedersha 2008).

For these reasons I investigated whether cellular stress in general affected RNAi by generating stress in control cells by addition of sodium arsenate. In other experiments I primed cells with type I interferon to look at the effects on RNAi. In addition I investigated the effects of SINV infection and polyI:C on RNAi.

Viral suppressors of RNAi are also a well-documented mechanism of evasion of the innate cellular defence. There are several examples: NS1 protein of influenza virus (de Vries JGV 2009, de Vries 2008, Int J biochem and cell bio), Vaccinia virus E3L, HCV core protein, PFV-1 Tas and the Ebola vp35 protein (Fabozzzi et al J Virol 85 2512-2523 2011, Haasnoot et al Plos pathogen 3 e86 2007). Viral suppressors of RNAi can bind to host RNAi molecules or sequester some components, and most of these proteins have also been shown to inhibit the interferon signal transduction pathway. For these reasons I used a known viral inhibitor of the interferon pathway to investigate whether it also blocked the RNAi pathway in human cells. The N-terminal protease N^{pro} from the pestivirus classical swine fever virus has been shown in our lab to degrade the transcripion factor IRF3, a central regulator of interferon synthesis (LA Rocca et al 2005). My work investigated if there was also a role for N^{pro} in the suppression of RNAi.

6.3. Results

6.3.1. Development of an RNAi functional assay

To assess the functionality of the siRNA pathway of the RNA interference system, a knockdown assay was developed. siRNA against a housekeeping gene (GAPDH) was transfected into HEK293C cells (both treated and control), and the effectiveness of the knockdown was assayed by monitoring the amount of GAPDH mRNA either by limited cycle RT-PCR or northern blotting. Should a treatment suppress the RNAi system, the assay will show GAPDH mRNA present in the treatment samples, as the effects of the transfected siRNA will be diminished. This is a semi-quantitative, but direct assay which gives an accurate picture of the quality of GAPDH mRNA present in the sample. Using two housekeeping genes instead of one would make it even more robust.

At first, limited cycle RT-PCR was chosen for its simplicity and speed (**Figure 6.1**). Further investigations showed that this method did not have the necessary accuracy (**Figure 6.8**). For this reason I have used northern blotting for this study, as this sensitive method allows for direct measurement of the amount of RNA present in the sample.

The RNAi assay was optimized by choosing JetPrime as the most effective transfection reagent. A concentration-series showed that 50nM final concentration if siRNA leads to effective knock-down in HEK293C cells. The efficiency of transfection was demonstrated using siGlow, a fluorescently tagged siRNA: 100% of the cells were transfected under these conditions (**Figure 6.2, Figure 6.3**). A time-course experiment showed that by 6 hrs post transfection the knockdown effect is total (**Figure 6.4**).
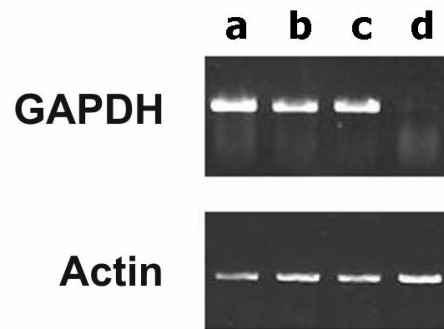
Figure 6.1. Limited cycle RT-PCR shows significantly lower GAPDH mRNA levels in GAPDH siRNA-treated cells. The knockdown experiment was conducted as described, and a limited cycle RT-PCR experiment carried out. The results show effective knockdown of GAPDH mRNA after 24hr using siRNA with 50nM final concentration. **a:** control cells, **b:** mock-treated cells, **c:** non-targeting siRNA treated cells, **d:** GAPDH siRNA treated cells.
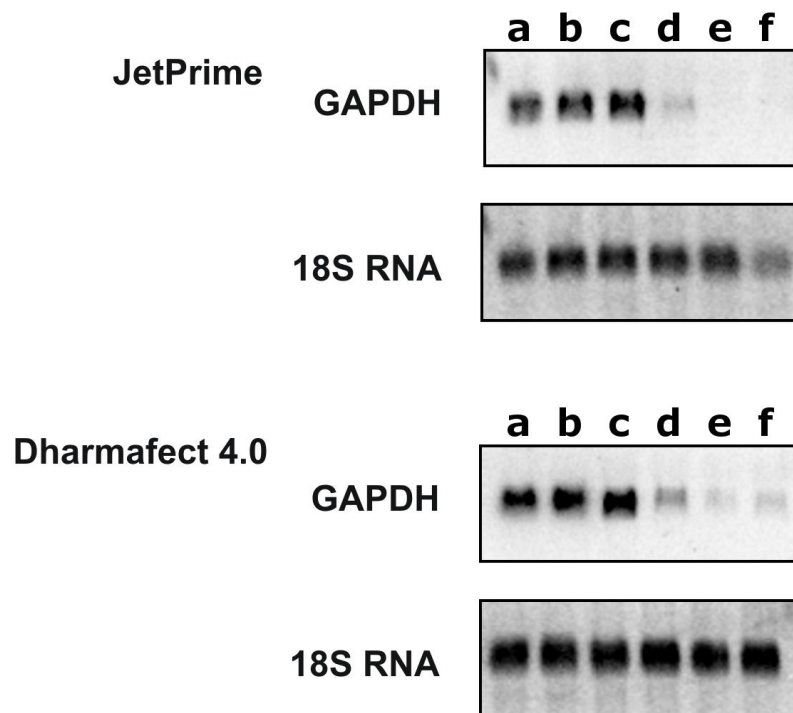
Figure 6.2 JetPrime is more efficient transfection reagent than Dharmafect 4.0 at knockdown of GAPDH mRNA. The efficiency of GAPDH siRNA transfection was tested using two different transfection reagents using the manufacturers' recommendations. The RNA was isolated from cells using Trizol, separated on a formaldehyde gel and blotted on a nitrocellulose membrane. The membrane was

hybridized with radioactive-labelled primer probes against GAPDH and 18S RNA (loading control). The results show that under these circumstances JetPrime achieved 100% knockdown on GAPDH using siRNA at 50nM final concentration, and that there was a visible GAPDH signal when using 100nM siRNA with Dharmafect 4.0 transfection reagent. **a:** control cells, b: mock treated cells, **c:** non-targeting siRNA treated cells, **d:** GAPDH siRNA 10nM final concentration, **e:** GAPDH siRNA 50nM final concentration, **f:** GAPDH siRNA 100nM final concentration. 18S RNA blot is shown for equal loading.

.
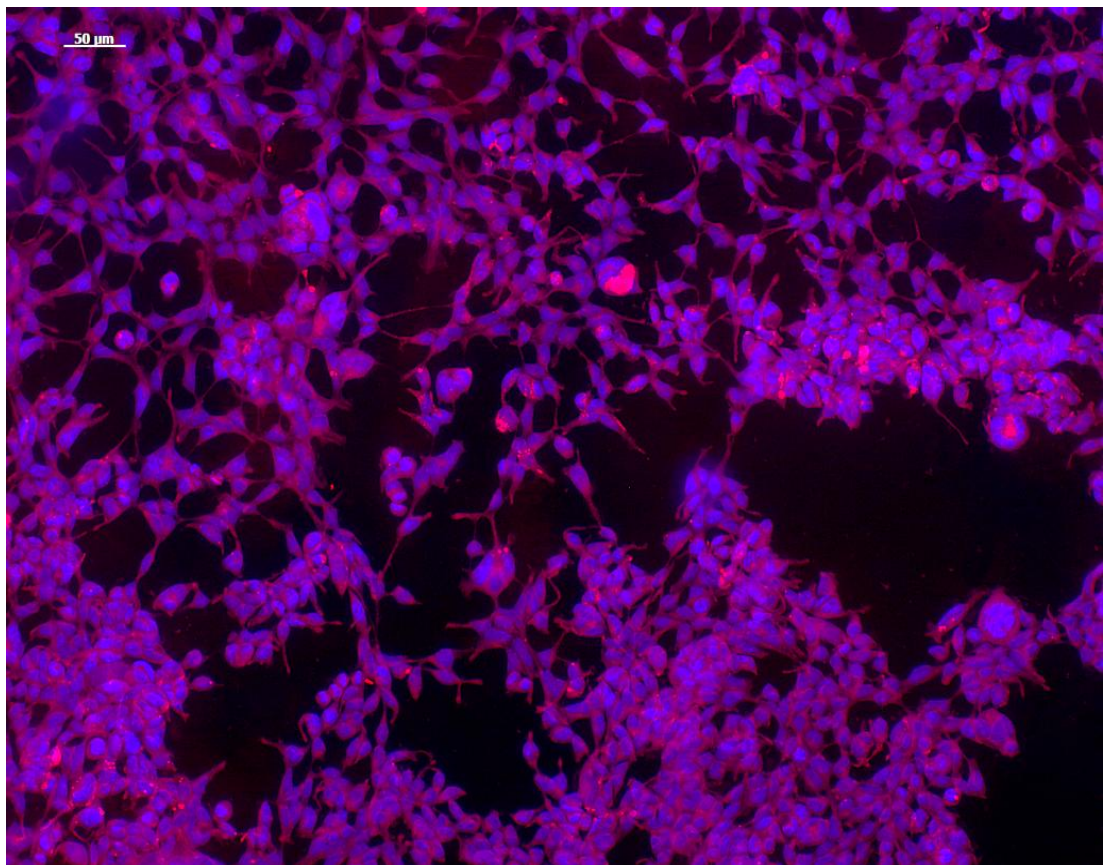
Figure 6.3 JetPrime effectively transfects 100% of the cells. Fluorescently labelled siGlow siRNA was used to monitor the effectiveness of transfection. 100% of the cells are transfected under the experimental conditions
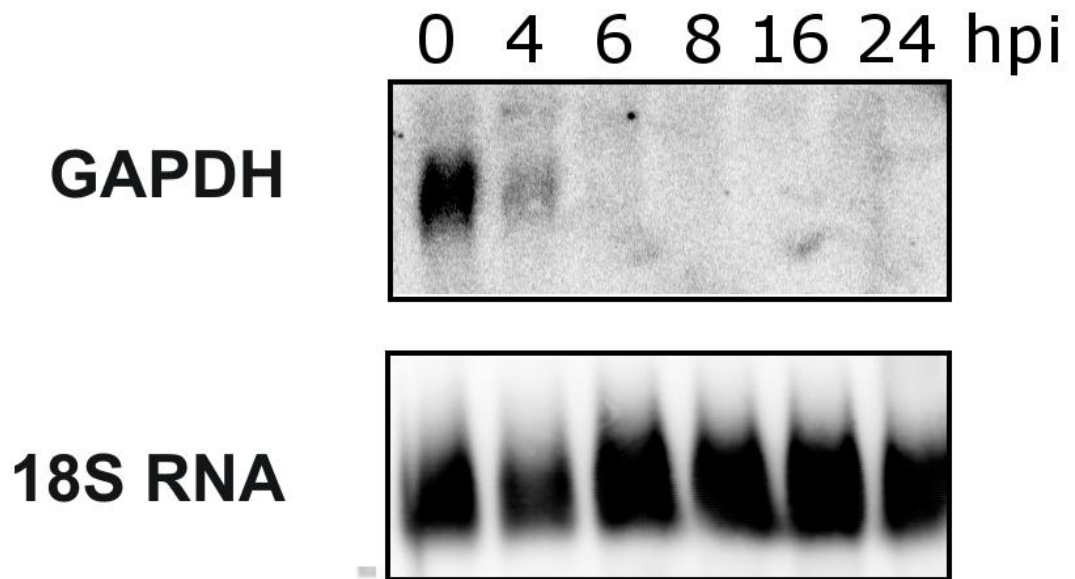
Figure 6.4. GAPDH siRNA effectively knocks down the level of GAPDH mRNA by 4hrs post-transfection. GAPDH siRNA was transfected into HEK293C cells and the RNA isolated, separated on formaldehyde gel and blotted on nitrocellulose membrane. The membrane was hybridized with radioactive-labelled primer probes against GAPDH. The Northern blot of the time course-series shows that the knockdown effect is total and persistent over 24hrs. The blot is a representative of several repeated experiments. 18S RNA blot is shown for equal loading.

6.3.2. The Effect of RHA on the siRNA pathway

Previous study (Robb & Rana 2007b) reported that RHA depleted cells have a compromised RNAi response using a similar assay. The study used HeLa cells stably expressing GFP. RHA was depleted using RHA specific siRNA, and 24hrs after transfection siRNA or shRNA targeting GFP was transfected into the cells. In the RHA depleted cells the level of GFP mRNA was equal to the control levels (control was no GFP-specific siRNA/shRNA treated HeLa-GFP cells) indicating that the siRNA pathway did not function. Ago2 specific siRNA was used as a positive control.

Since the study found that RHA depletion makes siRNA mediated RNA interference inoperable, RHA had the potential to be used as a positive control for my assay. However, when I repeated the GAPDH knockdown assay using HEK293C cells that were depleted of RHA using RHA specific siRNA, I found that their RNAi response does not differ from the control samples. The RNAi response was functional, and no difference was detected from the control group. The assay was repeated using RHA depleted HeLa cells, which the original study used, but the results were the same (**Figure 6.5**). RHA did not suppress siRNA mediated RNA interference in this system.
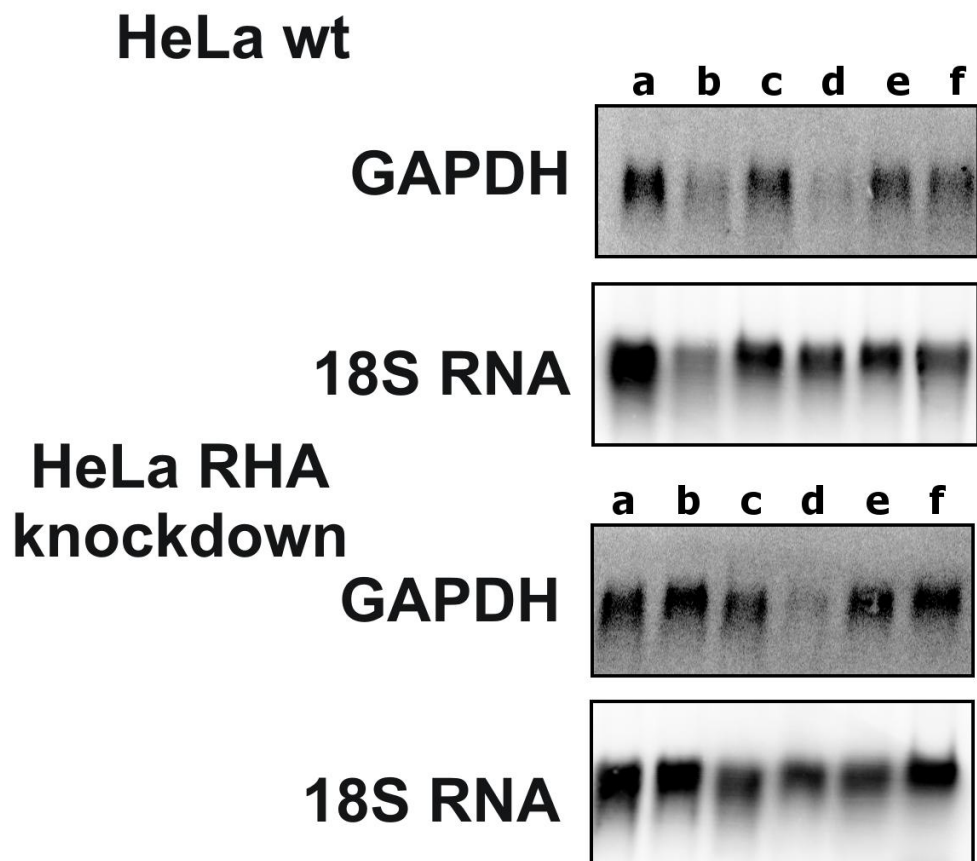
Figure 6.5 RHA knockdown does not have any effects on RNA interference. GAPDH knockdown assay in RHA depleted HeLa cells shows no suppression of RNAi; however dsRNA homologue (polyI:C) shows similar suppression as in HEK293C cells. The blot is a representative of several repeated experiments. **a:** control cells, **b:** mock treated cells, **c:** non-targeting siRNA treated cells, **d:** GAPDH siRNA treated cells, **e**: polyI:C treated cells, **f:** polyI:C/GAPDH siRNA treated cells. 18S RNA blot is shown for equal loading.

6.3.3. The Effect of Viral Infection, Double Stranded RNA, Interferon and Cellular Stress on RNAi

SINV has been shown to induce stress granules after infection of mammalian cells (Venticinque & Meruelo 2010). Translational regulation of gene expression offers the cells a required plasticity to react sudden changes, like different cellular stress signals (changes in pH, salinity, temperature, infection, etc.). Cytoplasmic granules (stress granules, processing bodies and neuronal granules) have shown to play important roles in posttranscriptional gene regulation. They contain mRNA, scaffold proteins, ribosomal subunits, translation factors, helicases, and more importantly, members of the RNAi and RNA decay machinery. Because of the proteins they contain, they are responsible for determining the localization, the stability and the translation of mRNA.

Stress signals will trigger a stress-response from eukaryotic cells, which leads to translation shutdown for the majority of proteins, and selective translational up regulation of stress related proteins, for example, chaperones (Harding et al. 2000). One of the major routes of stress response is through the phosphorylation of eukaryotic initiation factor 2 alpha (eIF2α). This effectively enacts a global protein synthesis shutdown through the blocking of CAP dependent translation, and up-regulates stress response gene expression, which is generally Internal Ribosome Entry Site (IRES)-regulated, and can be translated independently from CAP dependent translation mechanisms (Holcik & Sonenberg 2005). Many different stress signals can lead to eIF2α phosphorylation through different cellular sensors. These stress signals range from UV light, arsenate stress to viral dsRNA-activated PKR. The phosphorylation of eIF2α will lead to stress response, which either helps the cells to adopt the stress, clear the virus, or leads to ER mediated apoptosis. The translational shutdown leads to the accumulation of stress granules (SG), which holds the stalled mRNA-protein complexes

until they are either degraded in processing bodies (PB), or their translation is reinitialized. SGs are thought to be intermediate compartments for storage and remodelling of mRNPs. The fate of mRNA stored in SGs can either be reinitiation of translation in polysomes, or degradation in PBs (P. Anderson 2006). Studies by Nover et al. (1983) found that SGs forming in response to heat shock include the mRNA encoding most cellular proteins, but exclude the mRNA encoding for heat shock proteins; this phenomenon has been described by others as well. Both SG and PB are structures which are in dynamic equilibrium with the polysomes, the sites of translation. Both types of mRNP complexes contain multiple proteins, and some of them are common in both. These include Ago2 and other RISC components, which are required to be present in metazoan PBs. What they differ in is their roles: SGs mainly contain components of translation initiation, whereas PBs contain components for mRNA decay. Both can be taken as collectors of un-translated mRNA molecules that exceed the capacity of the translation and decay machinery, to hold them until further processing. They were also shown to be interacting with each other, raising the possibility of mRNA exchange between different mRNP granules.

A previous study showed that certain cellular stress signals down regulate the amount of Dicer present in cells, but the study did not assess the functionality of the RNAi system. The GAPDH siRNA knockdown assay is a functional assay, and it was used to examine how the function of siRNA mediated RNAi changes to different stress signals. Cells were treated with IFN-β, polyI:C, SINV (**Figure 6.6**) and arsenate. Arsenate had no effect; Interferon-β surprisingly did not affect the levels of GAPDH mRNA, but both polyI:C and SINV, however, did. Both treatments, that worked, are virus infection related; one is a dsRNA homologue, the other is an actual virus. (While the polyI:C results have been repeated in many different cell lines with consistent

results, the SINV-mediated RNAi suppression is a preliminary result, and should be treated as such.)

There are two hypotheses why polyI:C suppresses the siRNA-mediated RNAi response. The first is that the effect is non-specific: the large amount of long dsRNA present in the cytosol simply saturates Dicer, and renders it incapable to load the transfected GAPDH siRNA onto the RISC complex. The second hypothesis is that this is a result of a specific crosstalk between cellular signalling pathways of the innate immunity and the RNAi system.

Using the Dicer knockout colon cancer cell line DLD-1, it was possible to test these hypotheses. If the suppression is due to Dicer saturation, then all Argonauts within the RISC complexes would be flooded with short polyI:C duplexes, produced by Dicer, outcompeting any other short RNA present during RISC loading. In this case the GAPDH siRNA would be ineffectual as it would not be loaded onto RISC. In Dicer -/- cells, however, polyI:C is not processed into short fragments, and would not hinder the loading of GAPDH siRNA onto the RISC complexes. Therefore it should be possible to induce suppression of GAPDH mRNA using siRNA in Dicer -/- cells cotransfected with polyI:C.

Northen blot analysis of the experiment indicates that the first hypothesis is not true; the observed RNAi suppression may, therefore, be the result of crosstalk between the RNAi system and the innate immunity (**Figure 6.7**). We can observe the same pattern as with the previous blots: both wild-type and knockout cells show GAPDH suppression, while polyI:C abates the effects of siRNA in both cases. The analysis of the band intensities shows that in the wild-type cells, where both polyI:C and GAPDH were transfected, the knockdown effect decreases by 28% compared to the cells

transfected with GAPDH siRNA only. In the Dicer -/- cells cotransfected with both polyI:C and GAPDH siRNA, the decrease of the knockdown effect is 100% compared to the cells transfected with GAPDH siRNA only. Clearly the lack of Dicer activity increases the efficiency of polyI:C induced RNAi suppression, which might indicate that the inducing molecule is long dsRNA (as Dicer processes the long polyI:C chains into short fragments).
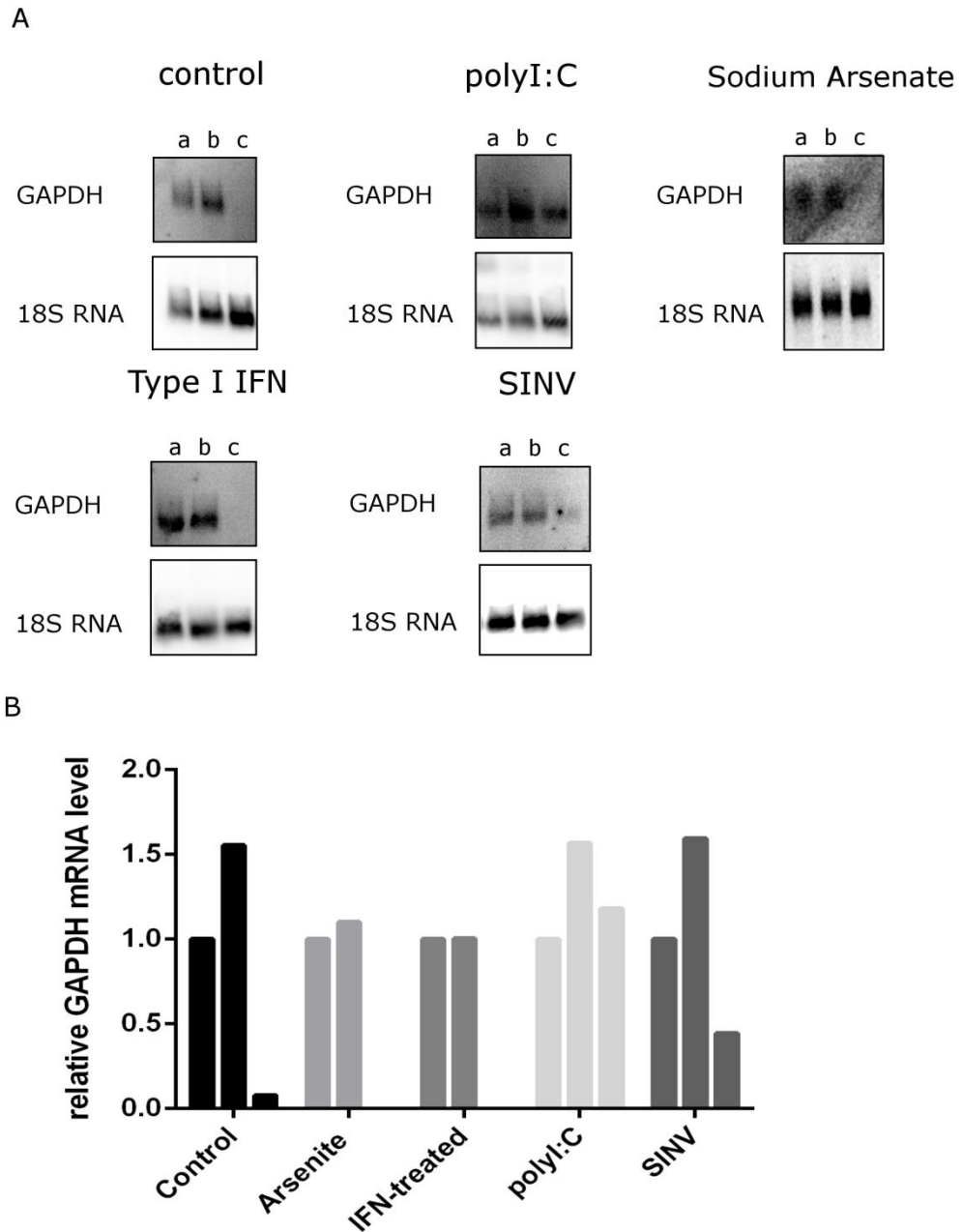
Figure 6.6 Double stranded RNA and SINV infection but not cellular stress and interferon can suppress RNA interference. (A) GAPDH knockdown assay was performed on cells subjected to different kinds of cellular stresses. **a:** mock treated cells, **b:** non-targeting siRNA treated cells, **c:** GAPDH siRNA treated cells. Double stranded RNA homologues (polyI:C) the RNAi machinery, demonstrated by the decreased efficiency of GAPDH siRNA. SINV infection shows a slight suppression, which needs to be investigated in the future. 18S RNA blot is shown for equal loading. (B) Densitometric analysis of the Northern blots. type I IFN treatment did not affect RNAi activity, but 43% of the control level GAPDH mRNA expression was restored in SINV infected, GAPDH siRNA treated samples.
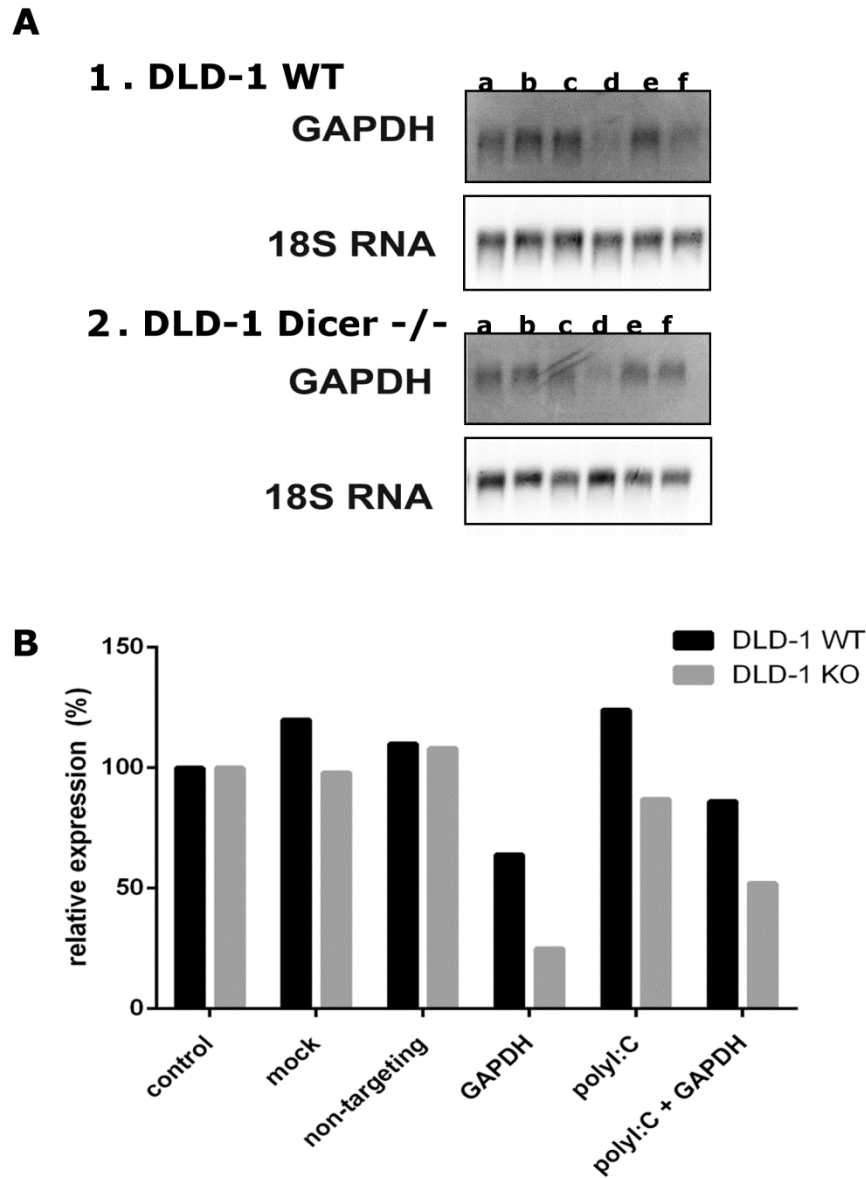
Figure 6.7 Suppression of RNAi in polyI:C treated cells is not due to saturation of Dicer with dsRNA. A.) The GAPDH knockdown assay was repeated using DLD-1 Dicer wild-type and KO cells, and the results are similar to the previous experiments. **a:** control cells, **b:** mock treated cells, **c:** non-targeting siRNA treated cells, **d:** GAPDH siRNA treated cells, **e**: polyI:C treated cells, **f:** polyI:C/GAPDH siRNA treated cells. The blots show strong GAPDH signal in the polyI:C-GAPDH siRNA cotransfected samples, while almost no signal in the GAPDH siRNA treated samples. 18S RNA blot is shown for equal loading. **B.)** densitometric analysis of the Northern blot. The graphs shows similar

trends on both Dicer -/- and WT cells, namely the restoration of GAPDH mRNA signal in polyI:C, GAPDH siRNA co-transfected cells.

6.3.4. The Effect of N^{pro} on RNAi

N^{pro} is the N-terminal protease of the Classical Swine Fever Virus (CSFV) of the Pestivirus family. This is a unique cysteine protease with no homologues in any other organism. It is a multifunctional viral protein that is responsible, among other things, for the autocatalytic cleavage of the virus polyprotein, and more importantly, the degradation of interferon response factor (IRF3). This renders the interferon system inoperable, facilitating virus replication (Bauhofer et al. 2007). N^{pro} also inhibits the transcription of IRF3 (La Rocca et al. 2005), demonstrating that the same host protein can be targeted by the virus at multiple levels. It has been shown to bind to IκBα and HAX-1, important regulators of apoptosis and immune response (Doceul et al. 2008; Johns et al. 2010).

Our laboratory demonstrated that N^{pro} binds to RNA Helicase A (RHA), and that it colocalizes with RHA in ribonuclear particles (unpublished results). RHA was shown to play an important role in RISC loading by other studies: RHA knockout HeLa cells had been reported to possess impeded RNAi response (Robb & Rana 2007b). It was our hypothesis that N^{pro} might be able to suppress the RNAi system by binding RHA.

Preparing cell lines that constantly and consistently express N^{pro} was proven difficult. After several approaches, I decided to use transiently expressing cell lines in all experiments, as N^{pro} expression diminished over time in every stably expressing cell lines created. This effect was observed regardless of the method N^{pro} was introduced (using stably expressing plasmids with selection agent or lentiviral vectors). N^{pro} is a cytotoxic protein and cells adapted to it by down-regulating its expression; this

phenomenon necessitated using freshly transfected transiently expressing cells. Plasmid encoding mCherry- N^{pro} was transfected 24hrs prior to the experiment to ensure strong expression of the protein, and the level of transfection was monitored using fluorescent microscopy. Fresh transfection before each experiment ensured a high, uniform expression of the viral protein (see Chapter 4).

This was the first series of knockdown assays performed, and at first I have used limited cycle RT-PCR to evaluate the results. The GAPDH assay was performed as described, and RT-PCR reactions were performed on 1 µg of the isolated total RNA using GAPDH, N^{pro} and β-Actin primers (see Methods). After separating the products on an agarose gel, there was a faint band present in the GAPDH siRNA treated N^{pro} expressing sample in all the replicate experiments, indicating the presence of GAPDH mRNA. This preliminary result indicated that N^{pro} might suppress the RNAi system (**Figure 6.8**).
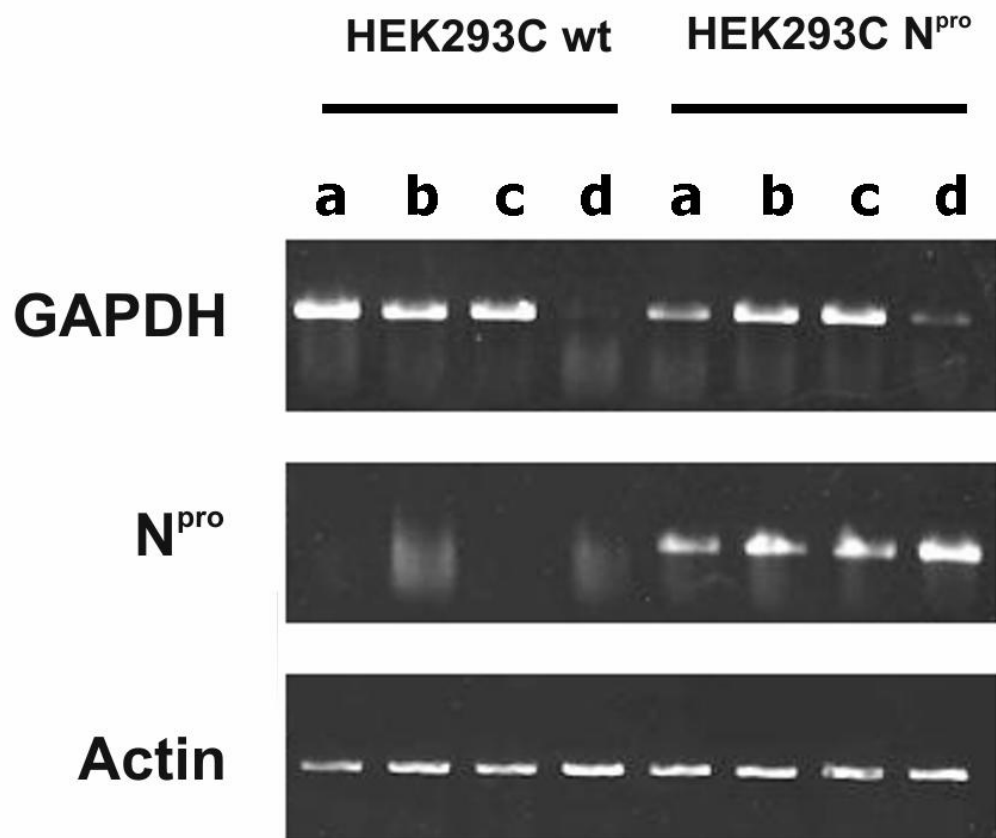
Figure 6.8 Preliminary results using limited cycle RT-PCR shows that in HEK293C cells expressing N^{pro} RNAi is suppressed. Control cells and N^{pro} expressing cells were used in a GAPDH knockdown assay to assert if N^{pro} effects RNAi. The RNA was analyzed using limited cycle RT-PCR. The PCR products were separated on an agarose gel. a **a:** control cells, **b:** mock treated cells, **c:** non-targeting siRNA treated cells, **d:** GAPDH siRNA treated cells. There was a stronger GAPDH band present in N^{pro} knockdown samples suggesting that N^{pro} suppresses RNAi. Actin RT-PCR is shown for equal loading.

The experiment was repeated using a much more accurate northern blotting technique to detect the mRNA signals, and in this system the band in the siRNA treated sample was not detectable (**Figure 6.9**). As northern blotting detects the RNA directly without reverse transcription or amplification steps, this is the accepted definite result. This convinced me to abandon the RT-PCR method, and switch to northern blotting.

Since N^{pro} is generally present in the whole cytosol and only translocates to RNP particles when the cells undergo cellular stress, or subjected to polyI:C, a double-stranded RNA homologue. It was hoped that the dsRNA homologue will provoke a strong cellular stress response, and this would translocate N^{pro} to the mRNPs. This way N^{pro} would be in the physical vicinity of the RNAi machinery, which is also localized in these granules. The results were surprising, however. As in previous experiments, N^{pro} by itself did not suppress RNAi, however, polyI:C did in both the control and treatment cells. The addition of a long dsRNA homologue, which is a very strong stress signal for the cell indicating viral infection, suppressed the RNAi answer. This result raises the very intriguing possibility of a crosstalk mechanism between the ancient RNAi and the more recent protein-based innate immunity.
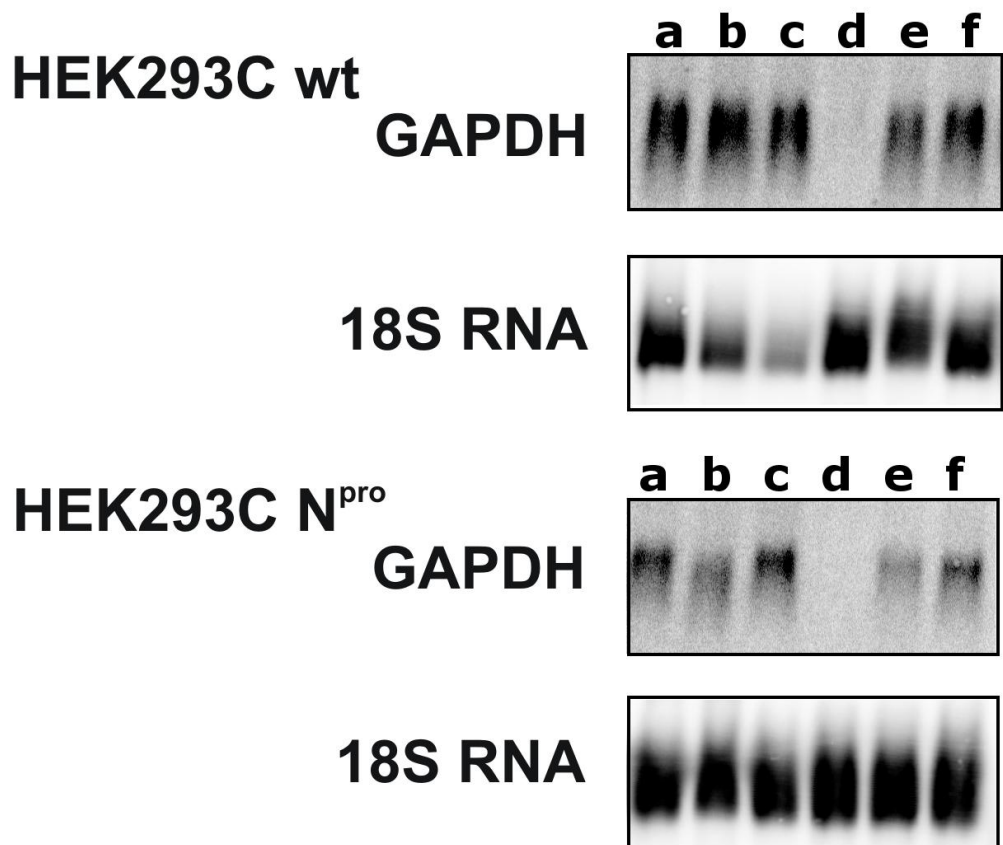
Figure 6.9 Northern blot analysis showed that N^{pro} does not suppress RNAi. The GAPDH knockdown assay was repeated and the RNA analyzed using Northern blotting. The results show that there is virtually no difference between control and Npro expressing cells. However, when polyI:C was added to the samples, we have seen a decrease of RNAi activity. The blot is a representative of many repeated experiments. **a:** control cells, **b:** mock treated cells, **c:** non-targeting siRNA treated cells, **d:** GAPDH siRNA treated cells, **e**: polyI:C treated cells, **f:** polyI:C/GAPDH siRNA treated cells. 18S RNA blot is shown for equal loading.

This result is in line with the study by Wiesen & Tomasi (2009) which showed down regulation of Dicer protein upon different cellular stress signals - such as the type I interferon response. With the GAPDH knockdown assay I have demonstrated a functional down regulation as well.

6.4. Discussion

Our hypothesis was that N^{pro}, a viral interferon inhibitor protein, may have suppressing effect on RNAi. There were two reasons behind this hypothesis. First and foremost, our laboratory has shown that N^{pro} binds to and colocalizes with a cellular helicase, RNA Helicase A (RHA, DDX9). This helicase has been shown to be important in RISC loading, as the RNA interference machinery was shown to be defective in cells depleted of RHA (Robb & Rana 2007b). This suggested that by binding RHA, N^{pro} might have a suppressing effect on RNA interference.

The second reason was the available literature on mammalian RNAi suppressors. Many publications demonstrated that viral interferon inhibitors may show RNAi suppression activity. N^{pro}, therefore, was an ideal candidate as a putative RNAi inhibitor.

I have developed a functional RNA interference assay to assay the effectiveness of putative RNAi suppressors. The assay works by monitoring the level of a chosen housekeeping gene (GAPDH). Small inhibitory RNA against this housekeeping gene is transfected into the cells in a level which should silence the gene. Should any treatment suppress RNA interference, the level of GAPDH mRNA should be increased over the detection limit in siRNA treated samples as well.

The first method of detection was semi-quantitative limited cycle RT-PCR. The assay had to be optimized for each primers; it was important to stop the polymerase chain reaction in the exponential phase, before it enters the plateau phase. This way the relative strength of the bands of the PCR products would give an indication of their relative abundance in the samples. As a control I have chosen β-actin, and I was monitoring the levels of GAPDH and N^{pro} in different samples.

The results were promising, as GAPDH mRNA was detected in GAPDH siRNA transfected N^{pro} expressing cells. This approach, however, is not ideal. It is only a semi-quantitative method, and another problem is that it does not detect RNA levels directly. RNA has to be reverse transcribed into cDNA first; the subsequent amplification steps of the polymerase chain reaction amplify small impurities present. Northern blotting can detect RNA directly, and was used to verify the preliminary results of the RT-PCR reactions.

Northern blotting, which detects RNA using end-labelled radioactive primer probes, found that N^{pro} does not affect RNA interference. Immunocytochemistry shows that N^{pro} is diffused in the cytosol of transfected cells, while both RHA and the RNAi machinery are located in distinct cytoplasmic granules. By subjecting the cells to stress signals, we hoped to bring N^{pro} into these granules, so that it may be able to interact with RHA and other proteins.

PolyI:C is a double stranded RNA homologue, and is widely used as an immunostimulant. Since double stranded RNA is a hallmark of viral replication, it is a very potent danger sign for the cell, which is detected by a host of different receptors (PKR, RIG-I, Toll-like receptor 3/7/8, OAS, etc.) By cotransfecting it into cells along with GAPDH siRNA it was hoped that any effects N^{pro} might have would materialize.

The results, however, showed that while N^{pro} did not have any effect on RNAi even under these circumstances, polyI:C itself did. As soon as the cells detected dsRNA, the effectiveness of siRNA mediated RNAi decreased, and the levels of GAPDH mRNA increased comparable to the control mRNA levels. This was a very intriguing and unexpected finding, which pointed to the possibility of crosstalk between RNA interference and the innate immunity.

The study by Robb & Rana (2007b) identified RNA Helicase A as a crucial player in RISC loading. Using a similar knockdown assay they found that RHA depleted cells exhibit an impaired RNAi response. I repeated this experiment using both HEK293C and HeLa cells, but the results were the same in both cases: RHA depleted cells did not have any decrease in silencing efficiency. The assays used in both cases are very similar; the Robb study used a transgene (GFP) as an indicator and Lipofectamine 2000 as a transfection reagent, whereas I used a housekeeping gene (GAPDH) and JetPrime. Nevertheless these factors do not explain the different results of the two studies.

To establish where this crosstalk happens between the two systems, HEK293C cells were subjected to different types of cellular stresses before repeating the GAPDH assay again. Arsenate and type I interferons did not have any effect, whereas SINV infection was shown to repress the silencing machinery's efficiency. Both polyI:C and Sindbis virus had similar effects on RNA interference; this suggests that the effect is due to the cellular reaction to viral infection. The lack of effect upon arsenate stress suggests that the responsible pathway is not the PKR pathway, as both act through Eukaryotic Initiation Factor 2-α (eIF2α) phosphorylation and translational repression. Lack of effect of type I interferon stimulation suggests that the crosstalk between the innate immunity and the RNA interference machinery happens early in the interferon pathway.

This can happen possibly at the PAMP receptor level, before the stimulation of IFNAR. Both the cytosolic RNA sensors (RIG-I family of receptors) and Dicer are members of the DEAD box family of helicases, and act as PRRs in a diverse range of organisms from plants to mammals. These findings indicate a crosstalk between these proteins in mammalian cells that makes sure that Dicer activity does not diminish the pool of dsRNA available for PRRs of the immune system.

7. Discussion

7.1. Overview

As reviewed in Chapter 1, it is a well-established fact that in plants and invertebrates RNAi acts as a primary innate immune response against viruses. First, vsRNA can be isolated and characterized from these organisms. Second, if RNAi is rendered inoperable, viral yields increase. Third, viruses of these organisms encode RNAi suppressors (VSRs). Fourth, the RNAi response usually has either an amplification mechanism, or a way to spread the RNAi response between cells, or both. (A new study by Cohen & Xiong (2011) describes a mammalian mechanism that is capable of spreading the RNAi response.) Fifth, the genes of siRNA pathway evolve faster than the genes involved in the miRNA pathway, which indicates a sort of "arms race" between virus and host. (The scope of this study did not include analysis of the evolutionary speed of different mammalian and viral genes.)

7.2. Cellular miRNA pathways are unaffected by SINV at the early stages of infection

The sequencing results show that svRNA is not produced from the SINV genome by the RNAi machinery in infected cells, and this argues that svRNAs are not used in mammalian cells against SINV infection. Sindbis virus is a good choice to test this hypothesis, as it is a positive stranded RNA virus, readily infects a wide range of cells, and most importantly, it was demonstrated in mosquitoes that it lacks RNAi suppressors (Campbell et al. 2008). The abundance of RNA mapping to the SINV genome was low in the sequencing data, and none of these sequences could be verified with northern blotting, even though highly sensitive LNA and riboprobes were used. In organisms where the role of svRNA was confirmed (such as plants and invertebrates), high-

throughput sequencing of virus infected cells results in very high number of reads mapping to the virus genome, which are readily detected using northern blotting.

MicroRNAs were found not to be effected by SINV infection in the early stages of viral infection (0-6hpi). We have not managed to find differentially expressed miRNAs in the sequencing data, and northern blot verification only reinforced this result.

7.3. siRNA pathway is suppressed in response to virus infection

Double stranded RNA and SINV infection showed that the siRNA pathway is suppressed during RNA virus infection at 24hpi. This effect does not seem to be Dicer-specific, as Dicer -/- cells show similar suppressing effect.

Based on the sequencing data and the northern blot validations, we can also state that the miRNA pathway is not affected in the early stages of infection. Northern blot analyses performed on longer time-series experiments (0-24hpi) showed that the levels of selected miRNAs do not change (data not shown). This hints that the miRNA pathway is not affected on a longer time-scale, either.

These results are incomplete and need further study to interpret them. My hypothesis for the siRNA pathway suppression is the importance of availability of dsRNA for the innate immune system (**Figure 7.1**). During the early stages of virus infection it is imperative that the cell effectively detects viral dsRNA. This might be assisted by the selective down regulation of the siRNA pathway, to prevent Dicer to process the long form of viral dsRNA into short fragments which are undetectable for the innate immunity. On the other hand, successful siRNA treatments are being developed against viral infections which demonstrate that the siRNA system is functional at some level, but only if it administered *prior* to infection. Unlike polyI:C, SINV infection did not cause complete suppression of the siRNA pathway. The

difference may be explained by the differences between the two treatments. PolyI:C is a very strong immune stimulant, and the cells were subjected to a high concentration; SINV infection, however is more close to the physiological conditions which virus infected cells are subjected to.

High throughput sequencing should be repeated at later time points (16, 24, 72hpi) to establish the changes in miRNA expression profiles, and to look for potential vsRNA sequences. (The costs of sequencing have gone down considerably in the last year.)
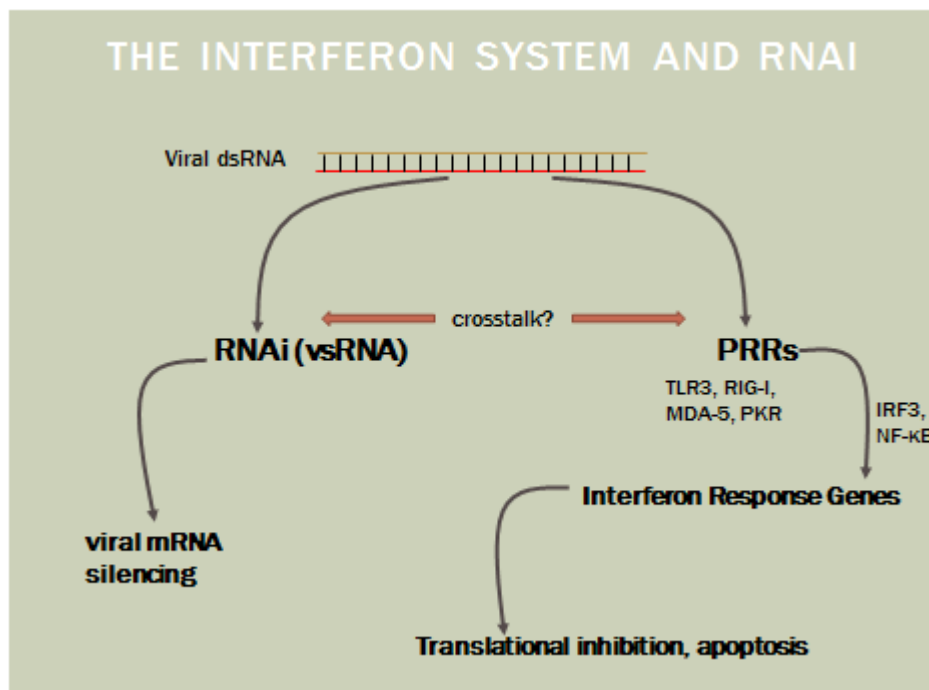
Figure 7.1. The proposed interaction between RNA interference and the innate immunity. dsRNA is a viral replication intermediate which is a substrate for Dicer and also a very important ligand for the pattern recognition receptors of the innate immunity. Dicer processes the long form of dsRNA (which is detectable to PRRs) into short, 20-23mer fragments, which are not detectable by the PRRs of innate immunity. This fact puts both systems into direct competition with each other for the same substrate/ligand, and a there needs to be a mechanism in place which enables the cell to prioritize the innate immune response when dsRNA is detected.

7.4. The lack of Dicer has an enhancing effect on SINV replication

Studies on Sindbis replication showed several interesting phenomena. Dicer deficient cells showed a significant difference in accumulation of viral RNA and proteins, but this did not translate into higher viral loads. The reason for this is the fact that DLD-1 cells are not permissive to SINV release. Using a different Dicer -/- cell line would help to shed light onto this issue. The result that Dicer knockout cells are more permissible to viral infection corresponds to the findings of other studies (Triboulet et al. 2007). This, by itself, does not mean that RNAi acts in a similar way as in plants and invertebrates. MicroRNAs have been shown to have antiviral effects (C. H. Lecellier et al. 2005; Muller & J. L. Imler 2007), however it also has been argued that miRNAs cannot play a role in antiviral immunity, as viruses can evolve faster than the conservative miRNA sequences (Saumet & C.-H. Lecellier 2006). It is true that any exogenous sequence targeting by human miRNA is most likely a fortuitous exception to the rule, but microRNAs may have non-virus specific effects on helping the cell establish an antiviral state. Another possibility is that Dicer –and the lack of it- has an indirect effect on viral replication. Our results, however, showed no differentially expressed miRNAs in the early stages of infection in HEK293C cells.

Dicer is an essential component of the cell homeostasis, which is demonstrated by the lethal phenotype of the Dicer -/- animals. The lack of Dicer –or even severely reduced Dicer activity- impacts the fitness of cells in a profound and negative way. This might cause the cells to be less able to mount an effective antiviral response, making it easier for the virus to replicate.

7.5. The lack of RHA has an enhancing effect on SINV replication

RHA depleted cells were shown to be significantly more permissible for virus replication; the virus titres measured from RHA knockdown cells were higher than in control cells. This finding underlies the role of RHA in defence against alphaviruses. As previous studies demonstrated the role of RHA in RISC loading, and showed that RHA-depleted cells have impeded RNAi response, there was a possibility that the observed effect of RHA above is carried out through the RNAi system, rather than the innate immunity. However, RHA-mediated RNAi suppression was not detected in our RNAi assay system under very similar circumstances. This suggests some sort of redundancy built into RISC loading system, or that RHA is not as essential as the previous study had shown. The cell types used, and the nature of the assay were very similar in both assays.

Further studies are needed to determine how RHA affects viral replication.

7.6. The lack of IRF3 has no effect on SINV replication

N^{pro}, a pestivirus protein, was used to decrease the levels of cellular IFR3, a crucial member of the signalling pathway leading to type I IFN-induction. The levels of IRF3 and the presence of N^{pro} had no visible effect on viral loads. This argues that SINV already has mechanisms in place to inhibit the type I IFN response, and the addition of another IFN inhibitor, N^{pro}, does not give a significant boost for the virus.

7.7. N^{pro} has no VSR function in mammalian cells

Since many viral IFN inhibitors were shown to be putative VSRs, and N^{pro} was shown to interact with RHA, an important player in RISC loading, it was interesting to take a look at the role of N^{pro} in the RNAi process. Functional RNAi assay showed that neither N^{pro} nor RHA have any effect on silencing. However, when polyI:C, a synthetic double stranded RNA analogue was used, I found that RNAi is inhibited. PolyI:C was

used to help N^{pro} localize to stress granules, as it was expected that it might help it interact with the members of the RNAi machinery which are also localized here. The results were exactly the opposite expected: polyI:C by itself was enough to suppress silencing.

Dicer -/- cell line helped to determine if this effect was the result overwhelming cells with dsRNA, which, in turn, saturated the RNAi pathway, or if it is the result of a specific crosstalk between RNAi system and the dsRNA sensors. The results from Dicer -/- cells indicate that the latter hypothesis is more likely.

7.8. The next steps

7.8.1. Sequencing

Further experiments would include the repetition of sequencing at several time points (0-4-6-24-48-72hpi) in triplicates using several cell lines. The later time points would make it possible to monitor the longer-term changes in both miRNA and vsRNA profiles, and the biological replicates would make sure that any effect detected is reproducible.

There is a possibility that later time points vsRNA may appear in the samples. This is unlikely; most authors who argue in favour of RNAi being a part of the innate immune response hypothesize that it serves as an immediate response until the protein based immunity takes over, but it is a possibility. It is also worth to sequence the small RNA populations isolated from different cell lines, as HEK293C is a tissue culture adapted line. Primary cells (HUVEC, for example), are attractive targets, and also embryonic stem cells, as they lack the IFN system and potentially use RNAi against

viral invaders. It would be very interesting to see if embryonic stem cells use RNAi against virus infection, unlike somatic cells from the same organism.

7.8.2. Determination of the nature of crosstalk between innate immunity and RNAi

The other important issue to address is the nature of the proposed crosstalk between the RNA interference machinery and innate immunity. There are no results yet that indicate the mechanism as of yet.

My hypothesis is focused on Dicer as a potential partner in this crosstalk. Dicer belongs to the family of Dead/Box helicases, the same family of proteins where the RIG-I and MDA-5 cytoplasmic PAMP receptors belong to. In invertebrates and plants Dicer fulfils the same role as RIG-I does in mammals: detection of viral RNA and activation of antiviral signalling pathways. It has been proposed that these helicases are members of an evolutionary conserved group of PAMP receptors. It might be possible that Dicer is able to signal into any of the signalling pathways of the type I IFN response, or the other way around: mammalian PAMP receptor Dead/Box helicases communicate with the RNAi pathway. The fact that Dicer -/- cells show similar suppression of RNAi as the control cells, complicates this issue. It is important to remember, however, these cells do have Dicer present, but this protein has impeded dicing function due to a point mutation. It is possible that while Dicer is unable to effectively cleave RNA, it might still be able to play its role in the signalling pathways important for the RNAi suppressing effect. Using Dicer depleted cells, or cell lines where Dicer has been rendered dysfunctional in a different way, it might be possible to determine if this is the case. Another, related question is if human Dicer can distinguish between external, viral RNA and pre-miRNA. Organisms, in which RNAi has been

proven to be a form of innate immunity, have several Dicer homologues which have different –although overlapping- functions.

Once these questions have been answered, it will be possible to map the exact signalling pathway leading to RNAi suppression. It is also possible to start looking for the connection between innate immunity and RNAi from the side of innate immunity. Cells, which are incapable of mounting an effective type I IFN response, showed higher concentration of vsRNA in studies. (Parameswaran et al. 2010) It would be interesting to see if RIG-I and other cytoplasmic PAMP receptor deficient cells produce vsRNA. As mentioned, embryonic stem cells are also very good candidates for cells that potentially use RNAi against viruses, as they do not mount interferon response, and have been shown to fight transposons and retro-transposons using RNAi.

The next step is to determine is the mechanism of suppression. As described previously, other studies showed that the level of Dicer decreased in response to type I IFN and cellular stress. In my studies I have shown a functional suppression of the siRNA pathway as well, which worked in wild type and Dicer -/- cells. It is not yet certain which step of the RNAi response is suppressed, but these results indicate that the suppression works in multiple levels of the RNAi system. (Most likely the process of RISC loading, or RISC function itself is affected.)

8. References

Ahluwalia, J.K., Khan, S.Z., Soni, K., Rawat, P., Gupta, A., Hariharan, M., Scaria, V., Lalwani, M., Pillai, B., Mitra, D., et al. (2008). Human cellular microRNA hsa-miR-29a interferes with viral nef protein expression and HIV-1 replication. Retrovirology *5*, 117.

Aliyari, R., and Ding, S.-W. (2009). RNA-based viral immunity initiated by the Dicer family of host immune receptors. Immunol. Rev *227*, 176–188.

Aliyari, R., Wu, Q., Li, H.-W., Wang, X.-H., Li, F., Green, L.D., Han, C.S., Li, W.-X., and Ding, S.-W. (2008). Mechanism of Induction and Suppression of Antiviral Immunity Directed by Virus-Derived Small RNAs in Drosophila. Cell Host & Microbe *4*, 387–397.

Anderson, P. (2006). RNA granules. The Journal of Cell Biology *172*, 803–808.

Andrew P. Byrnes,1 Joan E. Durbin,2 and Diane E. Griffin (2000). Control of Sindbis Virus Infection by Antibody in Interferon-Deficient Mice. J Virol *74*, 3905–3908.

Aravin, A.A., Klenov, M.S., Vagin, V.V., Bantignies, F., Cavalli, G., and Gvozdev, V.A. (2004). Dissection of a natural RNA silencing process in the Drosophila melanogaster germ line. Mol Cell Biol *24*, 6742 – 6750.

Attarzadeh-Yazdi, G., Fragkoudis, R., Chi, Y., Siu, R.W.C., Ülper, L., Barry, G., Rodriguez-Andres, J., Nash, A.A., Bouloy, M., Merits, A., et al. (2009). Cell-to-Cell Spread of the RNA Interference Response Suppresses Semliki Forest Virus (SFV) Infection of Mosquito Cell Cultures and Cannot Be Antagonized by SFV. Journal of Virology *83*, 5735–5748.

Bagasra, O., and Prilliman, K.R. (2004a). RNA interference: the molecular immune system. J. Mol. Histol *35*, 545–553.

Bagasra, O., and Prilliman, K.R. (2004b). RNA interference: The molecular immune system. Histochem J *35*, 545–553.

Bauhofer, O., Summerfield, A., Sakoda, Y., Tratschin, J.-D., Hofmann, M.A., and Ruggli, N. (2007). Classical Swine Fever Virus Npro Interacts with Interferon Regulatory Factor 3 and Induces Its Proteasomal Degradation. Journal of Virology *81*, 3087–3096.

Baum, A., Sachidanandam, R., and Garcia-Sastre, A. (2010). Preference of RIG-I for short viral RNA molecules in infected cells revealed by next-generation sequencing. Proceedings of the National Academy of Sciences *107*, 16303–16308.

Ben Berkhout, and Joost Haasnoot (2006). The interplay between virus infection and the cellular RNA interference machinery. FEBS Lett *580*, 2896–2902.

Bennasser, Y., Le, S.Y., Benkirane, M., and Jeang, K.T. (2005). Evidence that HIV-1 encodes an siRNA and a suppressor of RNA silencing. Immunity Flux capacitor *22*, 607 – 619.

Bergmann, M., Garcia-Sastre, A., Carnero, E., Pehamberger, H., Wolff, K., Palese, P., and Muster, T. (2000a). Influenza Virus NS1 Protein Counteracts PKR-Mediated Inhibition of Replication. J. Virol. *74*, 6203–6206.

Bergmann, M., Garcia-Sastre, A., Carnero, E., Pehamberger, H., Wolff, K., Palese, P., and Muster, T. (2000b). Influenza Virus NS1 Protein Counteracts PKR-Mediated Inhibition of Replication. J. Virol. *74*, 6203–6206.

Berkhout, B., and Jeang, K.T. (2007). RISCy business: MicroRNAs, pathogenesis, and viruses. J Biol Chem *282*, 26641 – 26645.

Blakqori, G., Delhaye, S., Habjan, M., Blair, C.D., Sánchez-Vargas, I., Olson, K.E., Attarzadeh-Yazdi, G., Fragkoudis, R., Kohl, A., Kalinke, U., et al. (2007). La Crosse Bunyavirus Nonstructural Protein NSs Serves To Suppress the Type I Interferon System of Mammalian Hosts. Journal of Virology *81*, 4991–4999.

Bucher, E., Hemmes, H., de Haan, P., Goldbach, R., and Prins, M. (2004). The influenza A virus NS1 protein binds small interfering RNAs and suppresses RNA silencing in plants. J Gen Virol *85*, 983–991.

Bürckstümmer, T., Baumann, C., Blüml, S., Dixit, E., Dürnberger, G., Jahn, H., Planyavsky, M., Bilban, M., Colinge, J., Bennett, K.L., et al. (2009). An orthogonal proteomic-genomic screen identifies AIM2 as a cytoplasmic DNA sensor for the inflammasome. Nat. Immunol *10*, 266–272.

Burke, C.W., Gardner, C.L., Steffan, J.J., Ryman, K.D., and Klimstra, W.B. (2009). Characteristics of alpha/beta interferon induction after infection of murine fibroblasts with wild-type and mutant alphaviruses. Virology *395*, 121–132.

C M Rice (1987). Production of infectious RNA transcripts from Sindbis virus cDNA clones: mapping of lethal mutations, rescue of a temperature-sensitive marker, and in vitro mutagenesis to generate defined mutants. J Virol. *61*, 3809–3819.

Campbell, C.L., Keene, K.M., Brackney, D.E., Olson, K.E., Blair, C.D., Wilusz, J., and Foy, B.D. (2008). Aedes aegypti uses RNA interference in defense against Sindbis virus infection. BMC Microbiol *8*, 47.

Carol D., B. (2011). Mosquito RNAi is the major innate immune pathway controlling arbovirus infection and transmission. Future Microbiology *6*, 265–277.

Carpenter, A., Jones, T., Lamprecht, M., Clarke, C., Kang, I., Friman, O., Guertin, D., Chang, J., Lindquist, R., Moffat, J., et al. (2006). CellProfiler: image analysis software for identifying and quantifying cell phenotypes. Genome Biology *7*, R100.

Chiu, Y.-L., and Rana, T.M. (2002). RNAi in Human Cells: Basic Structural and Functional Features of Small Interfering RNA. Mol Cell *10*, 549–561.

Cirimotich, C.M., Scott, J.C., Phillips, A.T., Geiss, B.J., and Olson, K.E. (2009). Suppression of RNA interference increases alphavirus replication and virus-associated mortality in Aedes aegypti mosquitoes. BMC Microbiology *9*, 49.

Cohen, H., and Xiong, M. (2011). Non-cell-autonomous RNA interference in mammalian cells: Implications for in vivo cell-based RNAi delivery. J RNAi Gene Silencing 456–463.

Collins, R.E., and Cheng, X. (2006). Structural and biochemical advances in mammalian RNAi. J. Cell. Biochem. *99*, 1251–1266.

Cullen, B.R. (2006a). Is RNA interference involved in intrinsic antiviral immunity in mammals? Nat Immunol *7*, 563 – 567.

Cullen, B.R. (2006b). Viruses and microRNAs. Nat Genet.

Cullen, B.R. (2013). MicroRNAs as mediators of viral evasion of the immune system. Nature Immunology *14*, 205–210.

Dhanushkodi, N.R., Mohankumar, V., and Raju, R. (2011). Sindbis virus induced phosphorylation of IRF3 in human embryonic kidney cells is not dependent on mTOR. Innate Immunity *18*, 325–332.

Ding, S.W., and Voinnet, O. (2007). Antiviral immunity directed by small RNAs. Cell *130*, 413 – 426.

Dixit, E., Boulant, S., Zhang, Y., Lee, A.S.Y., Odendall, C., Shum, B., Hacohen, N., Chen, Z.J., Whelan, S.P., Fransen, M., et al. (2010). Peroxisomes are signaling platforms for antiviral innate immunity. Cell *141*, 668–681.

Doceul, V., Charleston, B., Crooke, H., Reid, E., Powell, P.P., and Seago, J. (2008). The Npro product of classical swine fever virus interacts with I{kappa}B{alpha}, the NF-{kappa}B inhibitor. J Gen Virol *89*, 1881–1889.

Doench, J.G., Petersen, C.P., and Sharp, P.A. (2003). siRNAs can function as miRNAs. Gene Dev *17*, 438 – 442.

Du, L., Schageman, J.J., Subauste, M.C., Saber, B., Hammond, S.M., Prudkin, L., Wistuba, I.I., Ji, L., Roth, J.A., Minna, J.D., et al. (2009). miR-93, miR-98, and miR-197 Regulate Expression of Tumor Suppressor Gene FUS1. Molecular Cancer Research *7*, 1234–1243.

Dufour, J.H., Dziejman, M., Liu, M.T., Leung, J.H., Lane, T.E., and Luster, A.D. (2002). IFN-gamma-inducible protein 10 (IP-10; CXCL10)-deficient mice reveal a role for IP-10 in effector T cell generation and trafficking. J. Immunol. *168*, 3195–3204.

Farazi, T.A., Juranek, S.A., and Tuschl, T. (2008). The growing catalog of small RNAs and their association with distinct Argonaute/Piwi family members. Development *135*, 1201–1214.

Flint, S. (2004). Principles of virology : molecular biology, pathogenesis, and control of animal viruses (Washington D.C.: ASM Press).

Flynt, A., Liu, N., Martin, R., and Lai, E.C. (2009). Dicing of viral replication intermediates during silencing of latent Drosophila viruses. Proceedings of the National Academy of Sciences *106*, 5270–5275.

Forte, E., Salinas, R.E., Chang, C., Zhou, T., Linnstaedt, S.D., Gottwein, E., Jacobs, C., Jima, D., Li, Q.-J., Dave, S.S., et al. (2012). The Epstein-Barr Virus (EBV)-Induced Tumor Suppressor MicroRNA MiR-34a Is Growth Promoting in EBV-Infected B Cells. Journal of Virology *86*, 6889–6898.

Fragkoudis, R., Attarzadeh-Yazdi, G., Nash, A.A., Fazakerley, J.K., and Kohl, A. (2009). Advances in dissecting mosquito innate immune responses to arbovirus infection. Journal of General Virology *90*, 2061–2072.

Fuller-Pace, F.V. (2006). DExD/H box RNA helicases: multifunctional proteins with important roles in transcriptional regulation. Nucleic Acids Res. *34*, 4206–4215.

Gantier, M.P., Stunden, H.J., McCoy, C.E., Behlke, M.A., Wang, D., Kaparakis-Liaskos, M., Sarvestani, S.T., Yang, Y.H., Xu, D., Corr, S.C., et al. (2012). A miR-19 regulon that controls NF- B signaling. Nucleic Acids Research *40*, 8048–8058.

Garcia, S., Billecocq, A., Crance, J.-M., Prins, M., Garin, D., and Bouloy, M. (2006). Viral suppressors of RNA interference impair RNA silencing induced by a Semliki Forest virus replicon in tick cells. Journal of General Virology *87*, 1985–1989.

Gatignol, A., Lainé, S., and Clerzius, G. (2005). Dual role of TRBP in HIV replication and RNA interference: viral diversion of a cellular pathway or evasion from antiviral immunity? Retrovirology *2*, 65.

Gatto, G., Rossi, A., Rossi, D., Kroening, S., Bonatti, S., and Mallardo, M. (2008). Epstein-Barr virus latent membrane protein 1 trans-activates miR-155 transcription through the NF- B pathway. Nucleic Acids Research *36*, 6608–6619.

Ge, Q., Eisen, H.N., and Chen, J. (2004). Use of siRNAs to prevent and treat influenza virus infection. Virus Research *102*, 37–42.

Ghosh, Z., Mallick, B., and Chakrabarti, J. (2009). Cellular versus viral microRNAs in host–virus interaction. Nucleic Acids Research *37*, 1035–1048.

Gitlin, L., Barchet, W., Gilfillan, S., Cella, M., Beutler, B., Flavell, R.A., Diamond, M.S., and Colonna, M. (2006). Essential role of mda-5 in type I IFN responses to polyriboinosinic:polyribocytidylic acid and encephalomyocarditis picornavirus. Proc. Natl. Acad. Sci. U.S.A *103*, 8459–8464.

Gordon, K.H.J., and Waterhouse, P.M. (2006). Small RNA Viruses of Insects: Expression in Plants and RNA Silencing. In Advances in Virus Research, (Elsevier), pp. 459–502.

Gottwein, E., and Cullen, B.R. (2008). Viral and Cellular MicroRNAs as Determinants of Viral Pathogenesis and Immunity. Cell Host & Microbe *3*, 375–387.

Gregory, R.I., Yan, K., Amuthan, G., Chendrimada, T., Doratotaj, B., Cooch, N., and Shiekhattar, R. (2004). The Microprocessor complex mediates the genesis of microRNAs. Nature *432*, 235–240.

Griffiths-Jones, S., Saini, H.K., van Dongen, S., and Enright, A.J. (2008). miRBase: tools for microRNA genomics. Nucleic Acids Res. *36*, D154–158.

Gu, Y., Yang, Y., and Liu, Y. (2011). Imaging Early Steps of Sindbis Virus Infection by Total Internal Reflection Fluorescence Microscopy. Advances in Virology *2011*, 1–7.

Gupta, A., Gartner, J.J., Sethupathy, P., Hatzigeorgiou, A.G., and Fraser, N.W. (2006). Anti-apoptotic function of a microRNA encoded by the HSV-1 latency-associated transcript. Nature *442*, 82–85.

Haasnoot, J., Westerhout, E.M., and Berkhout, B. (2007a). RNA interference against viruses: strike and counterstrike. Nat. Biotechnol. *25*, 1435–1443.

Haasnoot, J., de, V.W., Geutjes, E.J., Prins, M., de, H.P., and Berkhout, B. (2007b). The Ebola virus VP35 protein is a suppressor of RNA silencing. PLoS Pathog *3*, e86.

Habjan, M., Andersson, I., Klingström, J., Schümann, M., Martin, A., Zimmermann, P., Wagner, V., Pichlmair, A., Schneider, U., Mühlberger, E., et al. (2008). Processing of genome 5' termini as a strategy of negative-strand RNA viruses to avoid RIG-I-dependent interferon induction. PLoS ONE *3*, e2032.

Haller, O., Kochs, G., and Weber, F. (2006). The interferon response circuit: Induction and suppression by pathogenic viruses. Virology *344*, 119–130.

Hamada, S., Satoh, K., Miura, S., Hirota, M., Kanno, A., Masamune, A., Kikuta, K., Kume, K., Unno, J., Egawa, S., et al. (2013). miR-197 induces epithelial-mesenchymal transition in pancreatic cancer cells by targeting p120 catenin. Journal of Cellular Physiology *228*, 1255–1263.

Han, J., Lee, Y., Yeom, K.-H., Kim, Y.-K., Jin, H., and Kim, V.N. (2004). The Drosha-DGCR8 complex in primary microRNA processing. Genes & Development *18*, 3016–3027.

Han, J., Lee, Y., Yeom, K.-H., Nam, J.-W., Heo, I., Rhee, J.-K., Sohn, S.Y., Cho, Y., Zhang, B.-T., and Kim, V.N. (2006). Molecular Basis for the Recognition of Primary microRNAs by the Drosha-DGCR8 Complex. Cell *125*, 887–901.

Harding, H.P., Zhang, Y., Bertolotti, A., Zeng, H., and Ron, D. (2000). Perk is essential for translational regulation and cell survival during the unfolded protein response. Mol. Cell *5*, 897–904.

Hariharan, M., Scaria, V., Pillai, B., and Brahmachari, S.K. (2005). Targets for human encoded microRNAs in HIV genes. Biochem. Biophys. Res. Commun *337*, 1214–1218.

Hassel, D., Cheng, P., White, M.P., Ivey, K.N., Kroll, J., Augustin, H.G., Katus, H.A., Stainier, D.Y.R., and Srivastava, D. (2012). MicroRNA-10 regulates the angiogenic behavior of zebrafish and human endothelial cells by promoting vascular endothelial growth factor signaling. Circ. Res. *111*, 1421–1433.

Henke, J.I., Goergen, D., Zheng, J., Song, Y., Schüttler, C.G., Fehr, C., Jünemann, C., and Niepmann, M. (2008). microRNA-122 stimulates translation of hepatitis C virus RNA. The EMBO Journal *27*, 3300–3310.

Ho, B.-C., Yu, S.-L., Chen, J.J.W., Chang, S.-Y., Yan, B.-S., Hong, Q.-S., Singh, S., Kao, C.-L., Chen, H.-Y., Su, K.-Y., et al. (2011). Enterovirus-Induced miR-141 Contributes to Shutoff of Host Protein Translation by Targeting the Translation Initiation Factor eIF4E. Cell Host & Microbe *9*, 58–69.

Ho, T., Pallett, D., Rusholme, R., Dalmay, T., and Wang, H. (2006). A simplified method for cloning of short interfering RNAs from Brassica juncea infected with Turnip mosaic potyvirus and Turnip crinkle carmovirus. Journal of Virological Methods *136*, 217–223.

Holcik, M., and Sonenberg, N. (2005). Translational control in stress and apoptosis. Nat Rev Mol Cell Biol *6*, 318–327.

Hornstein, E., Mansfield, J.H., Yekta, S., Hu, J.K.-H., Harfe, B.D., McManus, M.T., Baskerville, S., Bartel, D.P., and Tabin, C.J. (2005). The microRNA miR-196 acts upstream of Hoxb8 and Shh in limb development. Nature *438*, 671–674.

Hou, W., Tian, Q., Zheng, J., and Bonkovsky, H.L. (2010). MicroRNA-196 represses Bach1 protein and hepatitis C virus gene expression in human hepatoma cells expressing hepatitis C viral proteins. Hepatology *51*, 1494–1504.

Ishii, K.J., Koyama, S., Nakagawa, A., Coban, C., and Akira, S. (2008). Host Innate Immune Receptors and Beyond: Making Sense of Microbial Infections. Cell Host Microbe *3*, 352–363.

Itaya, A., Zhong, X., Bundschuh, R., Qi, Y., Wang, Y., Takeda, R., Harris, A.R., Molina, C., Nelson, R.S., and Ding, B. (2007). A Structured Viroid RNA Serves as a Substrate for Dicer-Like Cleavage To Produce Biologically Active Small RNAs but Is Resistant to RNA-Induced Silencing Complex-Mediated Degradation. J. Virol. *81*, 2980–2994.

J H Strauss and E G Strauss The alphaviruses: gene expression, replication, and evolution.

Jackson, R.J., and Standart, N. (2007). How Do MicroRNAs Regulate Gene Expression? Sci. STKE *2007*, re1–.

Jaronczyk, K., Carmichael, J.B., and Hobman, T.C. (2005). Exploring the functions of RNA interference pathway proteins: some functions are more RISCy than others? Biochem. J *387*, 561–571.

Jin, M.S., and Lee, J.-O. (2008). Structures of the Toll-like Receptor Family and Its Ligand Complexes. Immunity *29*, 182–191.

Jinek, M., and Doudna, J.A. (2009). A three-dimensional view of the molecular machinery of RNA interference. Nature *457*, 405–412.

Johns, H.L., Doceul, V., Everett, H., Crooke, H., Charleston, B., and Seago, J. (2010). The classical swine fever virus N-terminal protease Npro binds to cellular HAX-1. Journal of General Virology *91*, 2677–2686.

Jones, T.R., Carpenter, A.E., Lamprecht, M.R., Moffat, J., Silver, S.J., Grenier, J.K., Castoreno, A.B., Eggert, U.S., Root, D.E., Golland, P., et al. (2009). Scoring diverse cellular morphologies in image-based screens with iterative feedback and machine learning. Proceedings of the National Academy of Sciences *106*, 1826–1831.

Jopling, C.L., Yi, M., Lancaster, A.M., Lemon, S.M., and Sarnow, P. (2005). Modulation of hepatitis C virus RNA abundance by a liver-specific MicroRNA. Science *309*, 1577–1581.

JOSHUA-TOR, L. (2006). The Argonautes. Cold Spring Harbor Symposia on Quantitative Biology *71*, 67–72.

Kato, H., Takeuchi, O., Sato, S., Yoneyama, M., Yamamoto, M., Matsui, K., Uematsu, S., Jung, A., Kawai, T., Ishii, K.J., et al. (2006). Differential roles of MDA5 and RIG-I helicases in the recognition of RNA viruses. Nature *441*, 101–105.

Kawai, T., and Akira, S. (2006). Innate immune recognition of viral infection. Nat Immunol *7*, 131–137.

Kawai, T., and Akira, S. (2007). Antiviral Signaling Through Pattern Recognition Receptors. J Biochem *141*, 137–145.

Kemp, C., and Imler, J.-L. (2009). Antiviral immunity in drosophila. Current Opinion in Immunology *21*, 3–9.

Kim, K., Lee, Y.S., and Carthew, R.W. (2007). Conversion of pre-RISC to holo-RISC by Ago2 during assembly of RNAi complexes. RNA *13*, 22–29.

Kim, Y., Lee, S., Kim, S., Kim, D., Ahn, J.-H., and Ahn, K. (2012). Human Cytomegalovirus Clinical Strain-Specific microRNA miR-UL148D Targets the Human Chemokine RANTES during Infection. PLoS Pathogens *8*, e1002577.

Klimstra, W.B., Ryman, K.D., Bernard, K.A., Nguyen, K.B., Biron, C.A., and Johnston, R.E. (1999). Infection of Neonatal Mice with Sindbis Virus Results in a Systemic Inflammatory Response Syndrome. J. Virol. *73*, 10387–10398.

Koyama, S., Ishii, K.J., Coban, C., and Akira, S. (2008). Innate immune response to viral infection. Cytokine *43*, 336–341.

Kutter, C., and Svoboda, P. (2008). miRNA, siRNA, piRNA: Knowns of the unknown. RNA Biol *5*, 181–188.

Langland, J.O., Pettiford, S., Jiang, B., and Jacobs, B.L. (1994). Products of the porcine group C rotavirus NSP3 gene bind specifically to double-stranded RNA and inhibit activation of the interferon-induced protein kinase PKR. Journal of Virology *68*, 3821–3829.

Lawrence, P., and Rieder, E. (2009). Identification of RNA helicase A as a new host factor in the replication cycle of foot-and-mouth disease virus. J. Virol. *83*, 11356–11366.

Lecellier, C.H., Dunoyer, P., Arar, K., Lehmann-Che, J., Eyquem, S., Himber, C., Saib, A., and Voinnet, O. (2005). A cellular microRNA mediates antiviral defense in human cells. Science *308*, 557 – 560.

Lehmann, S.M., Krüger, C., Park, B., Derkow, K., Rosenberger, K., Baumgart, J., Trimbuch, T., Eom, G., Hinz, M., Kaul, D., et al. (2012). An unconventional role for miRNA: let-7 activates Toll-like receptor 7 and causes neurodegeneration. Nature Neuroscience *15*, 827–835.

Leonard, J.N., and Schaffer, D.V. (2005). Antiviral RNAi therapy: emerging approaches for hitting a moving target. Gene Ther *13*, 532–540.

Levy, D.E., and Garc�a-Sastre, A. (2001). The virus battles: IFN induction of the antiviral state and mechanisms of viral evasion. Cytokine & Growth Factor Reviews *12*, 143–156.

Lewis, B.P., Burge, C.B., and Bartel, D.P. (2005). Conserved Seed Pairing, Often Flanked by Adenosines, Indicates that Thousands of Human Genes are MicroRNA Targets. Cell *120*, 15–20.

Li, F., and Ding, S.-W. (2006). Virus counterdefense: diverse strategies for evading the RNA-silencing immunity. Annu. Rev. Microbiol *60*, 503–531.

Li, H.-W., and Ding, S.-W. (2005). Antiviral silencing in animals. FEBS Letters *579*, 5965–5973.

Li, W.-X., Li, H., Lu, R., Li, F., Dus, M., Atkinson, P., Brydon, E.W.A., Johnson, K.L., García-Sastre, A., Ball, L.A., et al. (2004a). Interferon antagonist proteins of influenza and vaccinia viruses are suppressors of RNA silencing. Proceedings of the National Academy of Sciences of the United States of America *101*, 1350–1355.

Li, W.-X., Li, H., Lu, R., Li, F., Dus, M., Atkinson, P., Brydon, E.W.A., Johnson, K.L., García-Sastre, A., Ball, L.A., et al. (2004b). Interferon antagonist proteins of influenza and vaccinia viruses are suppressors of RNA silencing. Proceedings of the National Academy of Sciences of the United States of America *101*, 1350–1355.

Lichner, Z., Silhavy, D., and Burgyan, J. (2003). Double-stranded RNA-binding proteins could suppress RNA interference-mediated antiviral defences. J Gen Virol *84*, 975–980.

Lin, L., Li, Y., Pyo, H.-M., Lu, X., Raman, S.N.T., Liu, Q., Brown, E.G., and Zhou, Y. (2012). Identification of RNA Helicase A as a Cellular Factor That Interacts with Influenza A Virus NS1 Protein and Its Role in the Virus Life Cycle. Journal of Virology *86*, 1942–1954.

Linssen, B., Richard M. Kinney, Patricia Aguilar, Kevin L. Russell, Douglas M. Watts, Oskar-Rüger Kaaden, and Martin Pfeffer (2000). Development of Reverse Transcription-PCR Assays Specific for Detection of Equine Encephalitis Viruses. J. Clin. Microbiol. *38*, 1527–1535.

Liu, N., Landreh, M., Cao, K., Abe, M., Hendriks, G.-J., Kennerdell, J.R., Zhu, Y., Wang, L.-S., and Bonini, N.M. (2012). The microRNA miR-34 modulates ageing and neurodegeneration in Drosophila. Nature *482*, 519–523.

Liu, Q., Rand, T.A., Kalidas, S., Du, F., Kim, H.-E., Smith, D.P., and Wang, X. (2003). R2D2, a bridge between the initiation and effector steps of the Drosophila RNAi pathway. Science *301*, 1921–1925.

Loo, Y.M. (2006). Viral and therapeutic control of IFN-[bgr] promoter stimulator 1 during hepatitis C virus infection. Proc. Natl Acad. Sci. USA *103*, 6001–6006.

M. Keene, K., and E. Olson, K. (2004). RNA interference acts as a natural antiviral response to O'nyong-nyong virus (Alphavirus; Togaviridae) infection of Anopheles gambiae. PNAS *101*, 17240–17245.

Ma, F., Xu, S., Liu, X., Zhang, Q., Xu, X., Liu, M., Hua, M., Li, N., Yao, H., and Cao, X. (2011). The microRNA miR-29 controls innate and adaptive immune responses to intracellular bacterial infection by targeting interferon-γ. Nat. Immunol. *12*, 861–869.

Macrae, I.J., Zhou, K., Li, F., Repic, A., Brooks, A.N., Cande, W.Z., Adams, P.D., and Doudna, J.A. (2006). Structural basis for double-stranded RNA processing by Dicer. Science *311*, 195–198.

MacRae, I.J., and Doudna, J.A. (2007). Ribonuclease revisited: structural insights into ribonuclease III family enzymes. Current Opinion in Structural Biology *17*, 138–145.

MacRae, I.J., Zhou, K., and Doudna, J.A. (2007). Structural determinants of RNA recognition and cleavage by Dicer. Nat Struct Mol Biol *14*, 934–940.

Malathi, K., Dong, B., Gale, M., and Silverman, R.H. (2007). Small self-RNA generated by RNase L amplifies antiviral innate immunity. Nature *448*, 816–819.

Manni, I., Artuso, S., Careccia, S., Rizzo, M.G., Baserga, R., Piaggio, G., and Sacchi, A. (2009). The microRNA miR-92 increases proliferation of myeloid cells and by targeting p63 modulates the abundance of its isoforms. The FASEB Journal *23*, 3957–3966.

Mardis, E.R. (2008). Next-Generation DNA Sequencing Methods. Annu. Rev. Genom. Human Genet. *9*, 387–402.

Marshall, O.J. (2004). PerlPrimer: cross-platform, graphical primer design for standard, bisulphite and real-time PCR. Bioinformatics *20*, 2471–2472.

McKnight, K.L., Simpson, D.A., Lin, S.C., Knott, T.A., Polo, J.M., Pence, D.F., Johannsen, D.B., Heidner, H.W., Davis, N.L., and Johnston, R.E. (1996). Deduced consensus sequence of Sindbis virus strain AR339: mutations contained in laboratory strains which affect cell culture and in vivo phenotypes. J. Virol. *70*, 1981–1989.

Meister, G., Landthaler, M., Patkaniowska, A., Dorsett, Y., Teng, G., and Tuschl, T. (2004). Human Argonaute2 Mediates RNA Cleavage Targeted by miRNAs and siRNAs. Mol Cell *15*, 185–197.

Metzker, M.L. (2009). Sequencing technologies — the next generation. Nat Rev Genet *11*, 31–46.

Moazed, D. (2009). Small RNAs in transcriptional gene silencing and genome defence. Nature *457*, 413–420.

Mohorianu, I., Schwach, F., Jing, R., Lopez-Gomollon, S., Moxon, S., Szittya, G., Sorefan, K., Moulton, V., and Dalmay, T. (2011). Profiling of short RNAs during fleshy fruit development reveals stage-specific sRNAome expression patterns. The Plant Journal *67*, 232–246.

Molnar, A., Csorba, T., Lakatos, L., Varallyay, E., Lacomme, C., and Burgyan, J. (2005). Plant Virus-Derived Small Interfering RNAs Originate Predominantly from Highly Structured Single-Stranded Viral RNAs. Journal of Virology *79*, 7812–7818.

Moxon, S., Schwach, F., Dalmay, T., MacLean, D., Studholme, D.J., and Moulton, V. (2008). A toolkit for analysing large-scale plant small RNA datasets. Bioinformatics *24*, 2252–2253.

Muller, S., and Imler, J.L. (2007). Dicing with viruses: microRNAs as antiviral factors. Immunity *27*, 1 – 3.

Myles, K.M., Morazzani, E.M., and Adelman, Z.N. (2009). Origins of alphavirus-derived small RNAs in mosquitoes. RNA Biology *6*, 387–391.

Nakhaei, P., Genin, P., Civas, A., and Hiscott, J. (2009). RIG-I-like receptors: sensing and responding to RNA virus infection. Semin. Immunol *21*, 215–222.

Nava, V.E., Rosen, A., Veliuona, M.A., Clem, R.J., Levine, B., and Hardwick, J.M. (1998). Sindbis virus induces apoptosis through a caspase-dependent, CrmA-sensitive pathway. J. Virol. *72*, 452–459.

Nover, L., Scharf, K.D., and Neumann, D. (1983). Formation of cytoplasmic heat shock granules in tomato cell cultures and leaves. Molecular and Cellular Biology *3*, 1648–1655.

O'Malley, P., and Mathews, M. (1986). A mechanism for the control of protein synthesis by adenovirus VA RNAI. Cell *44*, 391–400.

Obbard, D.J., Jiggins, F.M., Halligan, D.L., and Little, T.J. (2006). Natural Selection Drives Extremely Rapid Evolution in Antiviral RNAi Genes. Current Biology *16*, 580–585.

Obbard, D.J., Gordon, K.H.J., Buck, A.H., and Jiggins, F.M. (2009). The evolution of RNAi as a defence against viruses and transposable elements. Philosophical Transactions of the Royal Society B: Biological Sciences *364*, 99–115.

Otsuka, M., Jing, Q., Georgel, P., New, L., Chen, J., Mols, J., Kang, Y.J., Jiang, Z., Du, X., Cook, R., et al. (2007). Hypersusceptibility to vesicular stomatitis virus infection in Dicer1-deficient mice is due to impaired miR24 and miR93 expression. Immunity *27*, 123 – 134.

Parameswaran, P., Sklan, E., Wilkins, C., Burgon, T., Samuel, M.A., Lu, R., Ansel, K.M., Heissmeyer, V., Einav, S., Jackson, W., et al. (2010). Six RNA Viruses and Forty-One Hosts: Viral Small RNAs and Modulation of Small RNA Repertoires in Vertebrate and Invertebrate Systems. PLoS Pathog *6*, e1000764.

PERRY, A.K., CHEN, G., ZHENG, D., TANG, H., and CHENG, G. (2005). The host type I interferon response to viral and bacterial infections. Cell Res *15*, 407–422.

Pfeffer, S., Zavolan, M., Grässer, F.A., Chien, M., Russo, J.J., Ju, J., John, B., Enright, A.J., Marks, D., Sander, C., et al. (2004). Identification of virus-encoded microRNAs. Science *304*, 734–736.

Pichlmair, A., Schulz, O., Tan, C.-P., Rehwinkel, J., Kato, H., Takeuchi, O., Akira, S., Way, M., Schiavo, G., and Reis e Sousa, C. (2009). Activation of MDA5 Requires Higher-Order RNA Structures Generated during Virus Infection. Journal of Virology *83*, 10761–10769.

Pilcher, R.L.R., Moxon, S., Pakseresht, N., Moulton, V., Manning, K., Seymour, G., and Dalmay, T. (2007). Identification of novel small RNAs in tomato (Solanum lycopersicum). Planta *226*, 709–717.

Prufer, K., Stenzel, U., Dannemann, M., Green, R.E., Lachmann, M., and Kelso, J. (2008). PatMaN: rapid alignment of short sequences to large databases. Bioinformatics *24*, 1530–1531.

Randall, R.E., and Goodbourn, S. (2008). Interferons and viruses: an interplay between induction, signalling, antiviral responses and virus countermeasures. J Gen Virol *89*, 1–47.

van Rij, R.P., and Berezikov, E. (2009). Small RNAs and the control of transposons and viruses in Drosophila. Trends in Microbiology *17*, 163–171.

Rivas, F.V., Tolia, N.H., Song, J.-J., Aragon, J.P., Liu, J., Hannon, G.J., and Joshua-Tor, L. (2005). Purified Argonaute2 and an siRNA form recombinant human RISC. Nat Struct Mol Biol *12*, 340–349.

Robb, G.B., and Rana, T.M. (2007a). RNA Helicase A Interacts with RISC in Human Cells and Functions in RISC Loading. Molecular Cell *26*, 523–537.

Robb, G.B., and Rana, T.M. (2007b). RNA Helicase A Interacts with RISC in Human Cells and Functions in RISC Loading. *26*, 523–537.

La Rocca, S.A., Herbert, R.J., Crooke, H., Drew, T.W., Wileman, T.E., and Powell, P.P. (2005). Loss of Interferon Regulatory Factor 3 in Cells Infected with Classical Swine Fever Virus Involves the N-Terminal Protease, Npro. J. Virol. *79*, 7239–7247.

Rothenfusser, S., Goutagny, N., DiPerna, G., Gong, M., Monks, B.G., Schoenemeyer, A., Yamamoto, M., Akira, S., and Fitzgerald, K.A. (2005). The RNA helicase Lgp2 inhibits TLR-independent sensing of viral replication by retinoic acid-inducible gene-I. J. Immunol *175*, 5260–5268.

Ryman, K.D., Meier, K.C., Gardner, C.L., Adegboyega, P.A., and Klimstra, W.B. (2007). Non-pathogenic Sindbis virus causes hemorrhagic fever in the absence of alpha/beta and gamma interferons. Virology *368*, 273–285.

Sabbah, A., Chang, T.H., Harnack, R., Frohlich, V., Tominaga, K., Dube, P.H., Xiang, Y., and Bose, S. (2009). Activation of innate immune antiviral responses by Nod2. Nat Immunol *10*, 1073–1080.

Sadler, A.J., Latchoumanin, O., Hawkes, D., Mak, J., and Williams, B.R.G. (2009). An Antiviral Response Directed by PKR Phosphorylation of the RNA Helicase A. PLoS Pathogens *5*, e1000311.

Saito, T., Owen, D.M., Jiang, F., Marcotrigiano, J., and Gale Jr., M. (2008). Innate immunity induced by composition-dependent RIG-I recognition of hepatitis C virus RNA. Nature *454*, 523–527.

Saleh, M.-C., Tassetto, M., van Rij, R.P., Goic, B., Gausson, V., Berry, B., Jacquier, C., Antoniewski, C., and Andino, R. (2009). Antiviral immunity in Drosophila requires systemic RNA interference spread. Nature *458*, 346–350.

Sambrook, J. (2001). Molecular cloning : a laboratory manual (Cold Spring Harbor N.Y.: Cold Spring Harbor Laboratory Press).

Sanchez-Vargas, I., Travanty, E.A., Keene, K.M., Franz, A.W.E., Beaty, B.J., Blair, C.D., and Olson, K.E. (2004). RNA interference, arthropod-borne viruses, and mosquitoes. Virus Research *102*, 65–74.

Sánchez-Vargas, I., Scott, J.C., Poole-Smith, B.K., Franz, A.W.E., Barbosa-Solomieu, V., Wilusz, J., Olson, K.E., and Blair, C.D. (2009). Dengue Virus Type 2 Infections of Aedes aegypti Are Modulated by the Mosquito's RNA Interference Pathway. PLoS Pathogens *5*, e1000299.

Saumet, A., and Lecellier, C.-H. (2006). Anti-viral RNA silencing: do we look like plants ? Retrovirology *3*, 3.

Schickel, R., Boyerinas, B., Park, S.-M., and Peter, M.E. MicroRNAs: key players in the immune system, differentiation, tumorigenesis and cell death. Oncogene *27*, 5959–5974.

Schlee, M., Roth, A., Hornung, V., Hagmann, C.A., Wimmenauer, V., Barchet, W., Coch, C., Janke, M., Mihailovic, A., Wardle, G., et al. (2009). Recognition of 5' triphosphate by RIG-I helicase requires short blunt double-stranded RNA as contained in panhandle of negative-strand virus. Immunity *31*, 25–34.

Schmidt, A., Schwerd, T., Hamm, W., Hellmuth, J.C., Cui, S., Wenzel, M., Hoffmann, F.S., Michallet, M.-C., Besch, R., Hopfner, K.-P., et al. (2009). 5'-triphosphate RNA requires base-

paired structures to activate antiviral signaling via RIG-I. Proc. Natl. Acad. Sci. U.S.A *106*, 12067–12072.

Schoggins, J.W., and Rice, C.M. (2011). Interferon-stimulated genes and their antiviral effector functions. Curr Opin Virol *1*, 519–525.

Seth, R.B., Sun, L., and Chen, Z.J. Antiviral innate immunity pathways. Cell Res *16*, 141–147.

Seth, R.B., Sun, L., Ea, C.-K., and Chen, Z.J. (2005). Identification and characterization of MAVS, a mitochondrial antiviral signaling protein that activates NF-kappaB and IRF 3. Cell *122*, 669–682.

Siomi, H., and Siomi, M.C. (2009). On the road to reading the RNA-interference code. Nature *457*, 396–404.

Skalsky, R.L., and Cullen, B.R. (2010). Viruses, microRNAs, and Host Interactions. Annual Review of Microbiology *64*, 123–141.

Stein, P. (2003). RNAi: Mammalian oocytes do it without RNA-dependent RNA polymerase. RNA *9*, 187–192.

Stocks, M.B., Moxon, S., Mapleson, D., Woolfenden, H.C., Mohorianu, I., Folkes, L., Schwach, F., Dalmay, T., and Moulton, V. (2012). The UEA sRNA workbench: a suite of tools for analysing and visualizing next generation sequencing microRNA and small RNA datasets. Bioinformatics *28*, 2059–2061.

Sullivan, C.S., and Ganem, D. (2005). A Virus-Encoded Inhibitor That Blocks RNA Interference in Mammalian Cells. J. Virol. *79*, 7371–7379.

Sullivan, C.S., Grundhoff, A.T., Tevethia, S., Pipas, J.M., and Ganem, D. (2005). SV40-encoded microRNAs regulate viral gene expression and reduce susceptibility to cytotoxic T cells. Nature *435*, 682–686.

Svoboda P (2007). Off-targeting and other non-specific effects of RNAi experiments in mammalian cells. Curr Opin Mol Ther. *9*, 248–57.

Szittya, G., Moxon, S., Santos, D.M., Jing, R., Fevereiro, M.P., Moulton, V., and Dalmay, T. (2008). High-throughput sequencing of Medicago truncatula short RNAs identifies eight new miRNA families. BMC Genomics *9*, 593.

Takeda, A., Tsukuda, M., Mizumoto, H., Okamoto, K., Kaido, M., Mise, K., and Okuno, T. (2005). A plant RNA virus suppresses RNA silencing through viral RNA replication. EMBO J *24*, 3147–3157.

Takeuchi, O., and Akira, S. (2009). Innate immunity to virus infection. Immunological Reviews *227*, 75–86.

Tijsterman, M., and Plasterk, R.H.A. (2004). Dicers at RISC; the mechanism of RNAi. Cell *117*, 1–3.

Tong, L., Lin, L., Wu, S., Guo, Z., Wang, T., Qin, Y., Wang, R., Zhong, X., Wu, X., Wang, Y., et al. (2013). MiR-10a* up-regulates coxsackievirus B3 biosynthesis by targeting the 3D-coding sequence. Nucleic Acids Research *41*, 3760–3771.

Triboulet, R., Mari, B., Lin, Y.L., Chable-Bessia, C., Bennasser, Y., Lebrigand, K., Cardinaud, B., Maurin, T., Barbry, P., Baillat, V., et al. (2007). Suppression of microRNA-silencing pathway by HIV-1 during virus replication. Science *315*, 1579 – 1582.

Tsuchida, A., Ohno, S., Wu, W., Borjigin, N., Fujita, K., Aoki, T., Ueda, S., Takanashi, M., and Kuroda, M. (2011). miR-92 is a key oncogenic component of the miR-17-92 cluster in colon cancer. Cancer Science *102*, 2264–2271.

Umbach, J.L., and Cullen, B.R. (2009). The role of RNAi and microRNAs in animal virus replication and antiviral immunity. Genes & Development *23*, 1151–1164.

Uzri, D., and Gehrke, L. (2009). Nucleotide Sequences and Modifications That Determine RIG-I/RNA Binding and Signaling Activities. J. Virol. *83*, 4174–4184.

Vance, V., and Vaucheret, H. (2001). RNA Silencing in Plants--Defense and Counterdefense. Science *292*, 2277–2280.

Venkataraman, T., Valdes, M., Elsby, R., Kakuta, S., Caceres, G., Saijo, S., Iwakura, Y., and Barber, G.N. (2007). Loss of DExD/H box RNA helicase LGP2 manifests disparate antiviral responses. J. Immunol *178*, 6444–6455.

de Vries, W., and Berkhout, B. (2008). RNAi suppressors encoded by pathogenic human viruses. The International Journal of Biochemistry & Cell Biology *40*, 2007–2012.

de Vries, W., Haasnoot, J., van der Velden, J., van Montfort, T., Zorgdrager, F., Paxton, W., Cornelissen, M., van Kuppeveld, F., de Haan, P., and Berkhout, B. (2008). Increased virus replication in mammalian cells by blocking intracellular innate defense responses. Gene Ther *15*, 545–552.

Wiesen, J.L., and Tomasi, T.B. (2009). Dicer is regulated by cellular stresses and interferons. Molecular Immunology *46*, 1222–1228.

Williams, B.R. (1999). PKR; a sentinel kinase for cellular stress. Oncogene *18*, 6112–6120.

Xie, Q., and Guo, H.-S. (2006). Systemic antiviral silencing in plants. Virus Research *118*, 1–6.

Xie, Z., Johansen, L.K., Gustafson, A.M., Kasschau, K.D., Lellis, A.D., Zilberman, D., Jacobsen, S.E., and Carrington, J.C. (2004). Genetic and Functional Diversification of Small RNA Pathways in Plants. Plos Biol *2*, e104.

Yan, K.S., Yan, S., Farooq, A., Han, A., Zeng, L., and Zhou, M.-M. (2003). Structure and conserved RNA binding of the PAZ domain. Nature *426*, 469–474.

Yeung, M., Benkirane, M., and Jeang, K.-T. (2007). Small non-coding RNAs, mammalian cells, and viruses: regulatory interactions? Retrovirology *4*, 74.

Yoneyama, M., Kikuchi, M., Natsukawa, T., Shinobu, N., Imaizumi, T., Miyagishi, M., Taira, K., Akira, S., and Fujita, T. (2004). The RNA helicase RIG-I has an essential function in double-stranded RNA-induced innate antiviral responses. Nat. Immunol *5*, 730–737.

Yoneyama, M., Kikuchi, M., Matsumoto, K., Imaizumi, T., Miyagishi, M., Taira, K., Foy, E., Loo, Y.-M., Gale, M., Akira, S., et al. (2005). Shared and unique functions of the DExD/H-box helicases RIG-I, MDA5, and LGP2 in antiviral innate immunity. J. Immunol *175*, 2851–2858.

Zhou, J., and Rossi, J.J. (2011). Progress in RNAi-based antiviral therapeutics. Methods Mol. Biol. *721*, 67–75.

Zou, J., Chang, M., Nie, P., and Secombes, C. (2009). Origin and evolution of the RIG-I like RNA helicase gene family. BMC Evolutionary Biology *9*, 85.

(2007). Fields virology (Philadelphia: Wolters Kluwer Health/Lippincott Williams & Wilkins).

Small RNA Sample Prep Protocol v1.5, Part # 15002615, Rev. E.

Illumina - Sequencing Technology.

CellProfiler Project.